Strategy for understanding neutron star matter from HIHR/K1.1 physics

K. Miwa (Tohoku Univ.)
on behalf of the HIHR/K1.1 task force

Contents

- Hyperon puzzle in neutron stars
- Strategy for understanding neutron star matter from HIHR/K1.1 physics
- Λp scattering experiment at K1.1 beam line

From Quark to Neutron star

Bound system interacting by strong interaction with completely different scale.

Hadron

Nucleus, Hypernucleus

Neutron star

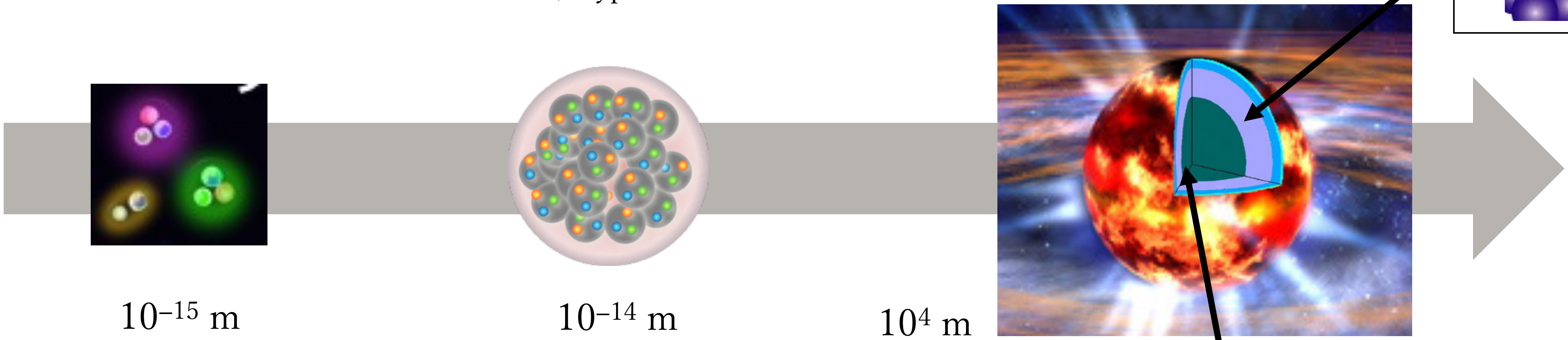

10^{-15} m

10^{-14} m

10^{4} m

Neutron matter

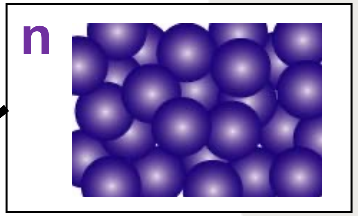

These system should be understood with the same framework based on the microscopic picture with strong interaction.

Strange hadronic matter ?

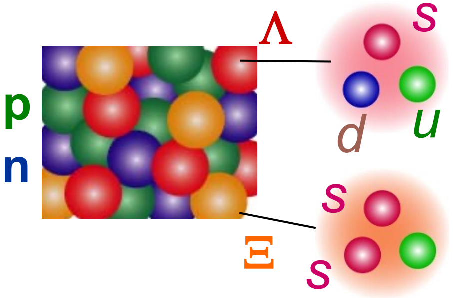

Hyperons

Inner core in neutron star

Extremely high-density nuclear matter where baryon-baryon interaction plays essential roles

✓ to judge the appearance of strange particles

✓ to understand the mechanism to support the massive neutron star.

Strategy of microscopic understanding of NS (neutron matter)

<u>Realistic NN interaction</u>

Meson-exchange models
- Paris potential
- Bonn potential
- Nijmegen potential

Potential models
- Urbana potential
- Argonne potential

Chiral EFT
- Up to N4LO

<u>3 Nucleon Force (3NF)</u>

Phenomenological model : Urbana UⅦ, U IX

Chiral 3NF

Microscopic approach to nuclear matter with the bare interaction model

<u>Theoretical approach to nuclear matter</u>

Ab-initio microscopic methods
- (Dirac) Brueckner-Hartree-Fock
- Self-consistent Green's function

:

Phenomenological approaches
- Relativistic mean-field

Nuclear structure → Nuclear saturation point → s.p. energy in pure neutron matter
EOS of neutron star

Constraints on EOS for neutron star from nuclear physics

G.F. Burgio et al., arXiv:2105.03747

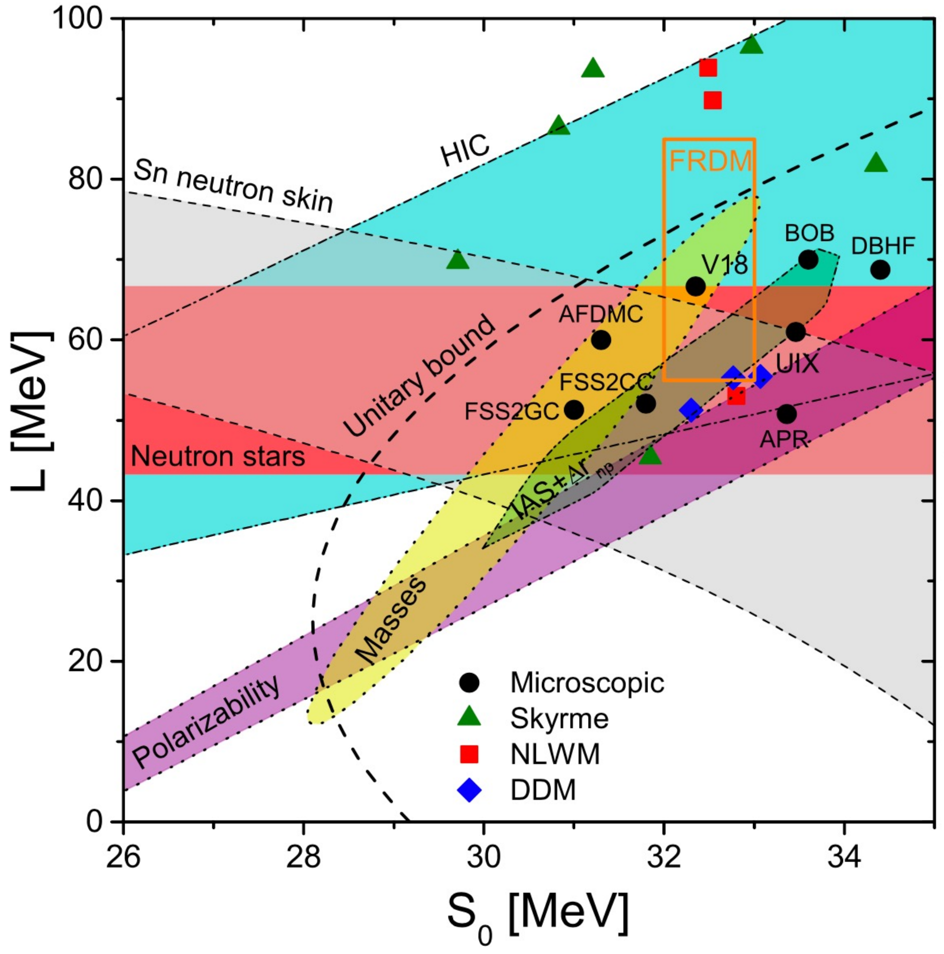

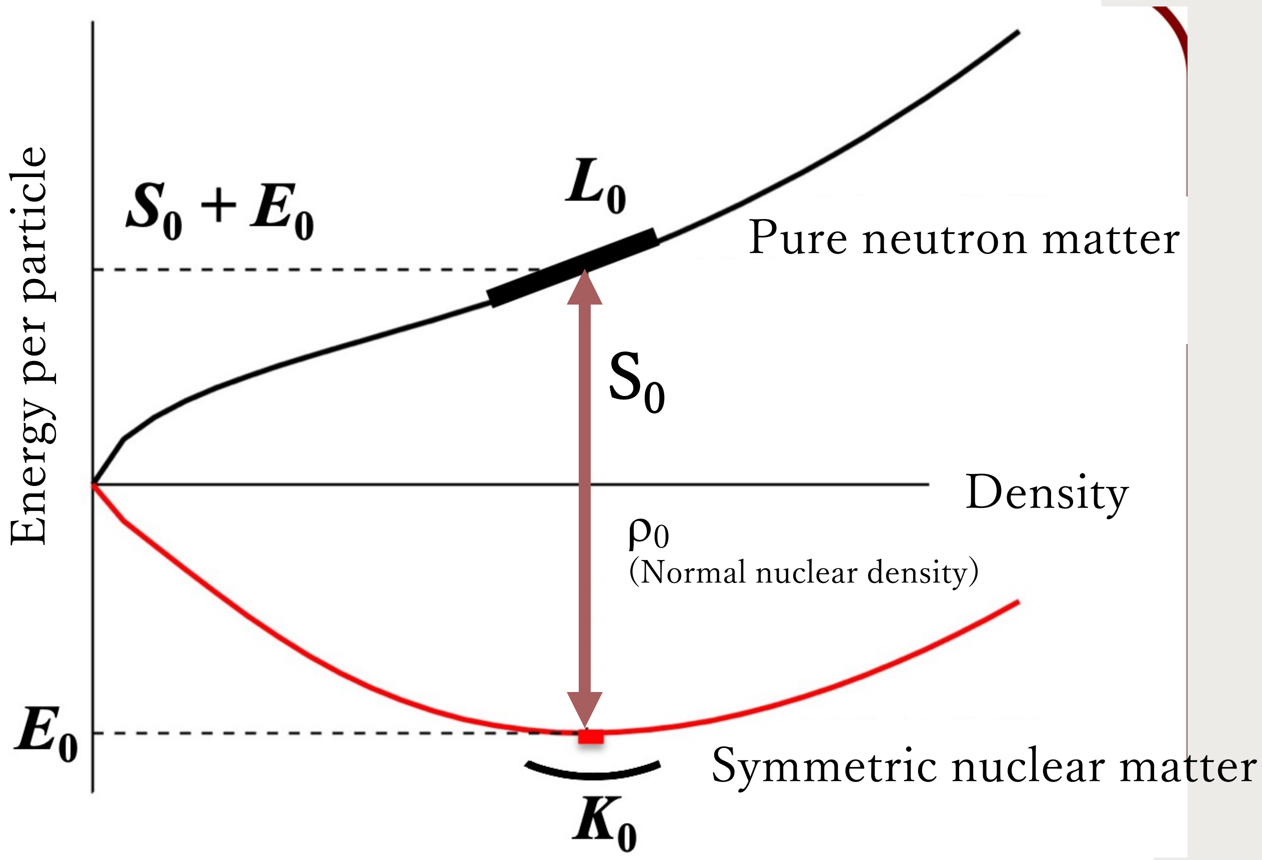

S_0 and L_0 values for symmetry energy are constrained from nuclear experiments

Constraints on EOS for neutron star from nuclear physics

G.F. Burgio et al., arXiv:2105.03747

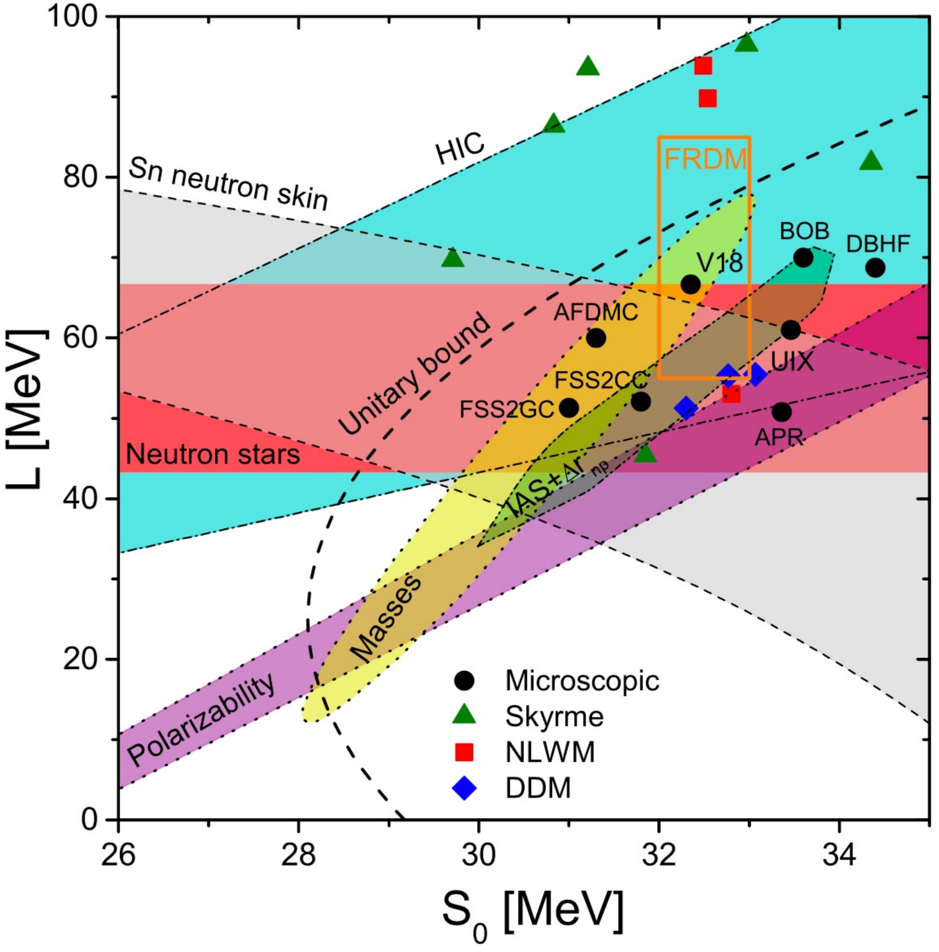

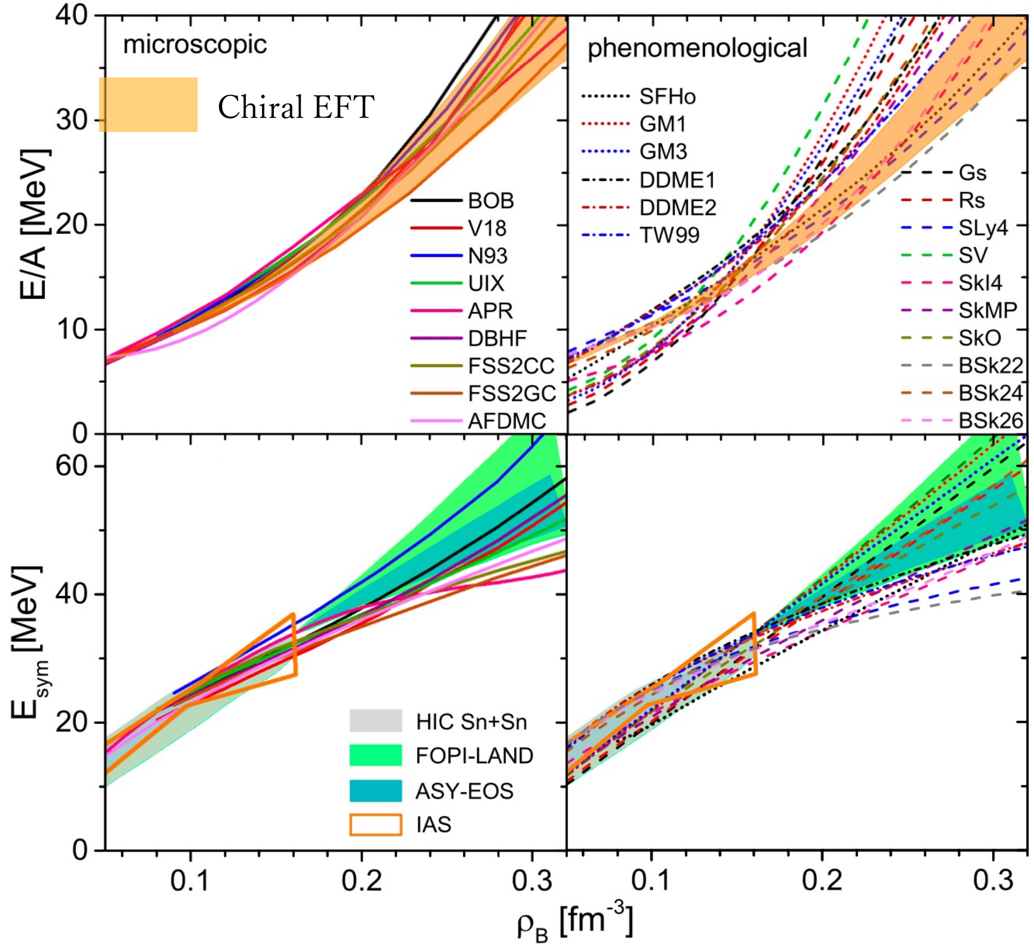

Rather consistent results are obtained up to $\sim 2\rho_0$ including chiral EFT calculation

Constraints on EOS from astrophysical observations

T.E. Riley et al., arXiv:2105.06980

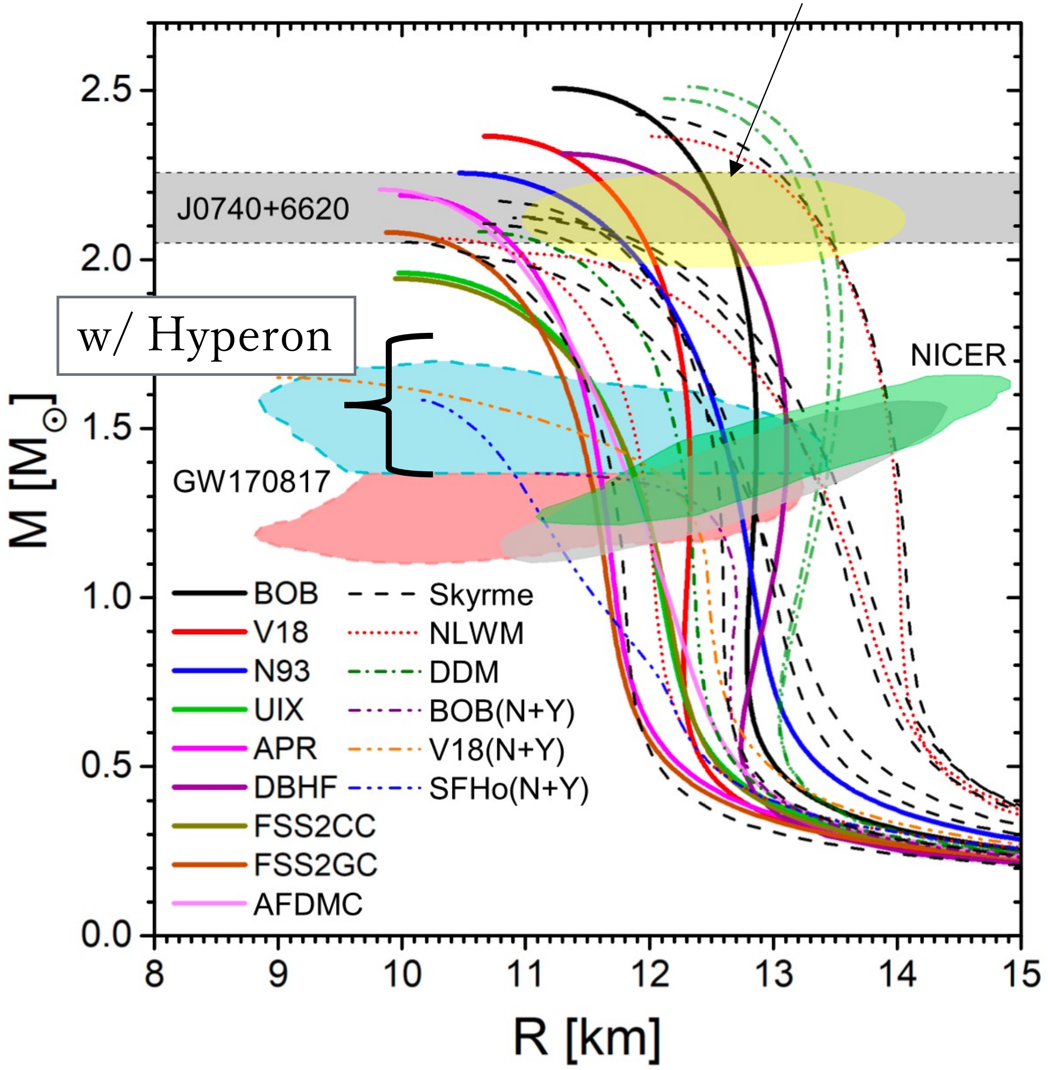

G.F. Burgio et al., arXiv:2105.03747

Gravitational waves

Tidal deformability of neutron star merger

NICER mission

Simultaneous measurement of both mass and radius

Heavy mass neutron star

Strong constraint on M-R relation

What is the key mechanism to make such M-R relation?
To answer this question, microscopic approach based on nuclear physics is necessary,
with strangeness degree of freedom

Hyperon puzzle in neutron star

Strange Hadronic Matter in neutron star ?

Hyperon's appearance is reasonable scenario from the attractive potential in nuclei.

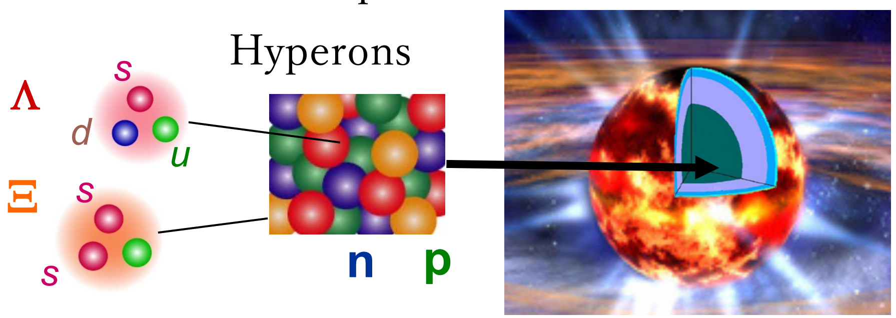

How can we reconcile ?

Softening of EOS w/ hyperon appearance

Two-solar-mass NS

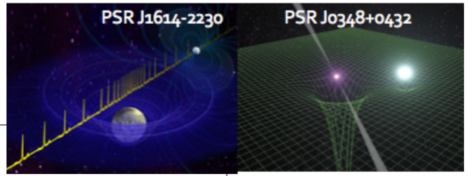

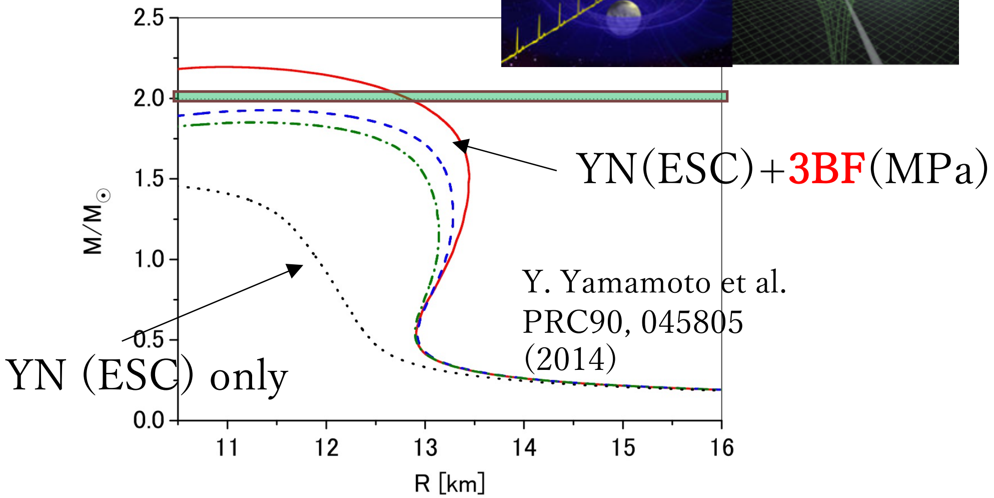

3 Baryon Force (3BF):

Significant repulsive contribution at high density

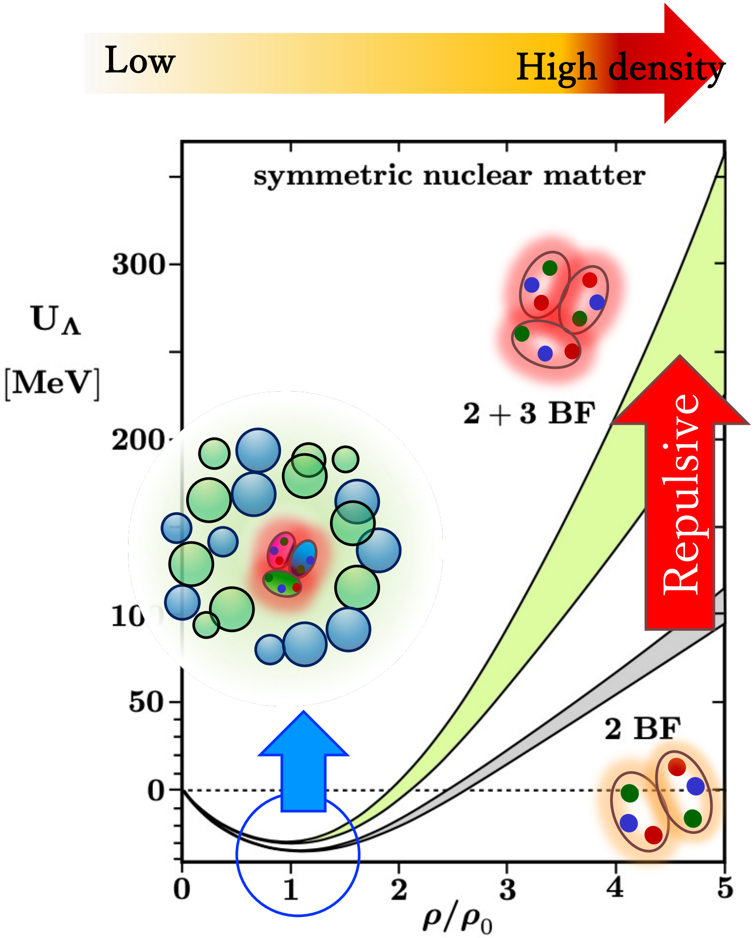

D. Gerstung et al., Eur. Phys. J. A(2020) 56:175

We have to derive the nature of the density dependence of ΛN interaction considering the ΛNN force.

Strategy of microscopic understanding of NS with strangeness

Realistic Baryon-Baryon (BB) interaction

Information of all BB interaction
ΛN, ΣN, ΞN, ΛΛ

$SU(3)_f$ meson exchange BB models

$SU(3)_f$ chiral EFT force
NLO at present

Lattice BB force

3 Baryon Force with hyperon (3BF)

Phenomenological 3BF
TFA + MP repulsion in Nijmegen

3BF in chiral EFT for YNN

Strength of ΛN-ΣN coupling and effect in nuclear medium

ΛN-ΣN coupling in free space or a few-body system

BB interaction in medium/nuclear matter

Ab initio calculation

No Core Shell Model

→ hypernuclei

BHF calculation →

Hyperon's single particle potential in neutron star matter

EOS with hyperon

This strategy is limited by the insufficient hypernuclear data

Quite scarce YN scattering data
→ Difficult to constrain BB interaction models.
More plenty of YN scattering data.

Limited hypernuclear data
Precise hypernuclear spectroscopic data for medium and heavy Λ hypernucleus to determine BE.

What have we provided from J-PARC experiments so far ?

Λ single particle potential at nuclear density

Accumulated hypernucler data

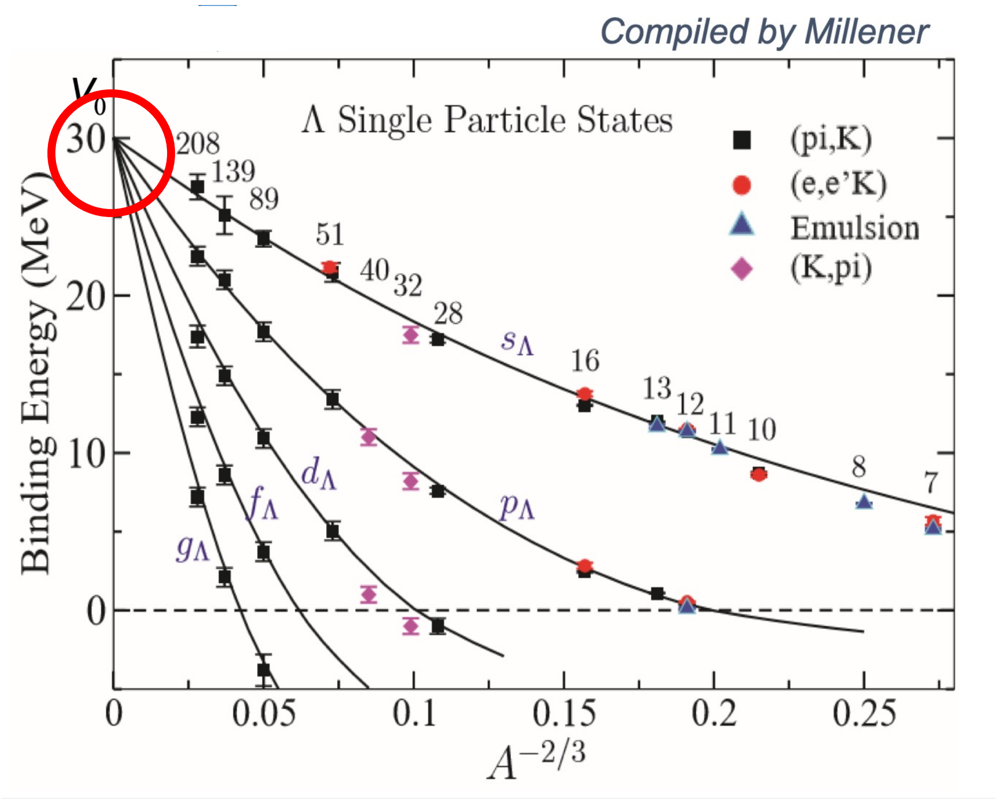

$U_\Lambda(\rho_0)$~-30 MeV

Attractive potential at normal nuclear density

This is a start point to consider Λ appearance in neutron star matter

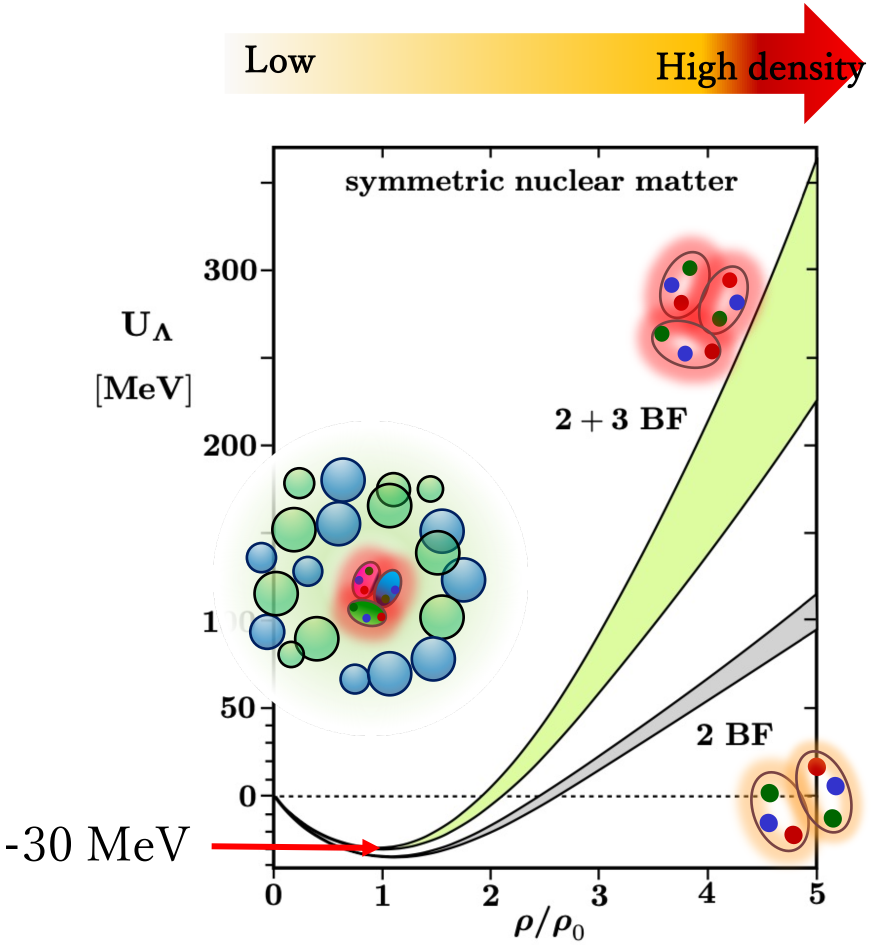

U_Λ can not be reproduced only with ΛN interaction

This potential value is essential constraint on the ΛNN 3BF at nuclear density

ΣN, ΞN interactions

J-PARC E10

T. Harada, R. Honda et al., Phys. Rev. C97, 024601 (2018)

Σ^--^{5}He system

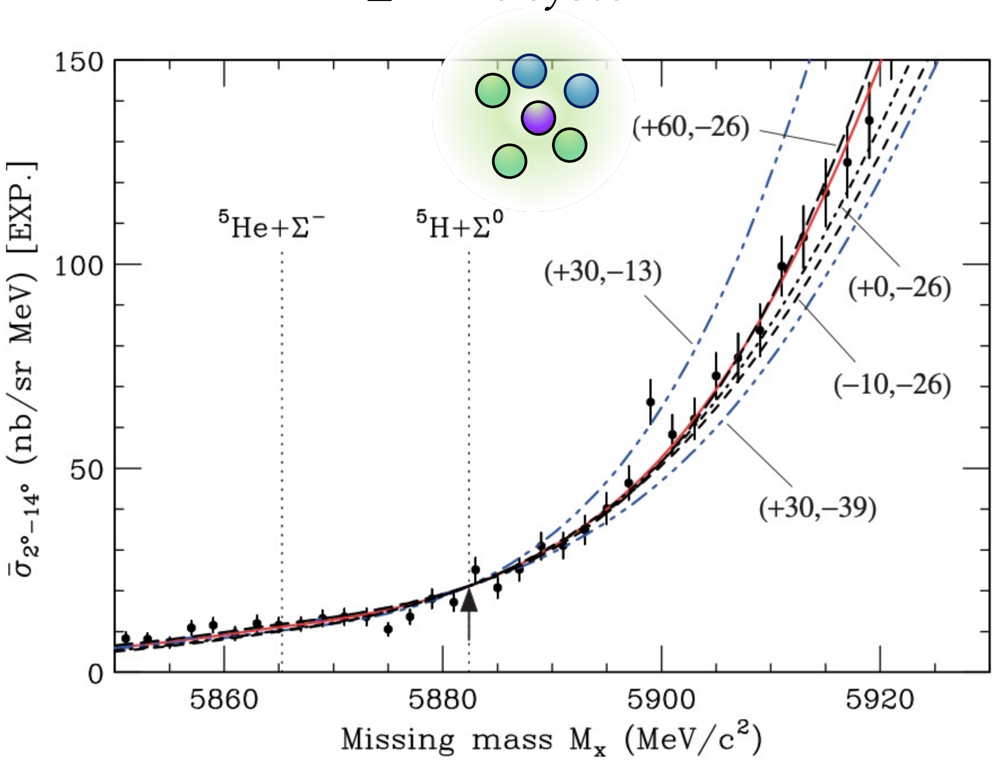

$U_\Sigma(\rho_0)$ = +30 ± 10 MeV (real part)

Repulsive potential for Σ-nucleus potential from Σ^--^{5}He system

J-PARC E07

Observation of Ξ hypernuclei

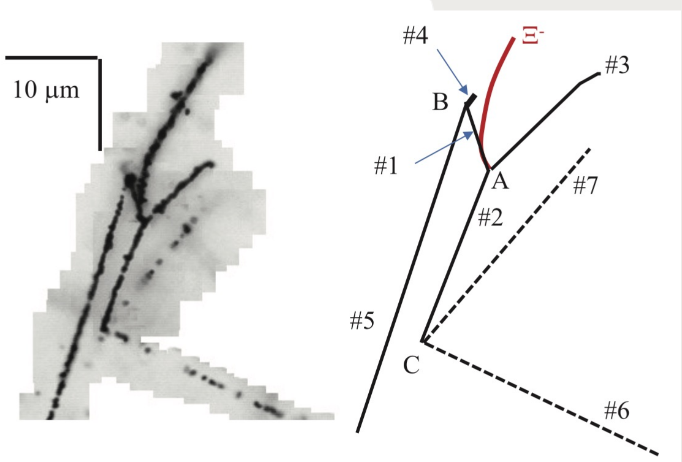

M. Yoshimoto et al., arXiv:2103.08793

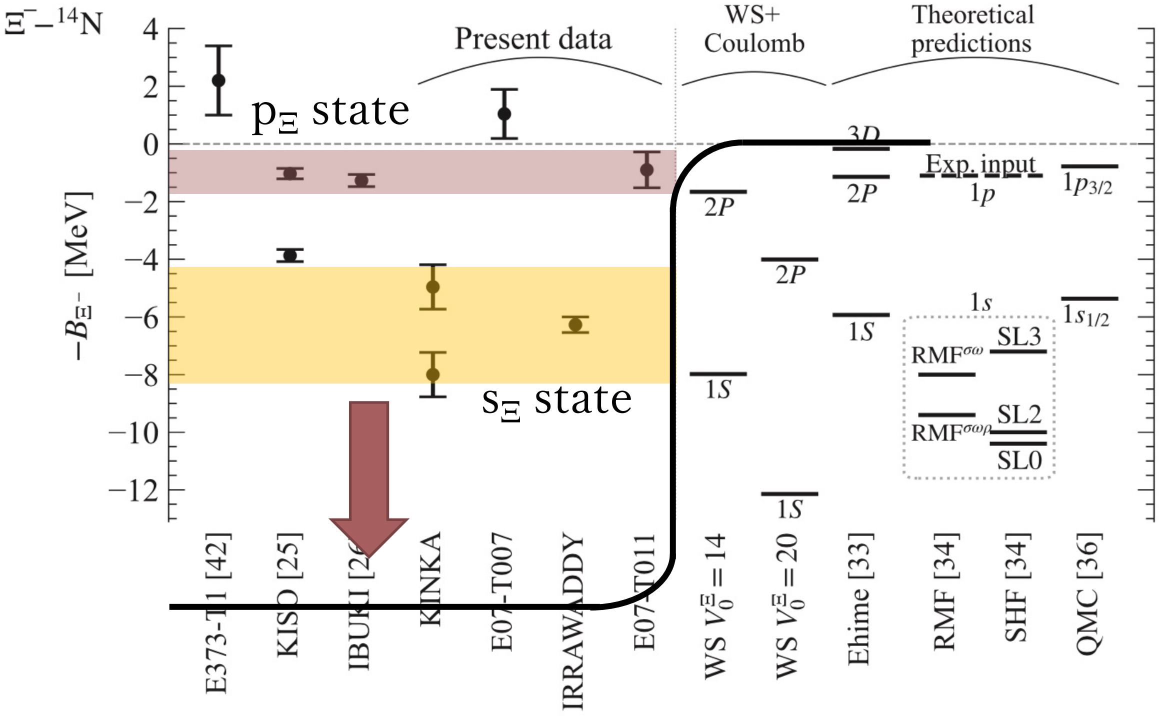

$U_\Xi(\rho_0)$ will be determined by J-PARC experiment
Emulsion (E07) + Ξ hypernuclear spectroscopy (E70)

Toward realistic YN interaction(Experimental side)

YN case

Link between here are connected

Base to construct reliable two-body BB interaction is being constructed both theoretically and experimentally.

2-body scattering data ⇄ **Derivation of YN potential**

Experimental progresses are realized.

Small relative-momentum region

ALICE Collaboration, arXiv:2104.04427

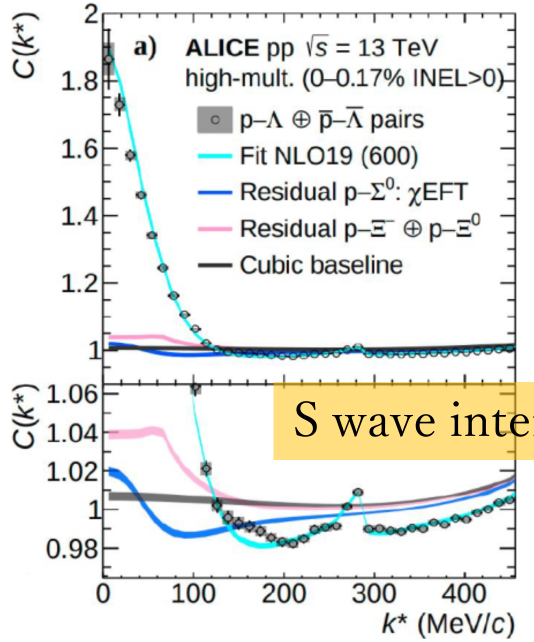

S wave interaction

Femtoscopy from HIC

Intermediate energy region

K. Miwa et al. arXiv:2104.13608

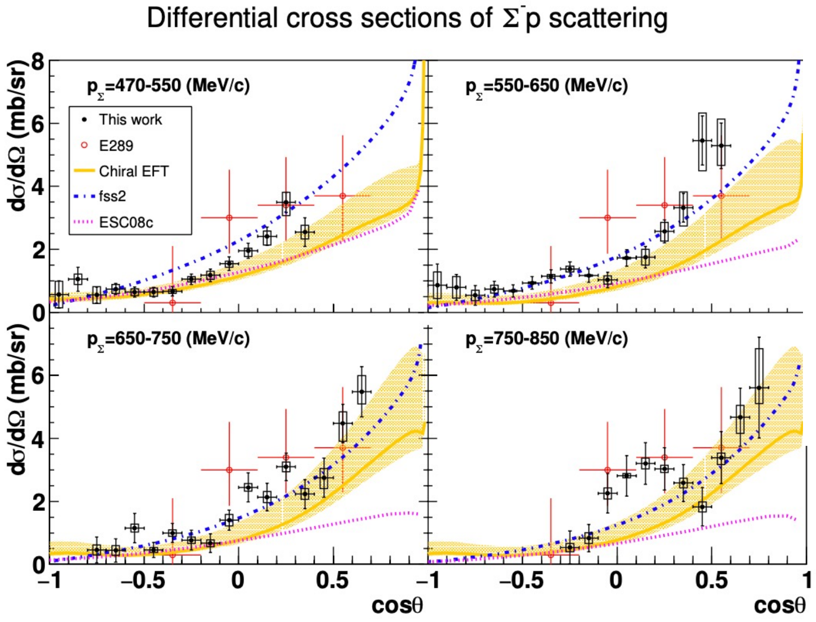

P and higher wave interaction

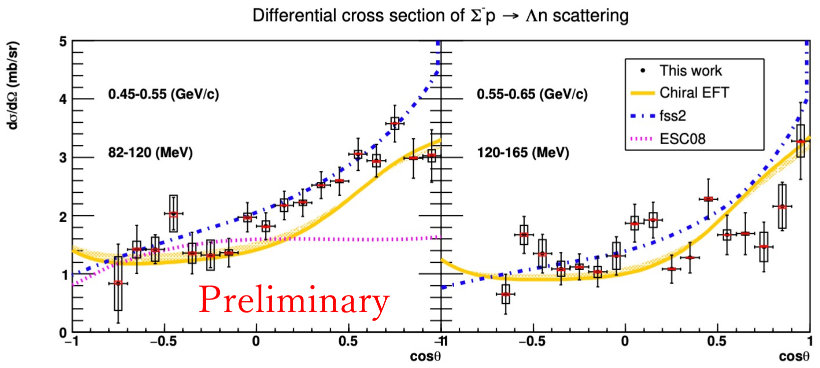

To be submitted soon

J-PARC E40

Experimental method for YN scattering was established.

Progress on theories

BB interaction
Hypernuclear structure

Lattice QCD

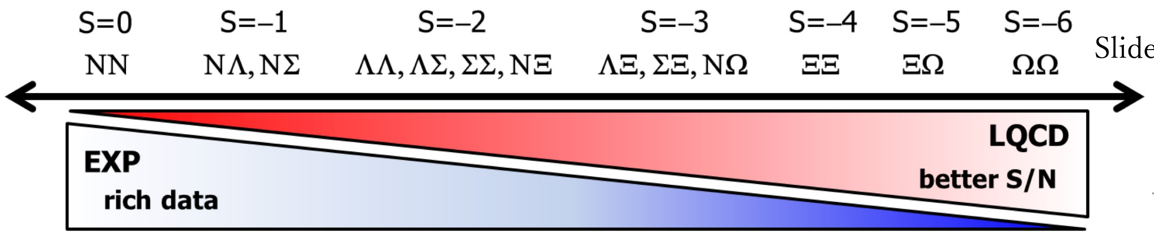

Slide from Doi-san

K. Sasaki et al., Nucl. Phys. A 998 (2020) 121737

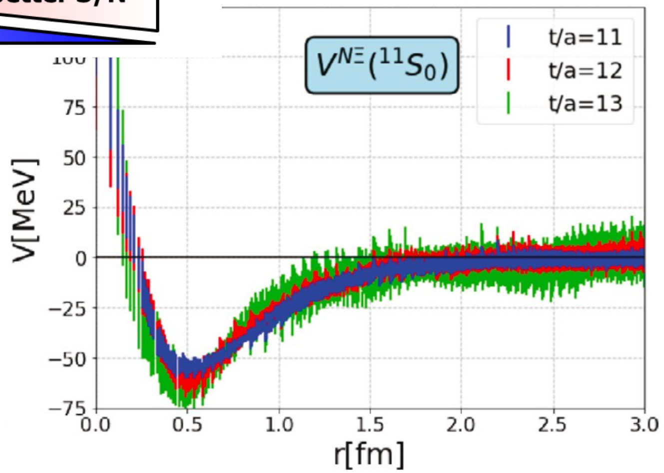

ALICE Collaboration, Nature 588 (2020) 232

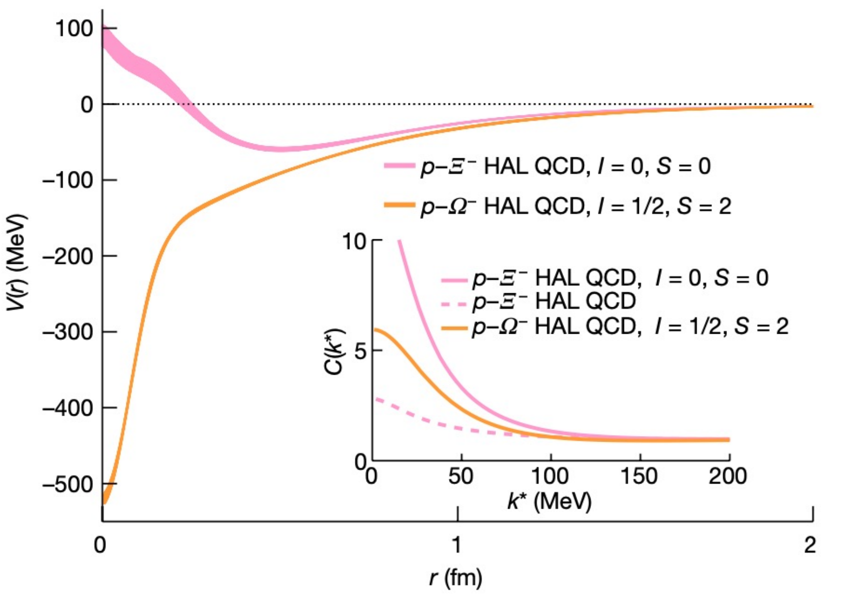

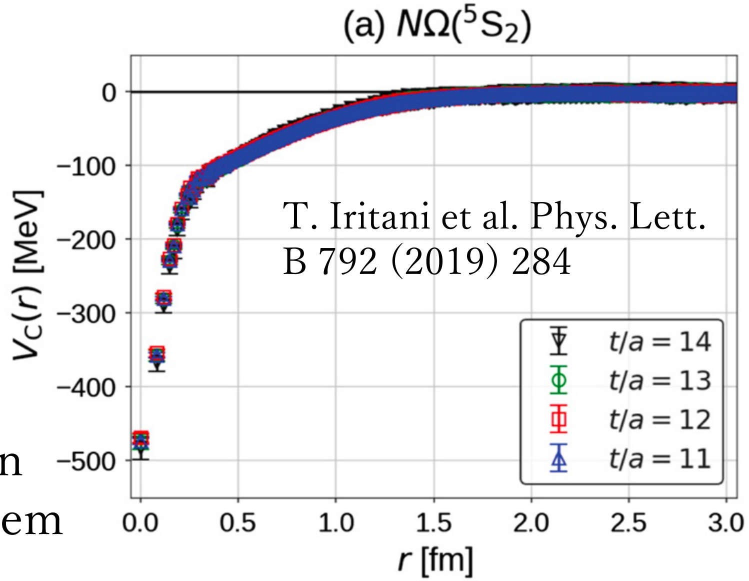

T. Iritani et al. Phys. Lett. B 792 (2019) 284

Attractive potential w/ NO Pauli exclusion

Decay suppression to ΛΞ, ΣΞ for S=2 system

Lattice QCD

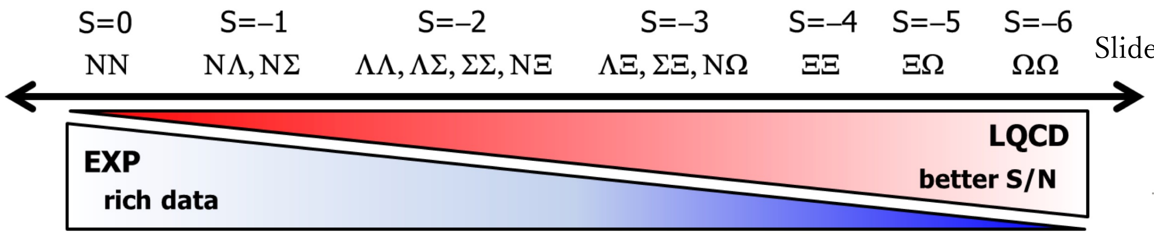

Slide from Doi-san

K. Sasaki et al., Nucl. Phys. A 998 (2020) 121737

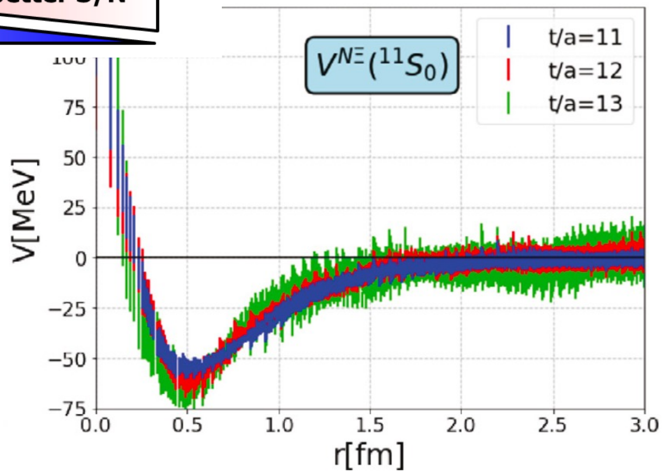

ALICE Collaboration, Nature 588 (2020) 232

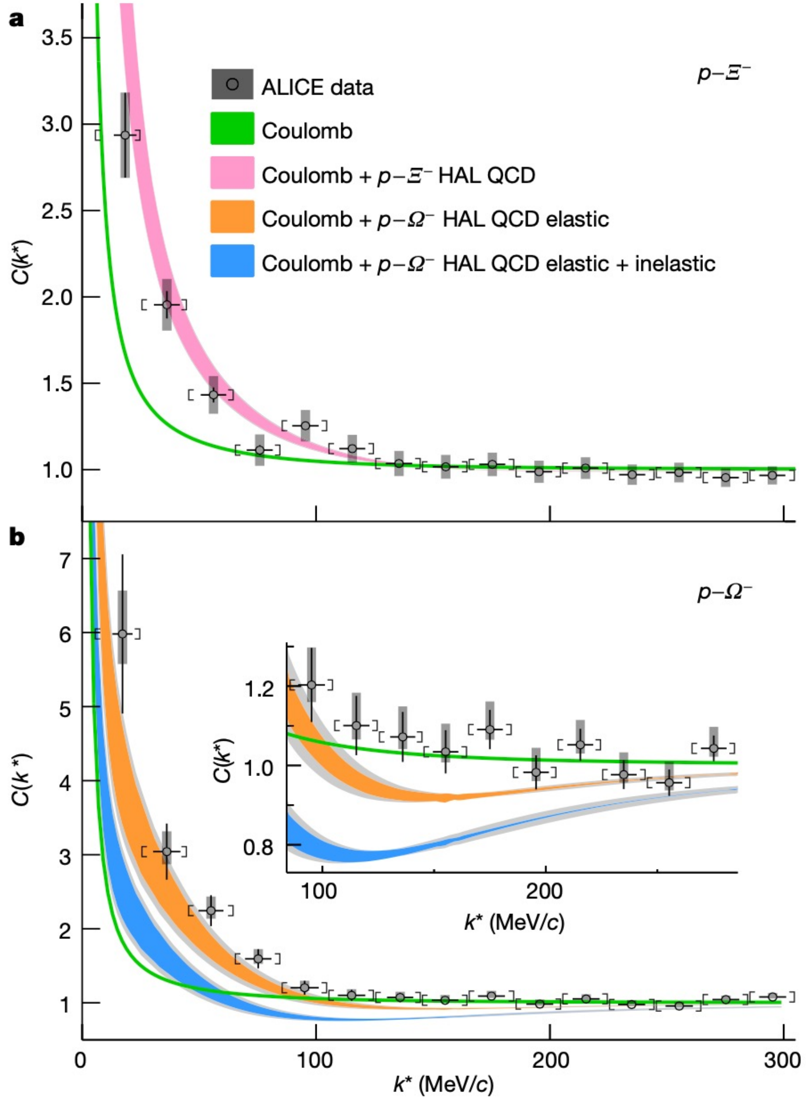

S=-1 system
Theoretical improvement with Misner's method (T. Miyamoto et al. Phys.Rev. D 101 (2020) 074514) are ongoing.

P-wave, LS-force, 3-body forces will be studied in Fugaku computer

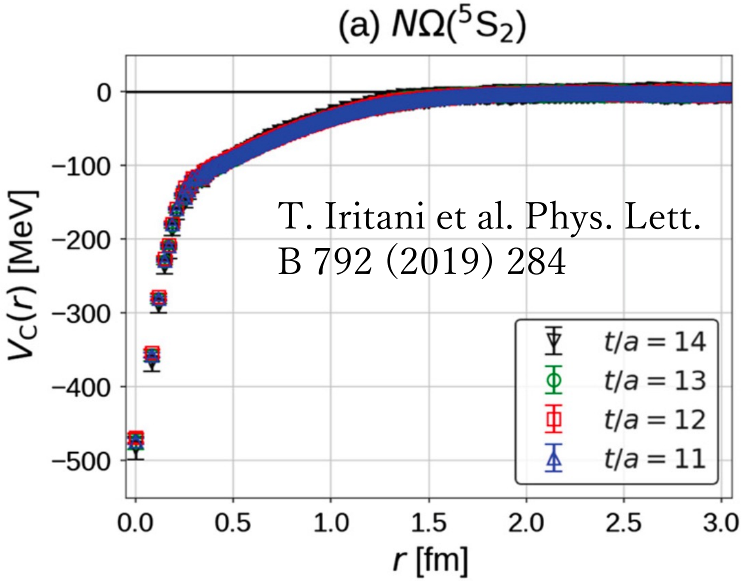

T. Iritani et al. Phys. Lett. B 792 (2019) 284

Chiral EFT

Underlying chiral symmetry in QCD

Power counting feature to improve calculation systematically by going to higher order

Multi baryon force appear naturally and automatically in a consistent implementation of the framework

YN interaction at NLO

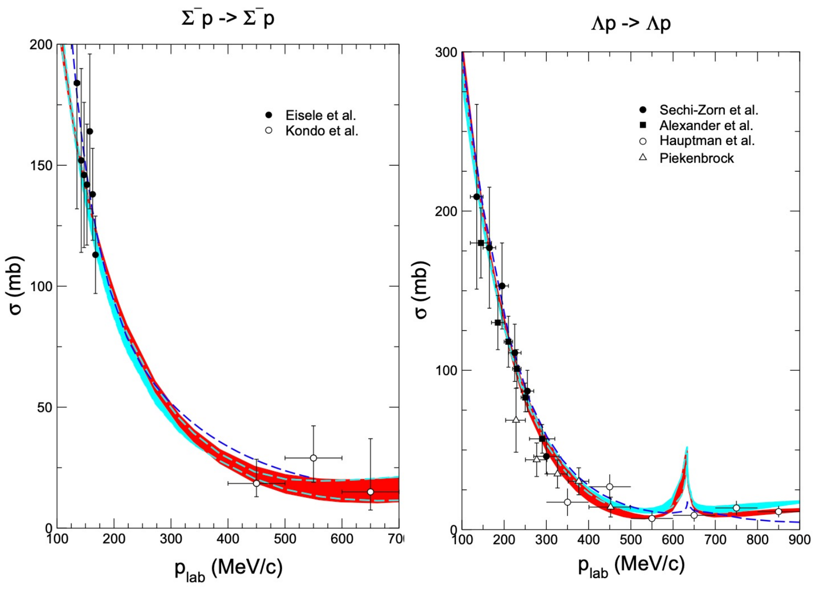

J. Haidenbauer et al., Eur. Phys. J. A (2020) 56:91

J. Haidenbauer et al., Nucl. Phys. A 915 (2013) 24

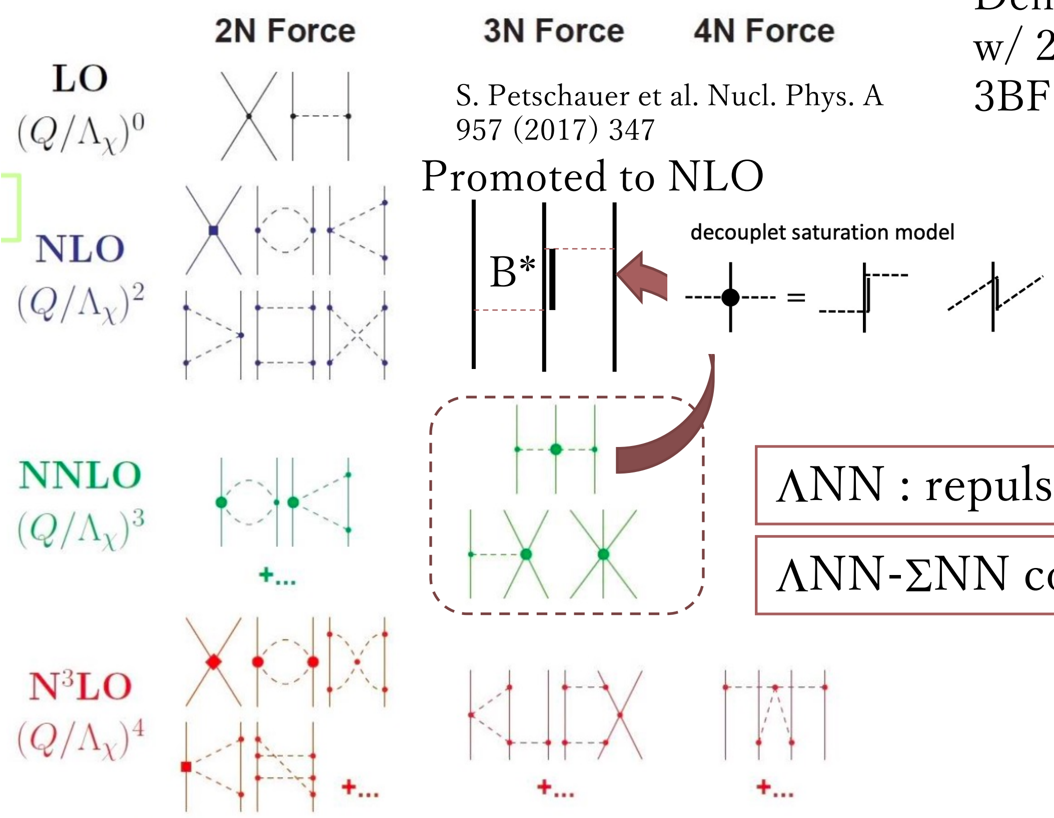

From slide by M. Kohno

Density-dependent effective potential w/ 2π-exchange ΛNN and ΛNN-ΣNN 3BF

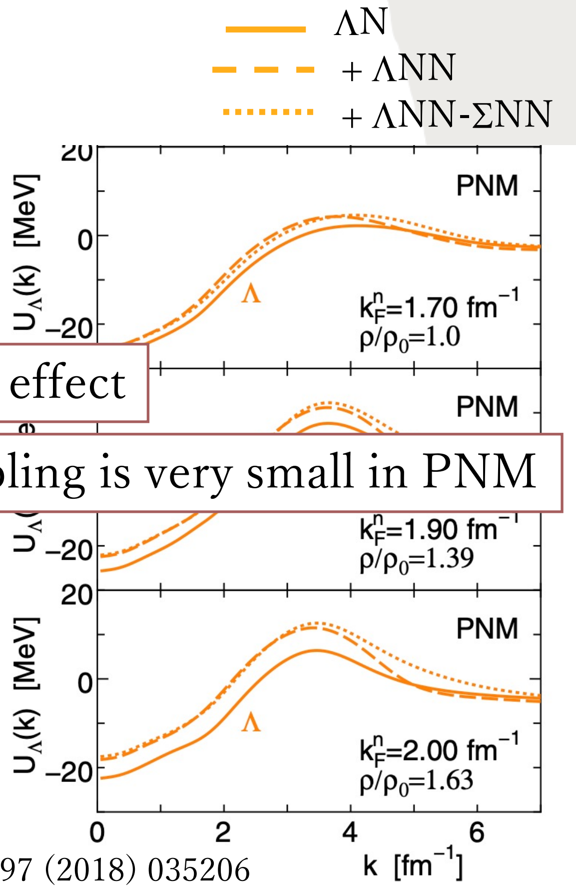

ΛNN : repulsive effect

ΛNN-ΣNN coupling is very small in PNM

M. Kohno, Phys. Rev. C 97 (2018) 035206

Source of attractive ΛN interaction ΛN-ΣN coupling

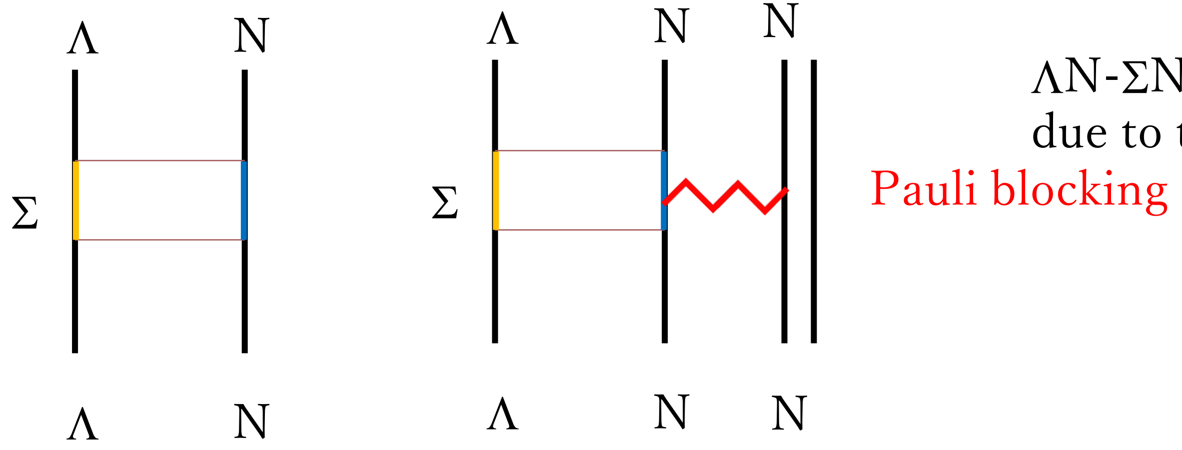

ΛN-ΣN coupling can be suppressed in nuclear medium due to the Pauli blocking at the intermediate N state

Artificially switch off ΛN-ΣN coupling potential

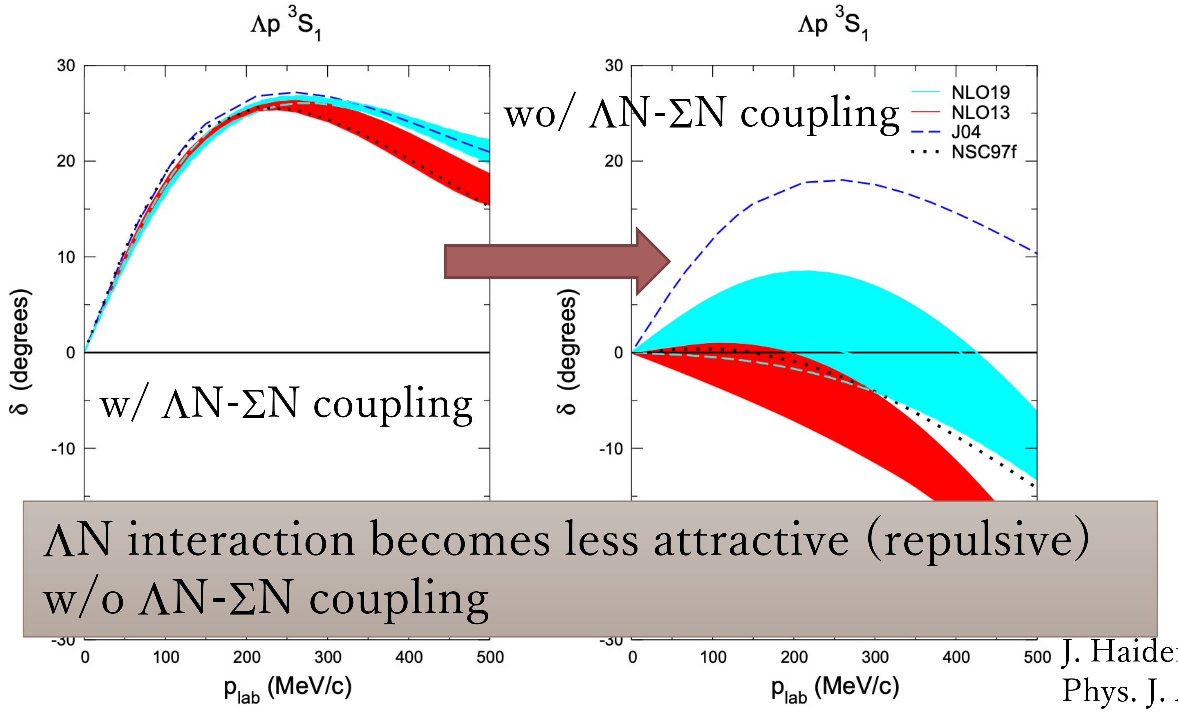

ΛN interaction becomes less attractive (repulsive) w/o ΛN-ΣN coupling

J. Haidenbauer et al., Eur. Phys. J. A (2020) 56:91

w/ ΛN interaction with large ΛN-ΣN coupling
+ ΛNN three-repulsive force (LECs for ΛNN are adjusted)

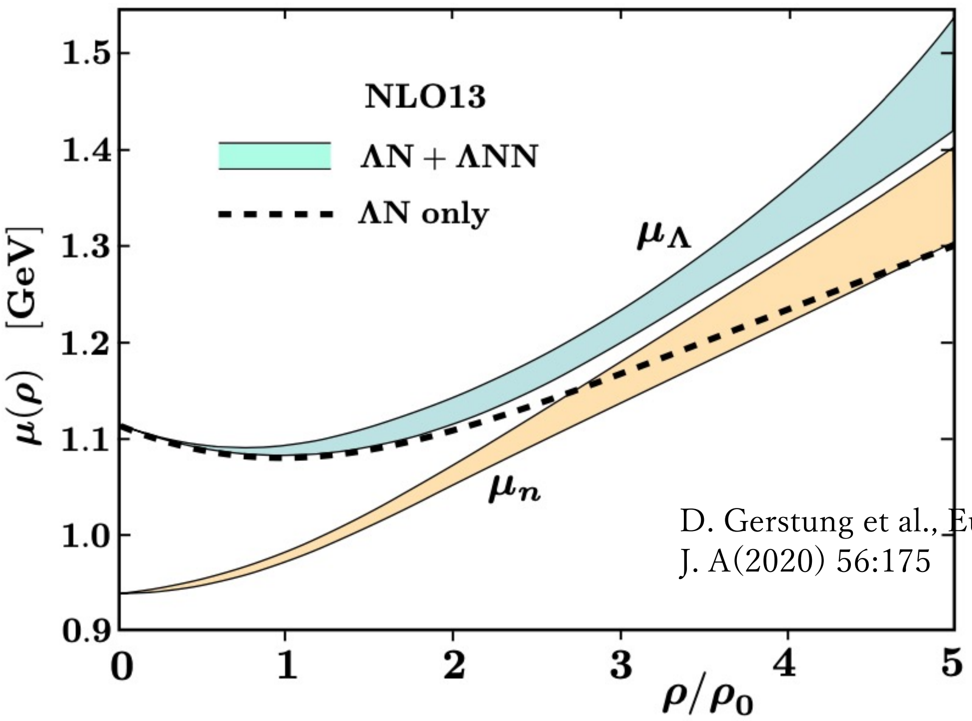

D. Gerstung et al., Eur. Phys. J. A(2020) 56:175

Λ does not appear in neutron star ?

Theoretical calculation of Λ binding energy for wide mass range

Comparison between experimental data and theoretical calculation of Λ hypernuclear mass (Λ binding energy) for wide mass range is important to extract the ΛNN force.

Energy spectra of $^{13}_{\Lambda}$C, $^{16}_{\Lambda}$O, $^{28}_{\Lambda}$Si, $^{51}_{\Lambda}$V, $^{89}_{\Lambda}$Y, $^{139}_{\Lambda}$La, $^{208}_{\Lambda}$Pb with ESC16 model

M.M. Nagels et al. Phys. Rev. C99, 044003 (2019)

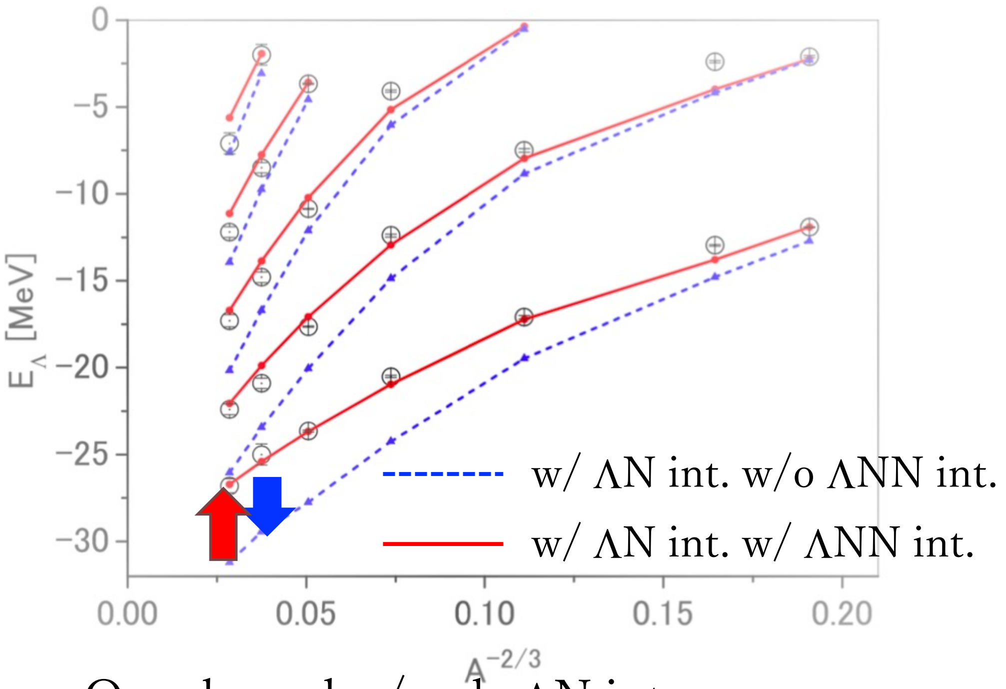

Over bound w/ only ΛN int.

ΛNN repulsive interaction is necessary to explain Λ hypernuclear bounding energy

Λ hypernuclei with chiral YN potential

J. Haidenbauer, I. Vidana, Eur. Phys. J. A (2020) 56:55

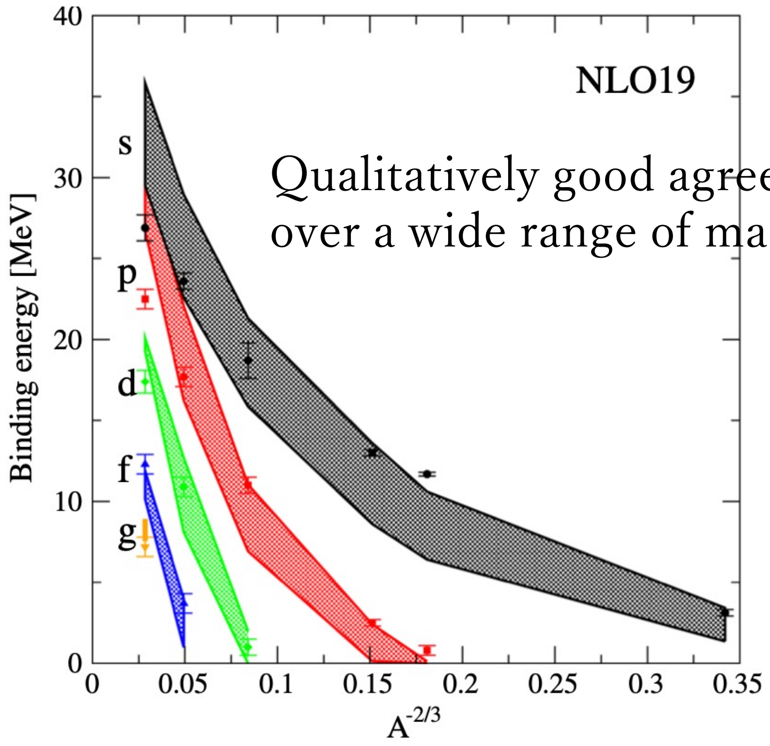

Qualitatively good agreement with data over a wide range of mass number

Sizable cutoff dependence
→ would be reduced at higher order and after inclusion of 3BF

Possibility of density dependence of ΛN int. from excited states

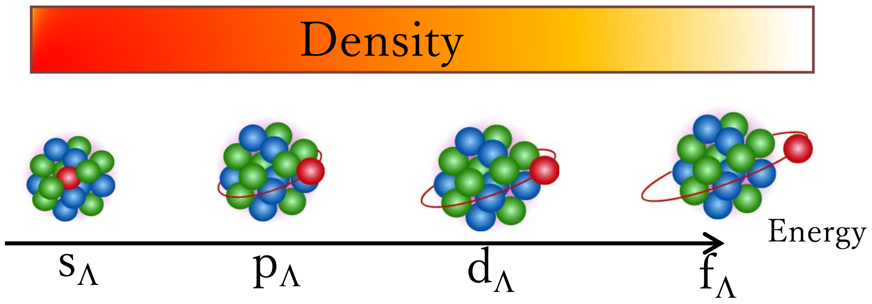

k_F from ADA

$^{40}{}_\Lambda$K(s): k_F = 1.26 fm^{-1}
$^{40}{}_\Lambda$K(p): k_F = 1.15 fm^{-1}
$^{40}{}_\Lambda$K(d): k_F = 1.02 fm^{-1}

Possibility to check the density dependent ΛN interaction from each Λ orbital state

- **Comparison between ESC14+MPP+TBA and ESC12+MPP'＋TBA'**

(MPP: original) (MPP': weakened)

Example: $^{40}_{\Lambda}$K

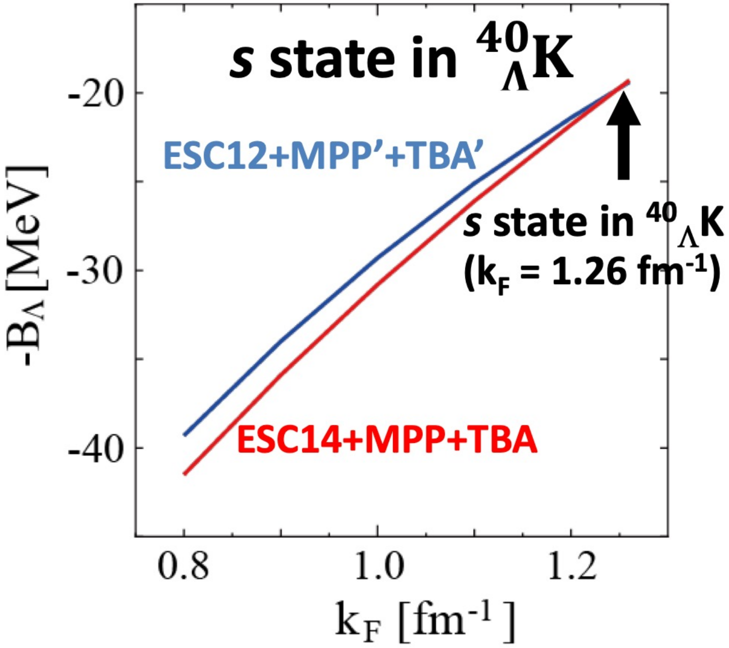

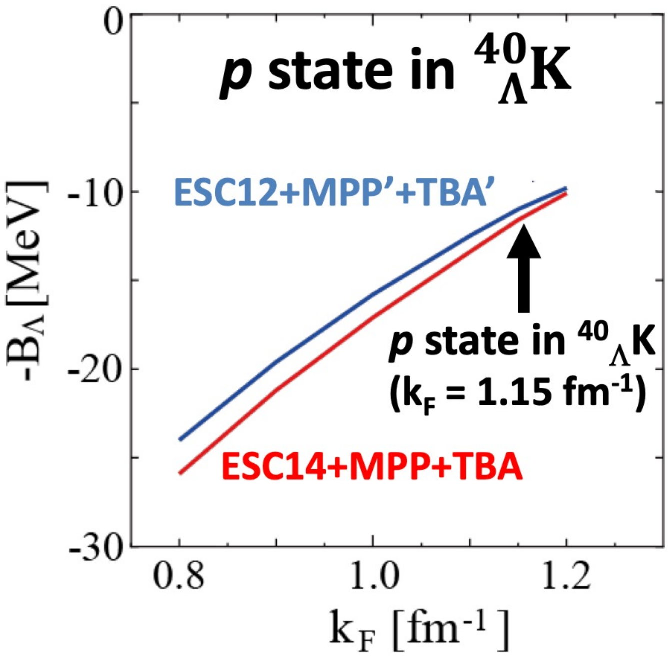

k_F from ADA

$^{40}{}_\Lambda$K(s): k_F = 1.26 fm^{-1}
$^{40}{}_\Lambda$K(p): k_F = 1.15 fm^{-1}
$^{40}{}_\Lambda$K(d): k_F = 1.02 fm^{-1}

M. Isaka's slide at HIHR/K1.1 WS

Calculated B_Λ values can be different in *p* states and *d* states

B_Λ values reliable?

Hotchi et al., PRC 64 (2001) 044302

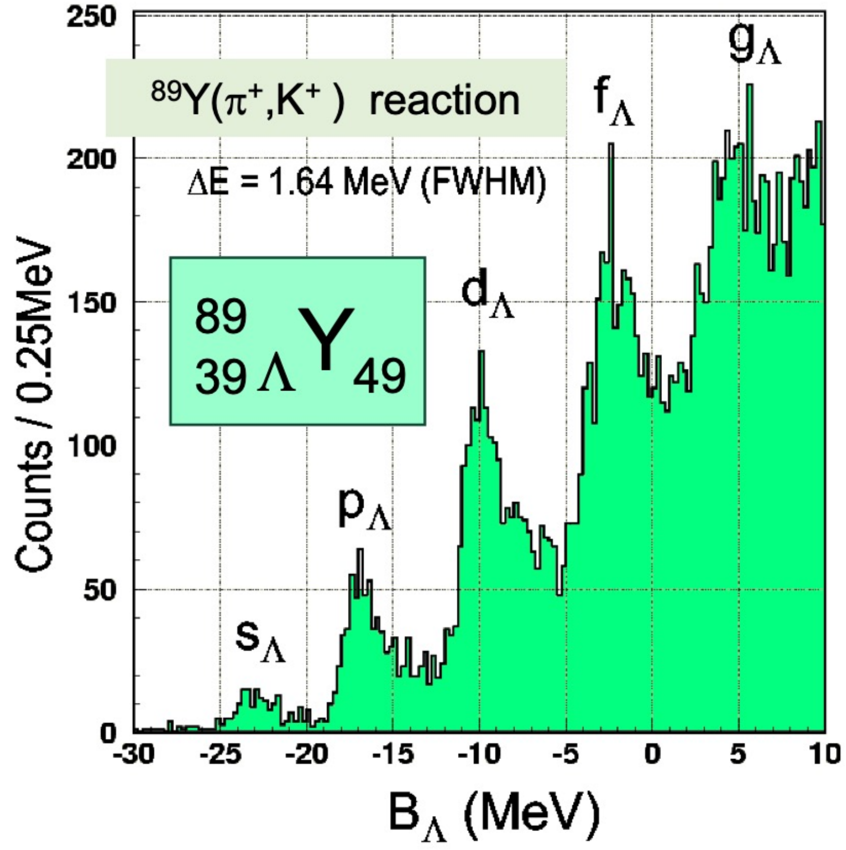

$^{139}La(\pi^+,K^+)^{139}_{\Lambda}La$, p_π = 1.06 GeV/c

Hasegawa et al., PRC 53 (1996) 1210

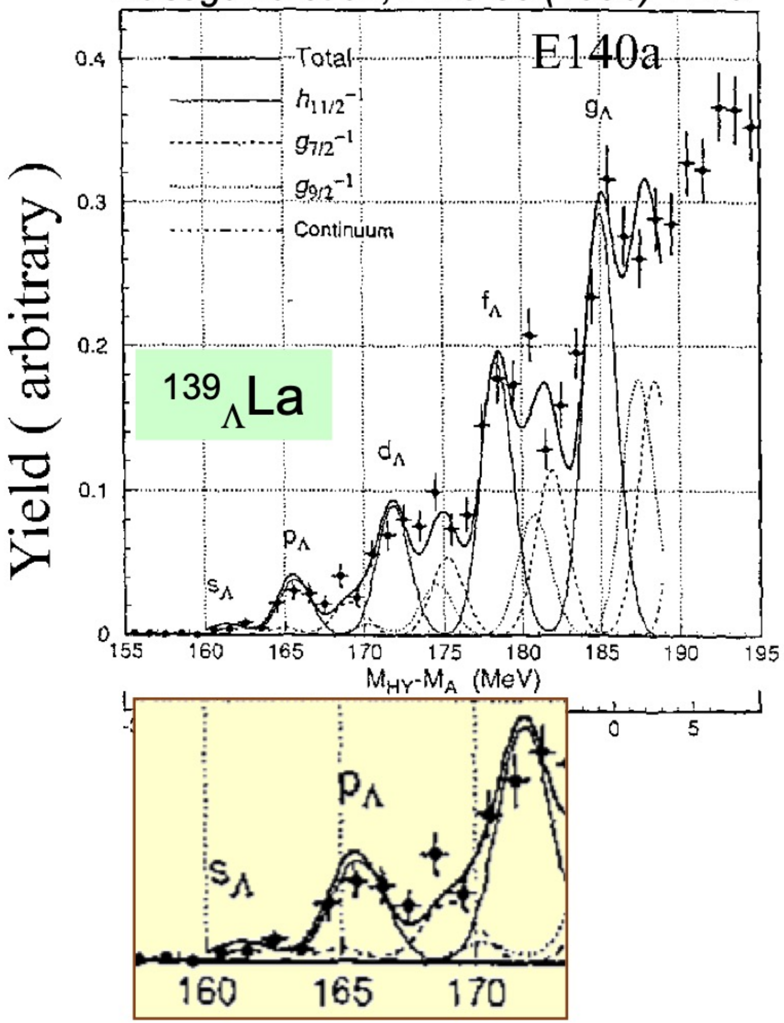

$^{208}Pb(\pi^+,K^+)^{208}_{\Lambda}Pb$, p_π = 1.06 GeV/c

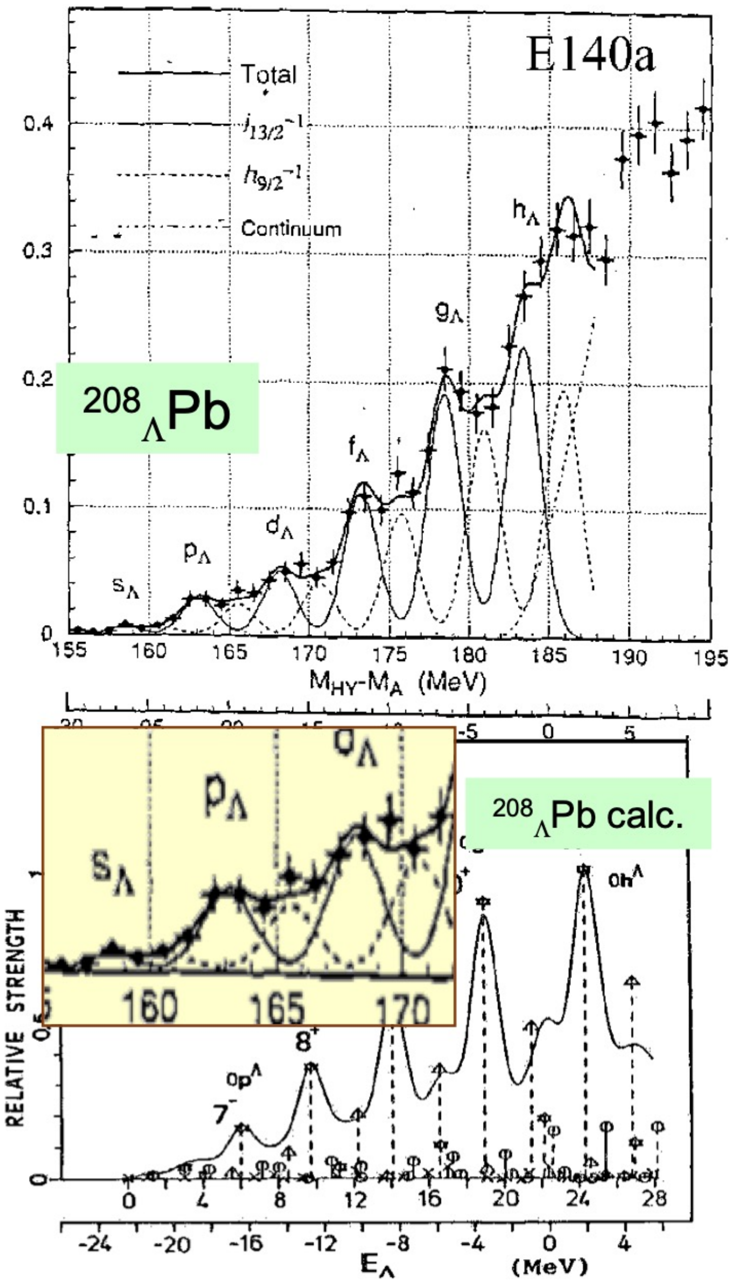

Λ's $\hbar\omega$ ~ 4MeV for $^{208}{}_\Lambda Pb$

Spacing of hole states (n orbit) ≳ 300 keV

=> a few 100 keV (FWHM) resolution is necessary to decompose the hole states

In the case of $^{208}_{\Lambda}$Pb

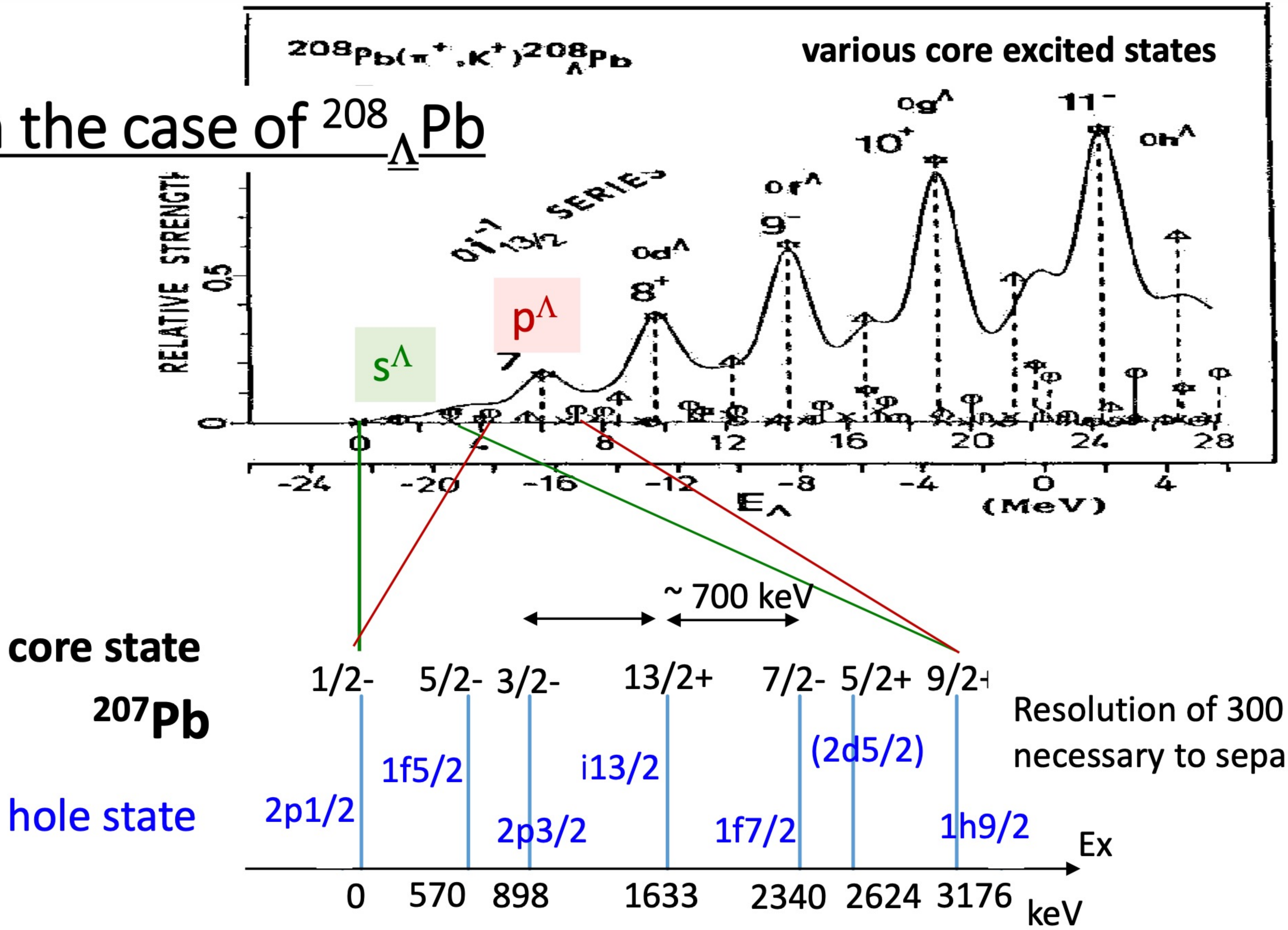

Resolution of 300 keV (FWHM) is necessary to separate the peaks.

HIHR/K1.1 strategy

Extend J-PARC Physics Capability

<u>Our strategy at J-PARC</u>

Go forward physics programs of S=-2 hypernuclei and Kaonic nuclei at existing beam lines

We need new beam lines for S=-1 physics

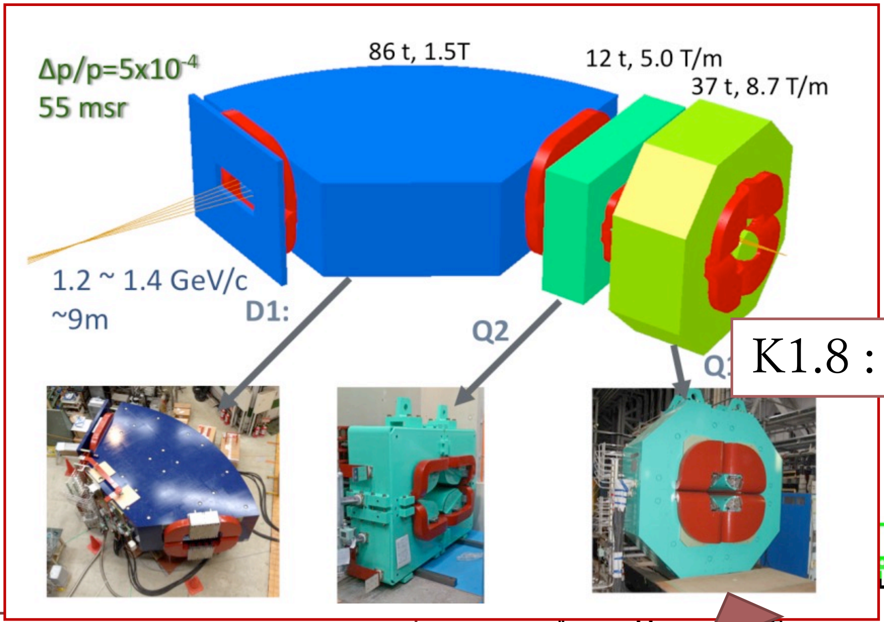

K1.8 : S=-2 physics

K1.8 BR : Kaon in nuclei

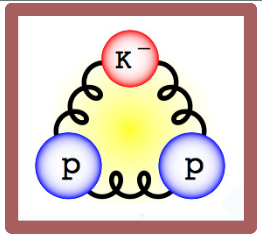

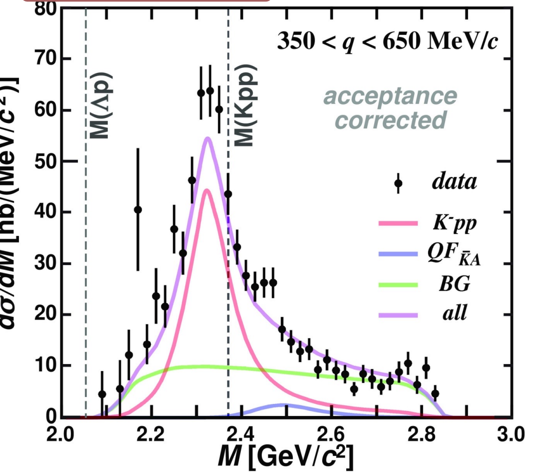

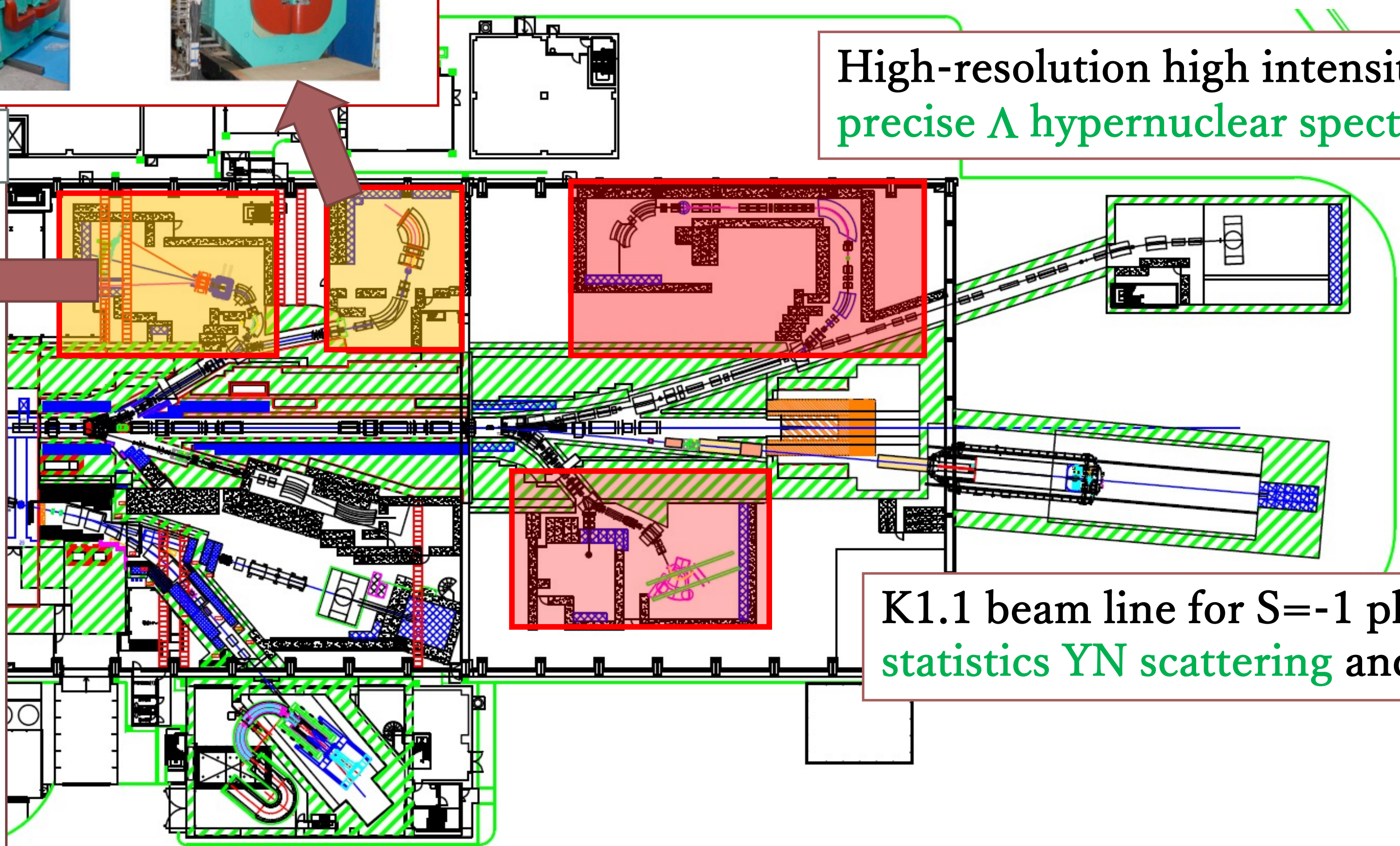

High-resolution high intensity beam line for precise Λ hypernuclear spectroscopy

K1.1 beam line for S=-1 physics for high statistics YN scattering and S=-1 physics

HIHR/K1.1 physics (microscopic understanding of NS matter)

<u>Hyperon puzzle in neutron star</u>

Softening of EOS w/ hyperon appearance

How can massive NS be supported ?

Understanding of 3Baryon Force (3BF) including hyperon is essential

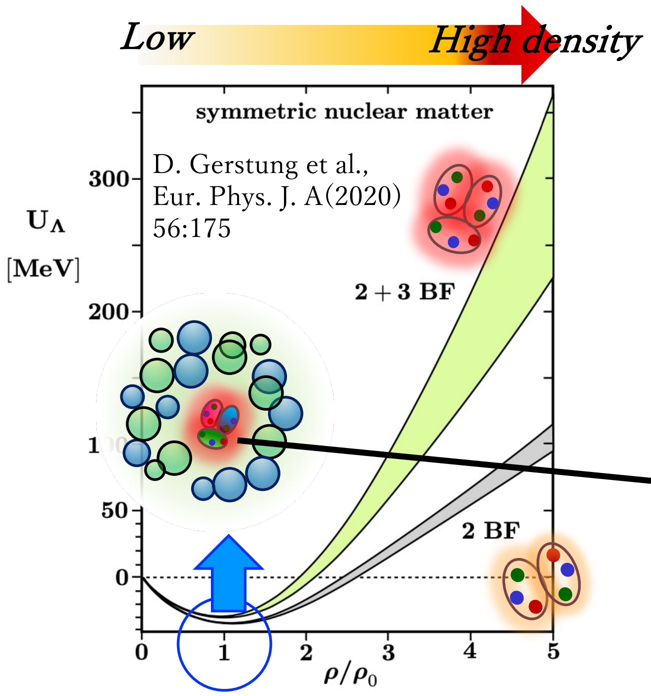

<u>ΛNN (3BF) effect in Λ hypernucleus should be measured</u>

- Realistic ΛN interaction based on Λp scattering experiment

→ K1.1 beam line : maximum Λ production cross section

<u>dσ/dΩ and Spin observables (100 times better statistics)</u>

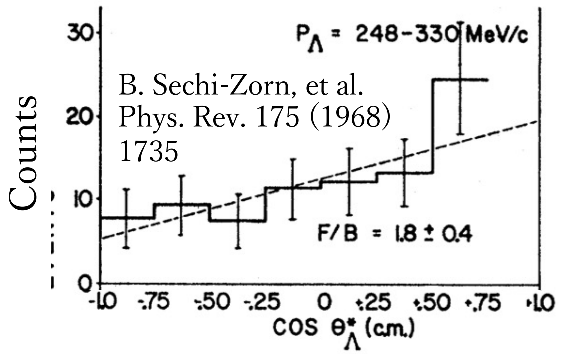

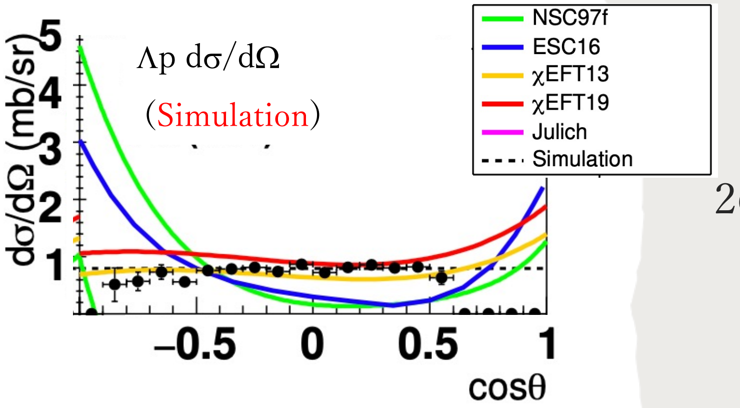

Essential input to establish realistic ΛN interaction

- Investigation of ΛNN 3BF by ultra high-resolution Λ hypernuclear spectroscopy

→HIHR beam line

<u>New generation spectroscopy with momentum-dispersion matching method</u>

High-resolution Λ hypernuclear spectroscopy at HIHR

ΛNN interaction :
Key of **Hyperon Puzzle**
Small effects to Λ binding energies

HIHR : Dispersion-matching beam line
→ Realize **high-resolution** spectroscopy **without beam intensity limit**

High intensity π beam of **> 10^8 /pulse**
(**~100 times stronger** than KEK-PS)

- Thin target can be used
  → High resolution and various target options

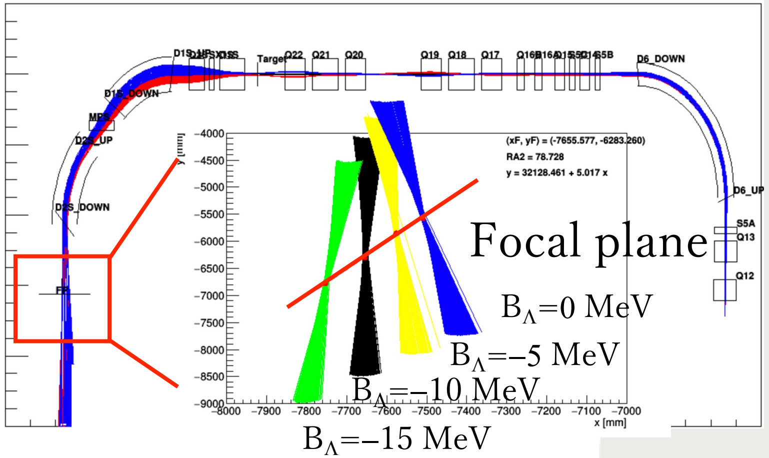

Impossible to separate peaks
with a few MeV resolution

Better than 0.4 MeV (FWHM) resolution

Clear separation of sub-major as well as major peaks

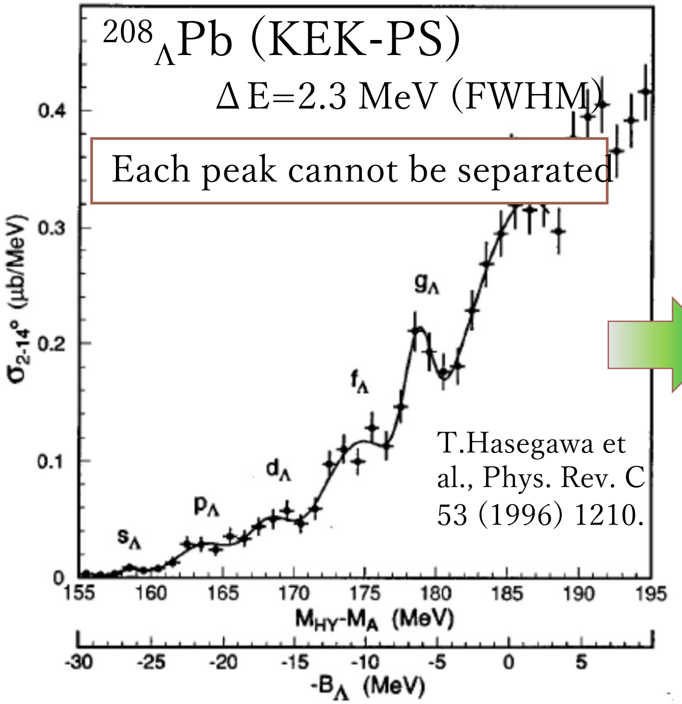

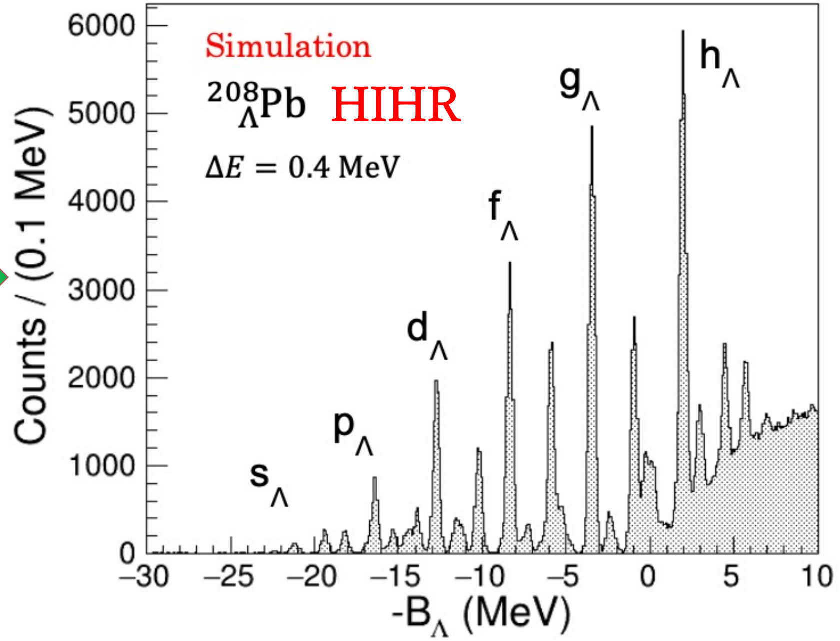

Precise Λ binding energies
for wide-mass range

Density dependence of ΛN interaction (ΛNN interaction)

Calculate U_Λ at high density region
Untangle hyperon puzzle in neutron star

Strategy of microscopic understanding of NS with strangeness

Realistic Baryon-Baryon (BB) interaction

3 Baryon Force with hyperon (3BF)

Strength of ΛN-ΣN coupling and effect in nuclear medium

- ✓ $SU(3)_f$ Boson-exchange model (Nijmegen, Julich)
- ✓ Chiral EFT
- ✓ Lattice QCD

Bridge from two-body and few-body data to BB interaction

More plenty of YN scattering data. (K1.1)
Much precise hypertriton data (Emulsion, Jlab)

Precise level structure in few-body Λ hypernuclei (HIHR)
Λd, Λα scattering (K1.1)

HIHR/K1.1 experiments will explore new data

Microscopic calculation based on realistic BB interaction

Density dependent ΛN interaction (ΛNN int.)

Much precise hypernuclear spectroscopic data for wide mass region

- Binding energy measurement w/ 300 keV resolution (HIHR)
- γ–ray measurement to assist a decomposition of high level density (K1.1)

BB interaction in medium/nuclear matter

Ab initio calculation

No Core Shell Model for hypernuclei

BHF calculation → hyperon's single particle potential in neutron star matter.
EOS with hyperons

Astrophysical observations

Short summary of HIHR/K1.1 physics

- We propose our strategy of hypernuclear physics based on the outputs from the HIHR/K1.1 beam lines

  We are going to provide
  - ✓ high-statistics YN scattering data at K1.1 beam line
  - ✓ Ultra precise Λ hypernuclear spectroscopic data at HIHR beam line

  By collaborating with theorist, we are going to establish "realistic YN interaction"
  Extract the strength of YNN 3BF phenomenologically (or determine LEC's for 3BF) by comparing reliable many-body calculations based on the realistic YN interaction and high precision hypernulear data.

- We expect the high-density matter can be microscopically examined in NN sector and also with YN/YY sectors.

- These strategies are essential for the understanding of baryonic matter in neutron star from the microscopic picture based on nuclear physics

New proposal for J-PARC experiment

Measurement of the differential cross section and spin observables of the Λp scattering with a polarized Λ beam

ΛN interaction and its uncertainty

Comparison between experimental data and theoretical calculation of Λ hypernuclear mass (Λ binding energy) for wide mass range is important to extract the ΛNN force.

Energy spectra of $^{13}_{\Lambda}$C, $^{16}_{\Lambda}$O, $^{28}_{\Lambda}$Si, $^{51}_{\Lambda}$V, $^{89}_{\Lambda}$Y, $^{139}_{\Lambda}$La, $^{208}_{\Lambda}$Pb with ESC16 model

M.M. Nagels et al. Phys. Rev. C99, 044003 (2019)

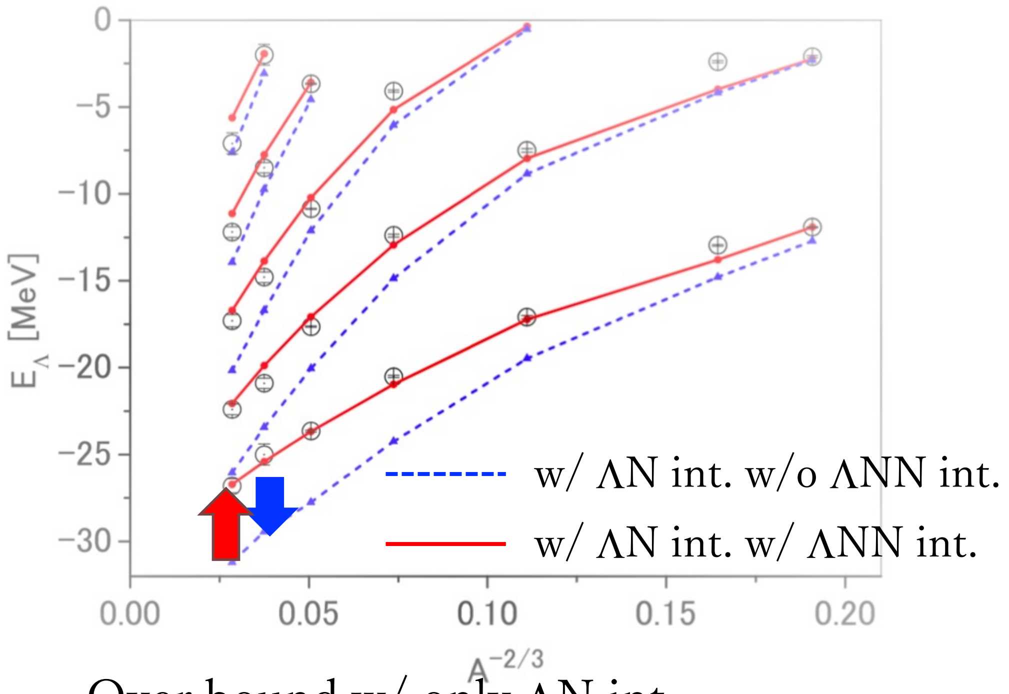

Over bound w/ only ΛN int.

ΛNN repulsive interaction is necessary to explain Λ hypernuclear bounding energy

Choice of two-body ΛN interaction has large effect of theoretical calculation

M. Isaka et al., Phys. Rev. C 95, 044308 (2017)

Calculation with only two-body interaction of different ESC versions

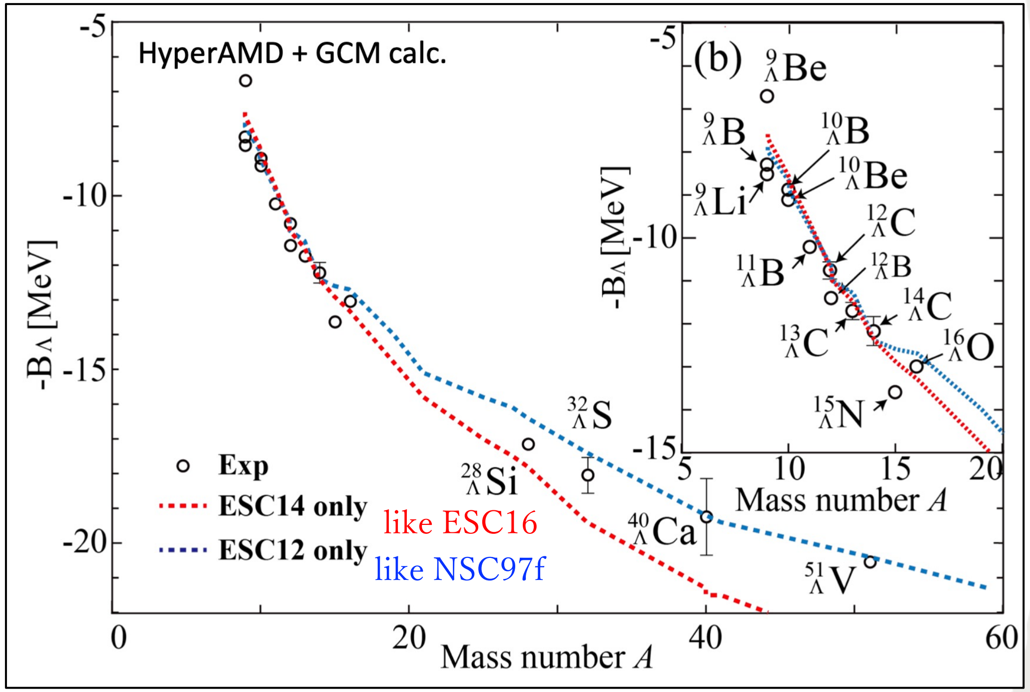

ESC12 can explain $-B_\Lambda$ w/o ΛNN repulsive int.

ESC14 need ΛNN repulsive int.

ΛN interaction and its uncertainty

M. Isaka et al., Phys. Rev. C 95, 044308 (2017)

Large uncertainty of P-wave potential

Calculation with only two-body interaction of different ESC versions

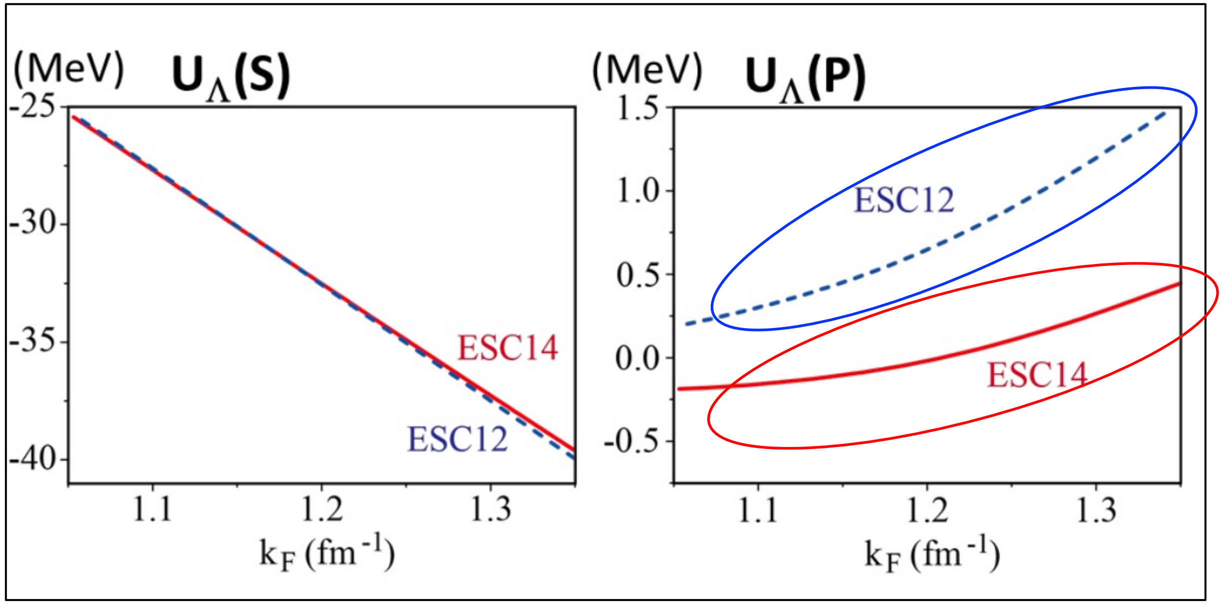

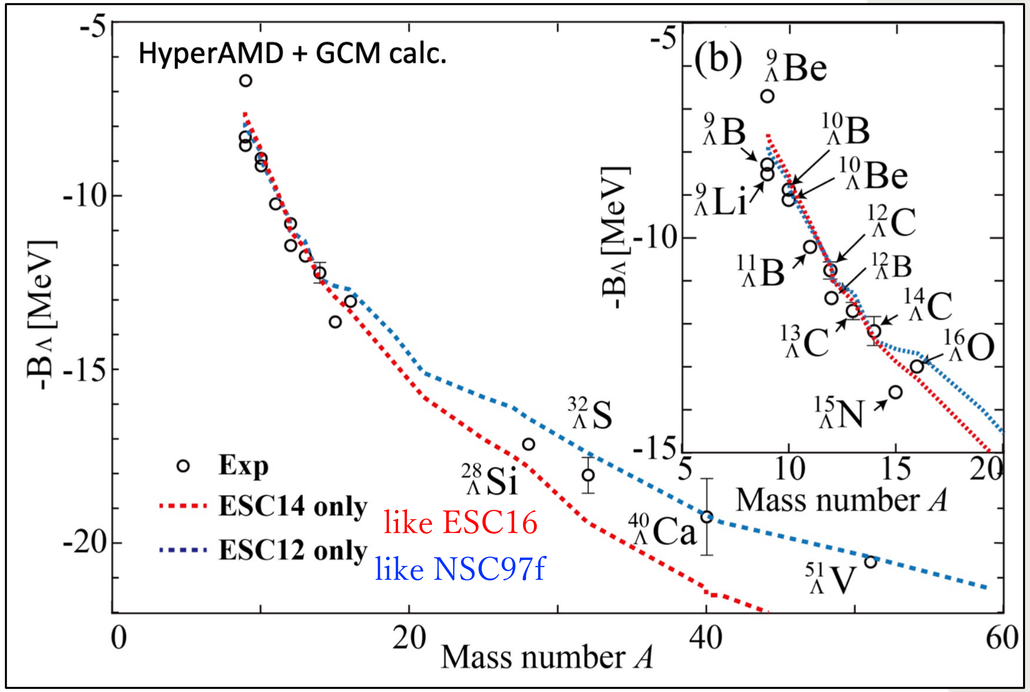

ESC12 : more repulsive in P-wave potential

→ Experimental Λ binding energy can be reproduced with only two-body ΛN interaction

ESC14 : moderately repulsive in P-wave potential

→ Λ binding energy with only two-body ΛN interaction is too large.
ΛNN repulsive force is necessary to reproduce experimental binding energy

Difference in P-wave contribution should appear as different angular distribution in dσ/dΩ of Λp scattering

ΛN interaction and its uncertainty

Paper of chiral EFT J. Haidenbauer et al. Eur. Phys. J. A. (2020) 56:91

allow one to pin down the interaction in the $S = -1$ sector. It should be emphasized that the aspects discussed above apply only to the interaction in the S waves. Since there are practically no data for differential observables, it is impossible to fix the YN contact terms in the P-waves. In this case, imple-

Total cross section data exist for Λp scattering.
But no differential cross section data.

Total cross section might be similar for each model.

However, there are large uncertainty in the P-wave interaction.

(1) ESC16 (Nijmegen)

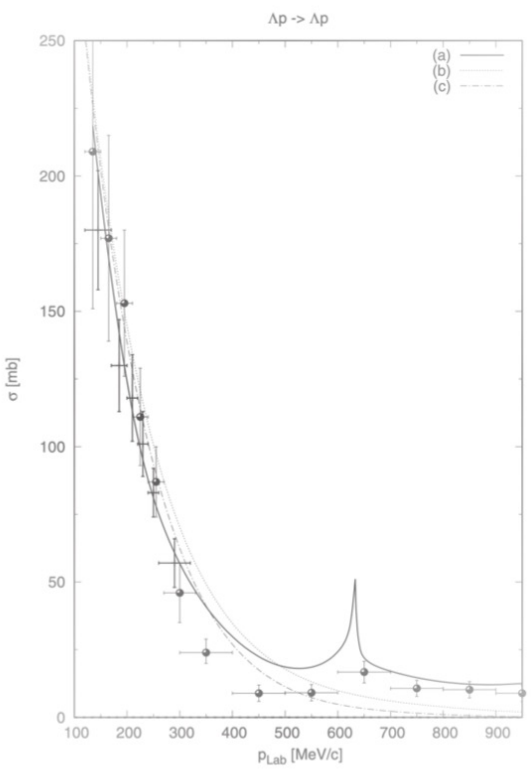

(2) Chiral EFT

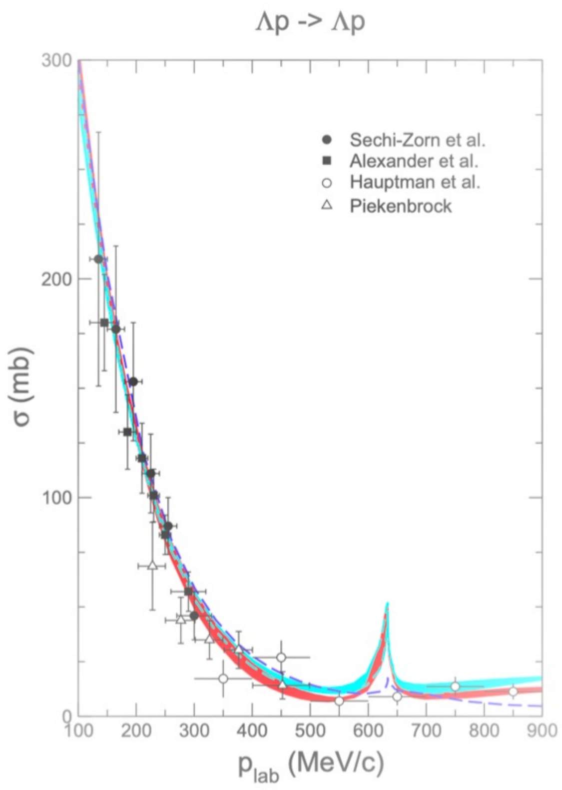

ΛN Differential information at ΣN threshold

NSC97f
Julich 04
Chiral EFT(NLO13)
Chiral EFT(NLO19)

Differential cross section

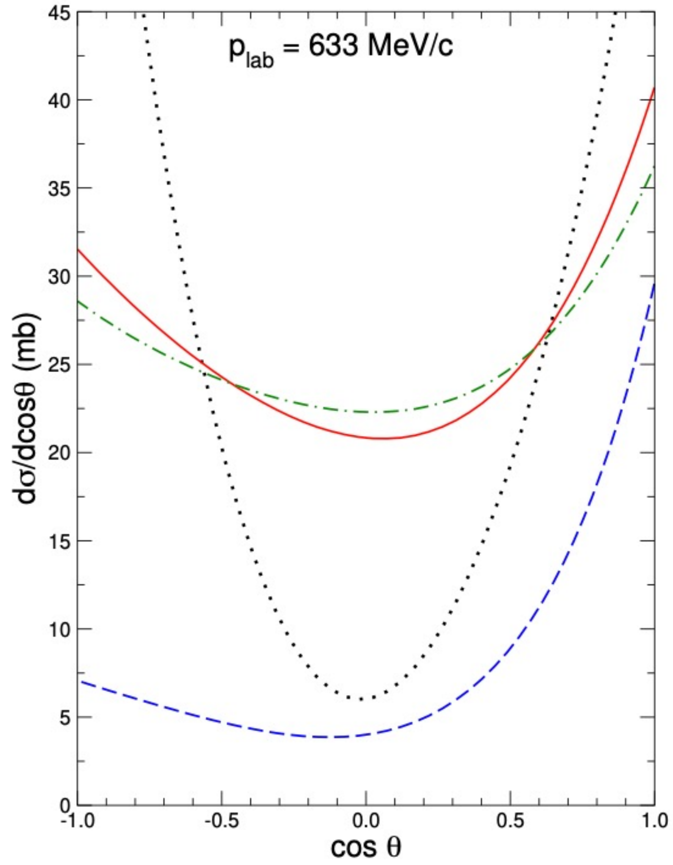

Polarization (Λ)

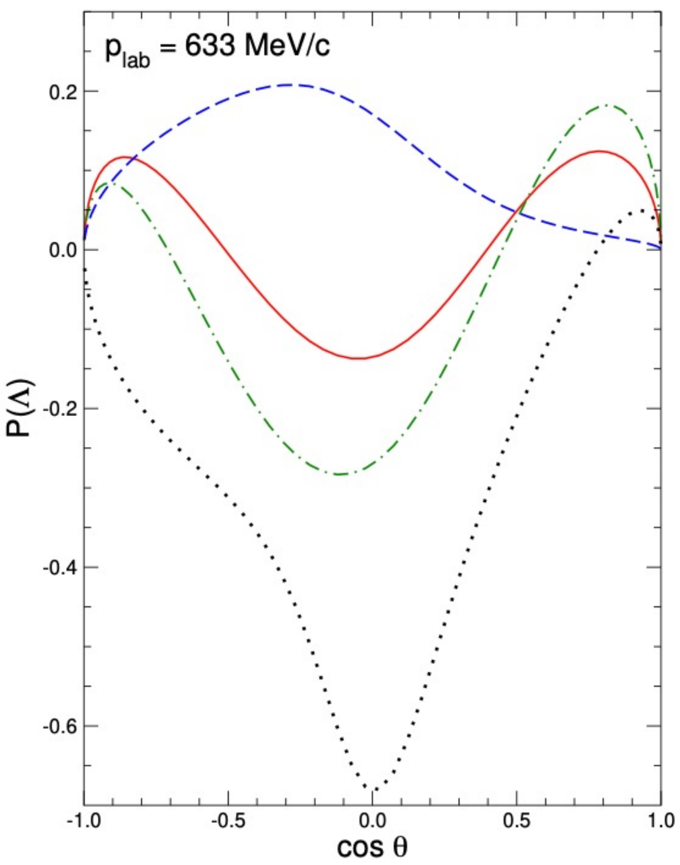

Depolarization (D_{NN})

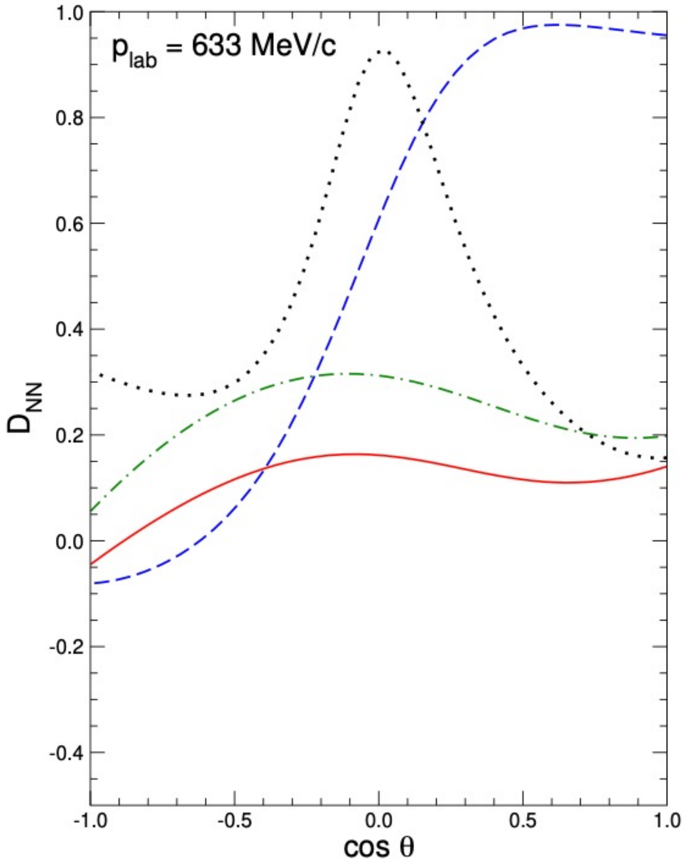

J. Haidenbauer, U.G. Meißner arXiv:2105.00836

Such difference clearly appears in differential observables !
We should measure these differential cross sections and spin observables to constrain theoretical model significantly.

Conventional representation of elastic scattering

From S. Ishikawa et al.
PRC 69, 034001 (2004)

Scattering amplitude in $\frac{\vec{1}}{2}+\frac{\vec{1}}{2}\rightarrow\frac{\vec{1}}{2}+\frac{\vec{1}}{2}$ scattering : → 4 x 4 matrix

→ 6 components from the restriction of parity conservation and time-reversal invariance

spin-independent spin-spin symmetric LS (ΔS=0) anti-symmetric LS (ΔS=1) Tensor

T matrix

$$\boldsymbol{M} = V_c + V_\sigma(\boldsymbol{s}_a\cdot\boldsymbol{s}_b) + V_{SLS}(\boldsymbol{s}_a+\boldsymbol{s}_b)\cdot\boldsymbol{L} + V_{ALS}(\boldsymbol{s}_a-\boldsymbol{s}_b)\cdot\boldsymbol{L} + V_T([\boldsymbol{s}_a\otimes\boldsymbol{s}_b]^{(2)}\cdot\boldsymbol{Y}_2(\hat{\boldsymbol{r}})),$$

Scalar amplitude

$U_\alpha \equiv < \boldsymbol{k}_f|V_c|\boldsymbol{k}_i >, U_\beta \equiv < \boldsymbol{k}_f|V_\sigma|\boldsymbol{k}_i >$

Vector amplitude

$S_{ALS} \equiv < \boldsymbol{k}_f|V_{ALS}L_1|\boldsymbol{k}_i >, S_{ALS} \equiv < \boldsymbol{k}_f|V_{SLS}L_1|\boldsymbol{k}_i >$

Tensor amplitude

$T_j = \frac{1}{2} < \boldsymbol{k}_f|V_T Y_{2j-1}|\boldsymbol{k}_i >$

<u>We are going to measure following observables.</u>

Differential cross section

$$\left(\frac{d\sigma}{d\Omega}\right) = \frac{1}{4}\mathrm{Tr}(MM^\dagger) = |U_\alpha|^2 + \frac{3}{16}|U_\beta|^2 + \frac{1}{2}(|S_{SLS}|^2+|S_{ALS}|^2) + \frac{1}{4}|T_1|^2 + \frac{1}{2}(|T_2|^2+|T_3|^2).$$

Analyzing power (Polarization)

$$A_y(Y) = -\frac{1}{\sqrt{2}\sigma(\theta)}\mathrm{Im}\left\{(U_\alpha+\frac{1}{4}U_\beta)^*S_{SLS} + (U_\alpha-\frac{1}{4}U_\beta)^*S_{ALS} - \frac{1}{2}T_\alpha^*(-S_{ALS}+S_{SLS})\right\},$$

Depolarization

$$D_y^y = \frac{1}{\sigma(\theta)}\mathrm{Re}\left\{\frac{1}{2\sqrt{3}}\left(U_0+\frac{1}{\sqrt{3}}U_1\right)^* U_1 + \frac{1}{2}\left(U_0-\frac{1}{\sqrt{3}}U_1\right)^*\left(\frac{1}{\sqrt{6}}T_1+T_3\right) - S_1^*S_2 + \frac{1}{2}|S_3|^2 - \frac{1}{\sqrt{6}}T_1^*\left(\frac{1}{\sqrt{6}}T_1-T_3\right) - \frac{1}{2}|T_2|^2\right\}.$$

Number of observables is still limited to determine each component separately.
But measurements of many observables contribute to impose constraints on YN theoretical models.

Conventional representation of elastic scattering

Analyzing power

Left/Right asymmetry of Λp scattering

Left scattered event

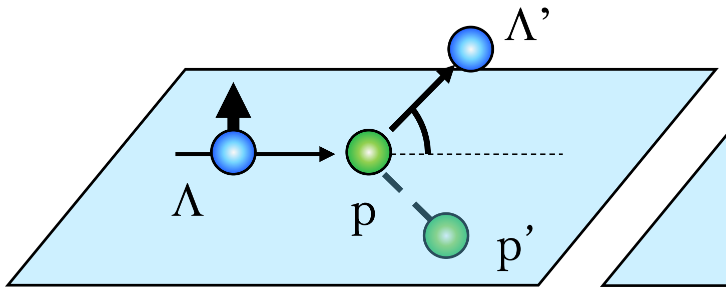

Right scattered event

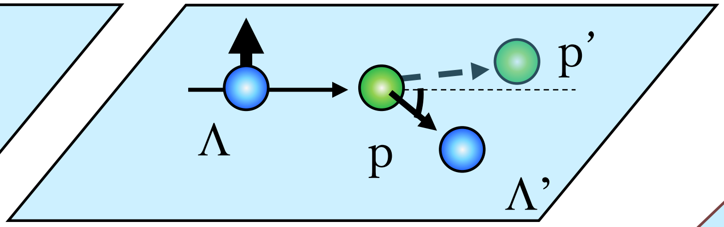

Depolarization ($D_y^{\,y}$)

Change the spin polarization after the Λp scattering

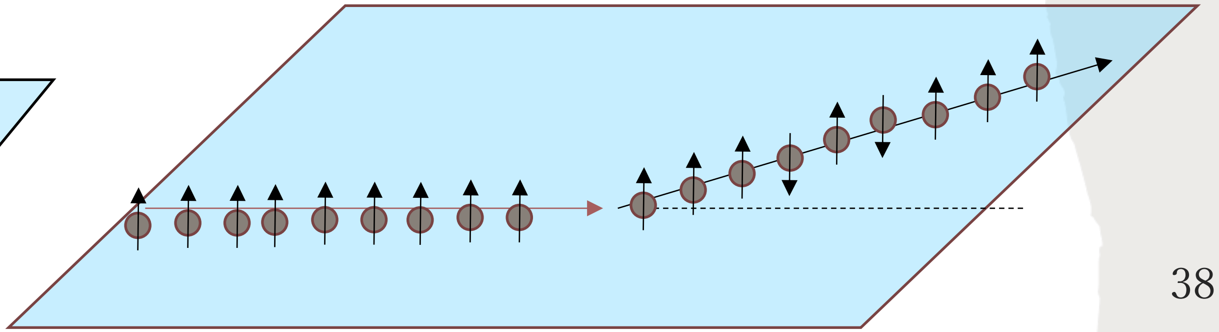

We are going to measure following observables.

Differential cross section

$$\left(\frac{d\sigma}{d\Omega}\right) = \frac{1}{4}\mathrm{Tr}(MM^{\dagger}) = |U_{\alpha}|^2 + \frac{3}{16}|U_{\beta}|^2 + \frac{1}{2}(|S_{SLS}|^2 + |S_{ALS}|^2) + \frac{1}{4}|T_1|^2 + \frac{1}{2}(|T_2|^2 + |T_3|^2).$$

Analyzing power (Polarization)

$$A_y(Y) = -\frac{1}{\sqrt{2}\sigma(\theta)}\mathrm{Im}\left\{(U_{\alpha} + \frac{1}{4}U_{\beta})^{*}S_{SLS} + (U_{\alpha} - \frac{1}{4}U_{\beta})^{*}S_{ALS} - \frac{1}{2}T_{\alpha}^{*}(-S_{ALS} + S_{SLS})\right\},$$

Depolarization

$$D_y^y = \frac{1}{\sigma(\theta)}\mathrm{Re}\left\{\frac{1}{2\sqrt{3}}\left(U_0 + \frac{1}{\sqrt{3}}U_1\right)^{*}U_1 + \frac{1}{2}\left(U_0 - \frac{1}{\sqrt{3}}U_1\right)^{*}\left(\frac{1}{\sqrt{6}}T_1 + T_3\right) - S_1^{*}S_2 + \frac{1}{2}|S_3|^2 - \frac{1}{\sqrt{6}}T_1^{*}\left(\frac{1}{\sqrt{6}}T_1 - T_3\right) - \frac{1}{2}|T_2|^2\right\}.$$

Number of observables is still limited to determine each component separately.
But many observables contribute to impose constraints on YN theoretical models.

New project: Λp scattering experiment at K1.1 beam line with polarized Λ beam

Proposal for an experiment at the 50-GeV PS

Measurement of the differential cross section and spin observables of the Λp scattering with a polarized Λ beam

K. Miwa(spokesperson), S. H. Hayakawa, Y. Ishikawa, K. Itabashi, K. Kamada, T. Kitaoka, T. Morino, S. Nagao, S. N. Nakamura, F. Oura, T. Sakao, H. Tamura, H. Umetsu, S. Wada
Tohoku University, Japan

M. Fujita, Y. Ichikawa, T. O. Yamamoto
Japan Atomic Energy Agency (JAEA), Japan

R. Honda, M. Ieiri, T. Takahashi, M. Ukai
High Energy Accelerator Research Organization (KEK), Japan

T. Nanamura
Kyoto University, Japan

K. Shirotori
Research Center for Nuclear Physics (RCNP), Osaka University, Japan

P. Evtoukhovitch
Joint Institute for Nuclear Research (JINR), Russia

Z. Tsamalaidze
Joint Institute for Nuclear Research (JINR), Russia
Georgian Technical University (GTU), Tbilisi, Georgia

K1.1 beam line at extended hadron hall

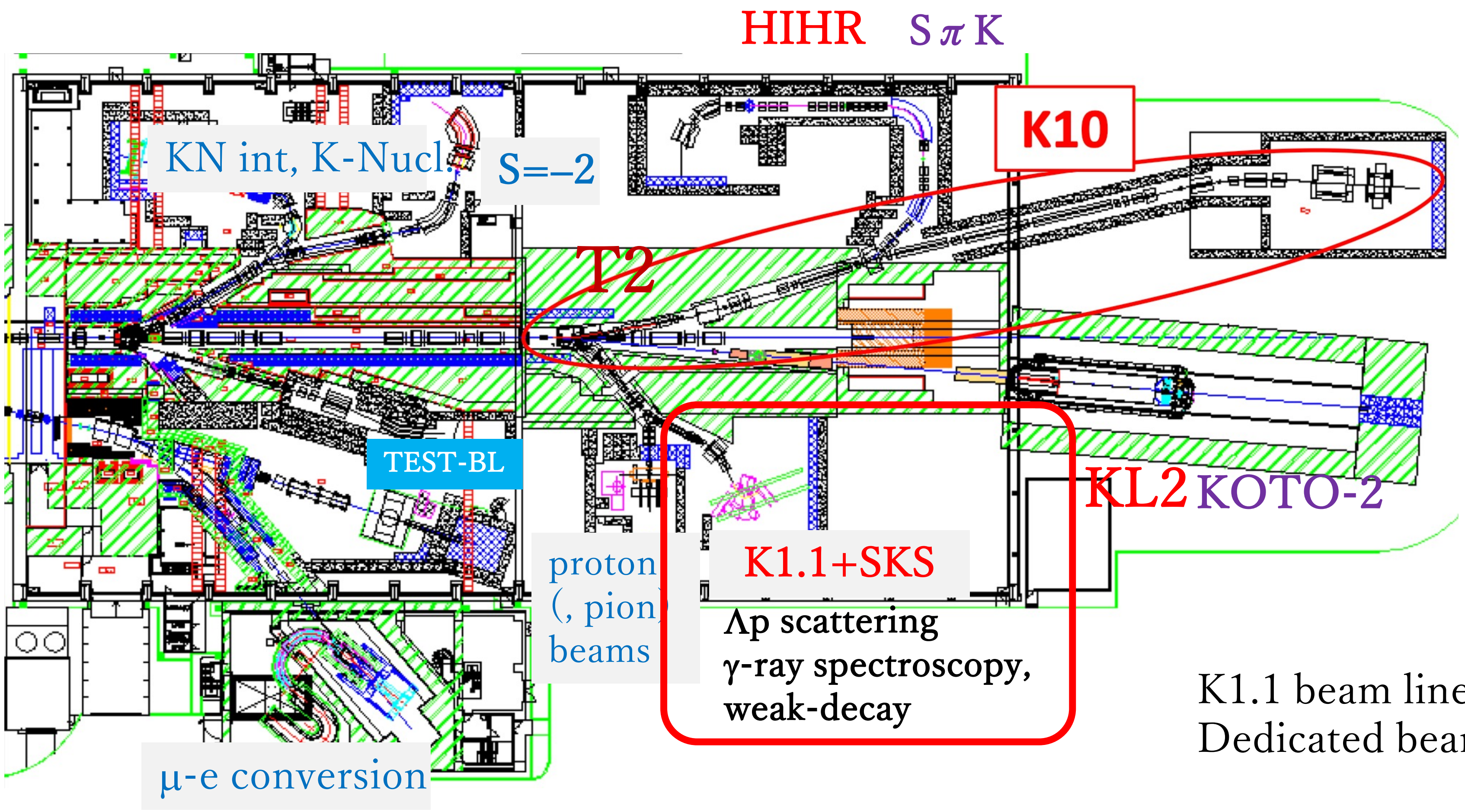

K1.1 beam line :
Dedicated beam line for S=-1 physics

Pmax = 1.2 GeV/c
Two stages of Elec. Separator

Advantage of Λ production at 1.05 GeV/c

Maximum Λ production cross section

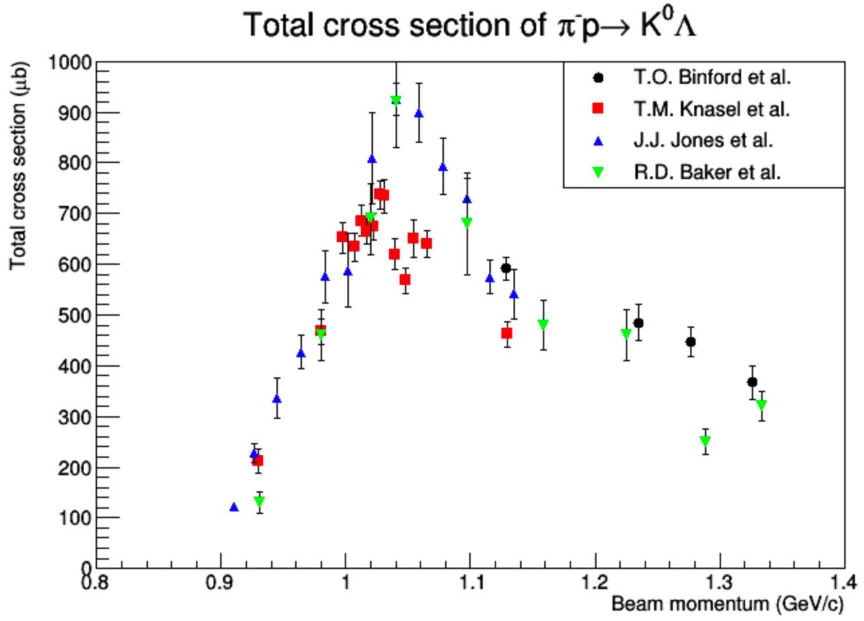

High spin polarization of Λ for Λ production plane

R.D. Baker et al. , Nucl. Phys. B141 (1978) 29

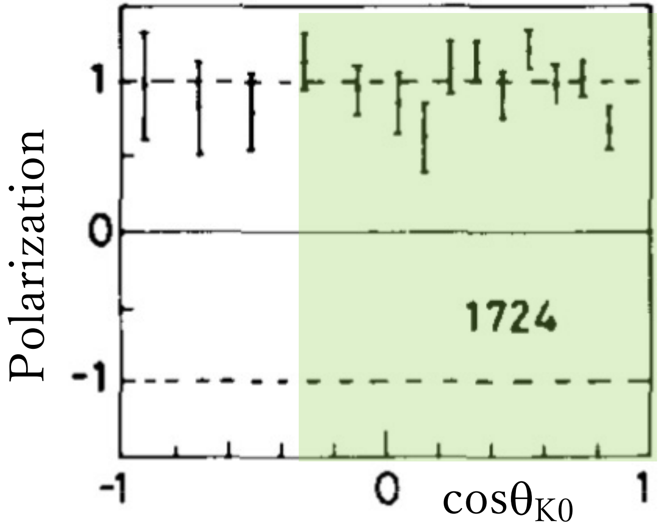

Angular distribution of decay proton

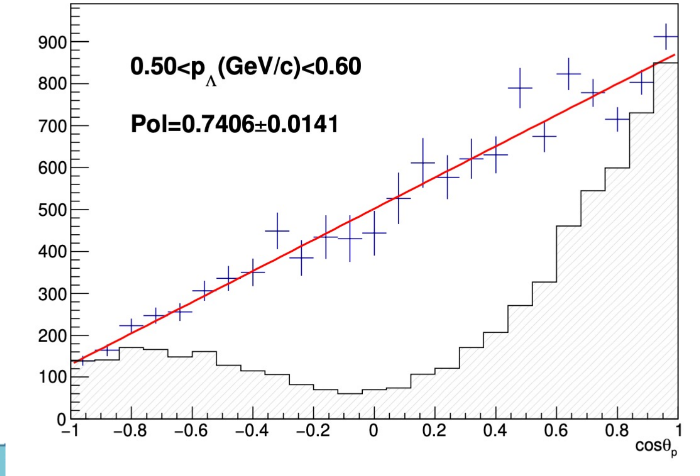

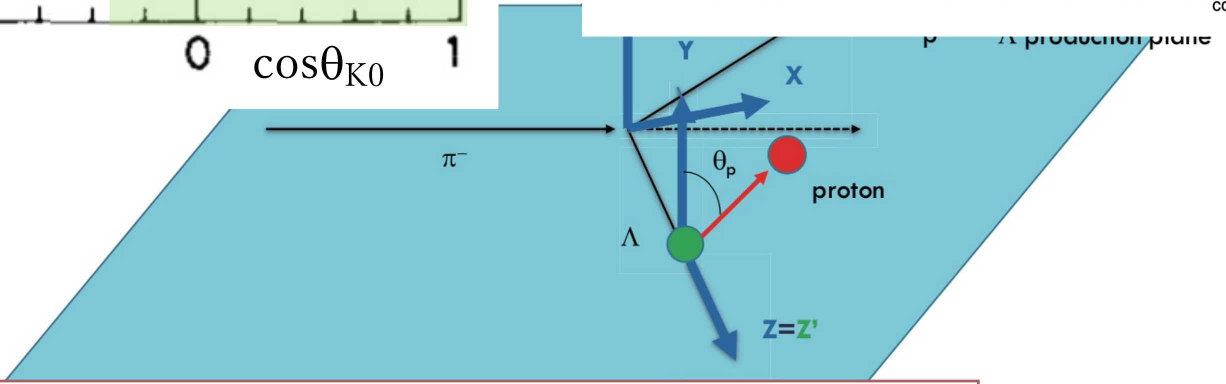

- ✓ By using 30 M/spill π^- beam, 1.72 M Λ beam can be tagged in one day
- ✓ Λ beam is automatically polarized with ~100% level
- ✓ Λ beam polarization can be measured from angular dependence of decay proton

Λp scattering experiment at K1.1 beam line

Λ beam identification

Tagged by $\pi^- p \rightarrow K^0\Lambda$ reaction at p=1.05 GeV/c

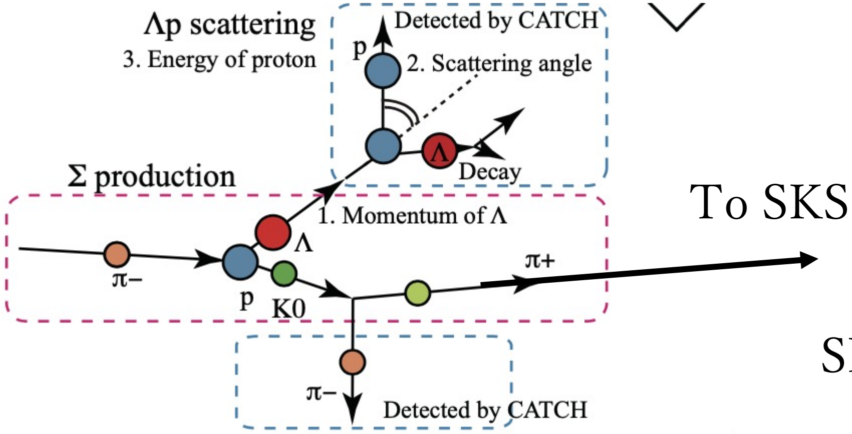

To SKS spectrometer

SKS spectrometer

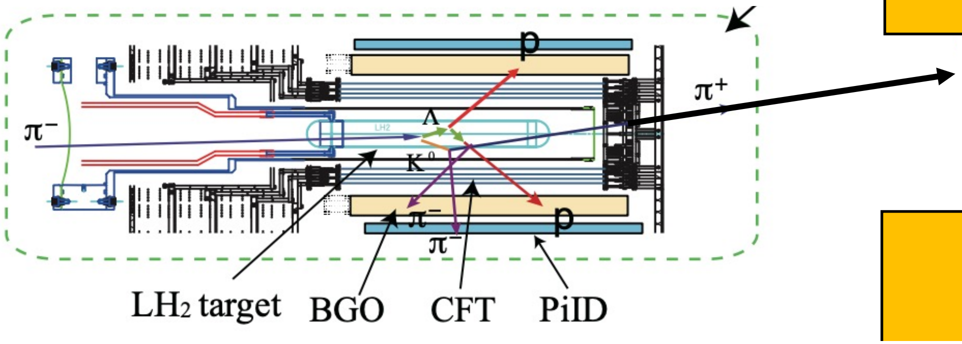

Λp scattering identification

Detected by CATCH

Almost same setup with E40

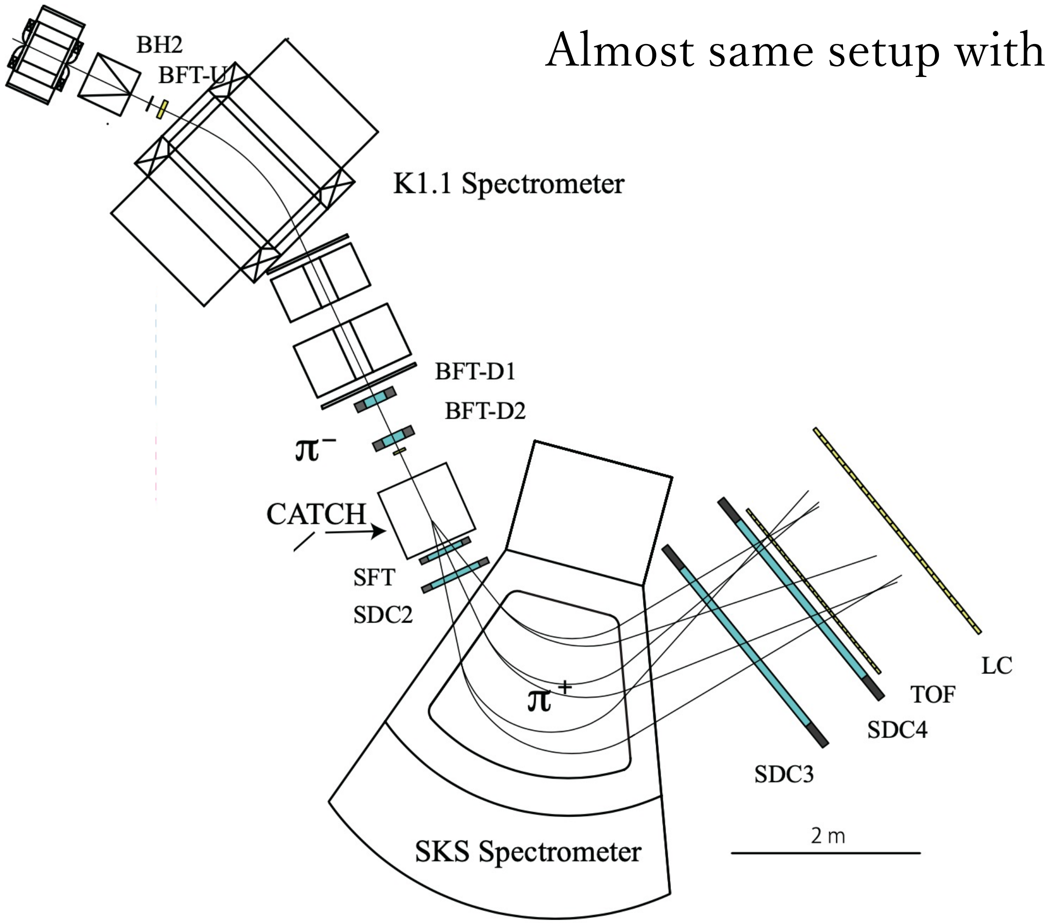

Λp scattering experiment at K1.1 beam line

Λ beam identification

Tagged by $\pi^- p \rightarrow K^0 \Lambda$ reaction at p=1.05 GeV/c

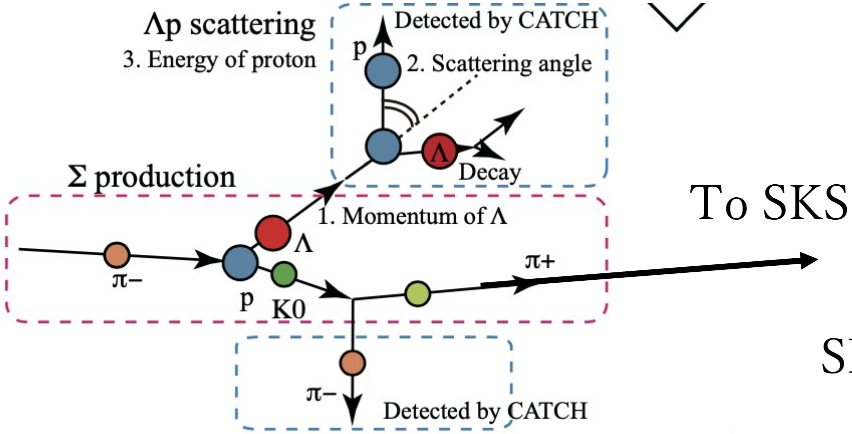

To SKS spectrometer

SKS spectrometer

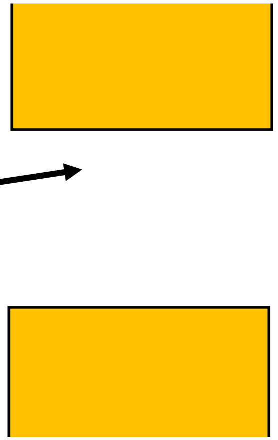

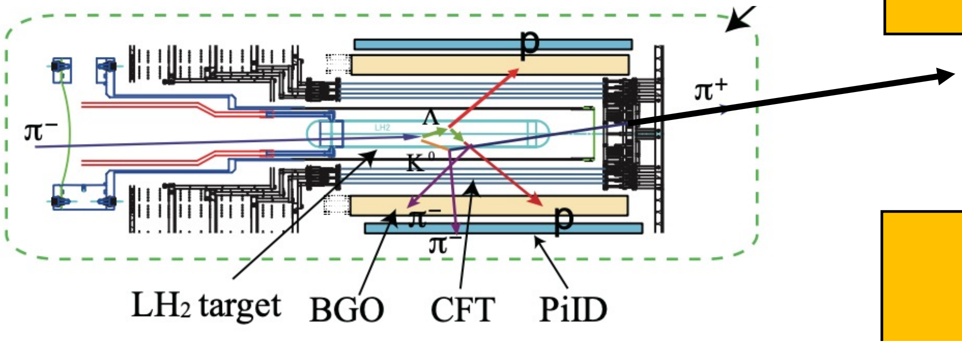

Λp scattering identification

Detected by CATCH

Momentum-tagged Λ beam

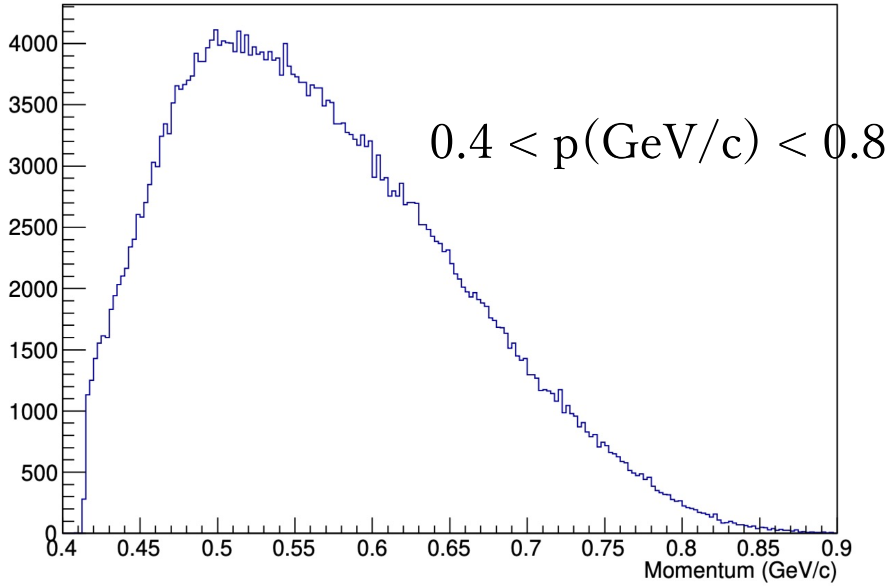

Goal of experiment

30 days production : 50 M Λ beam
→ $(d\sigma/d\Omega)_0$, $A_y(\Lambda)$

+30 days production : 100 M Λ beam in total
→ $D^y{}_y$ + ($d\sigma/d\Omega$, $A_y(\Lambda)$ w/ improved statistics)

Feasibility study in E40 (Σp scattering)

By using by-product data in E40, we already checked feasibility of Λp scattering

New K^0 identify method
π^+ : magnetic spectrometer
π^- : CATCH

We can keep large acceptance for K^0

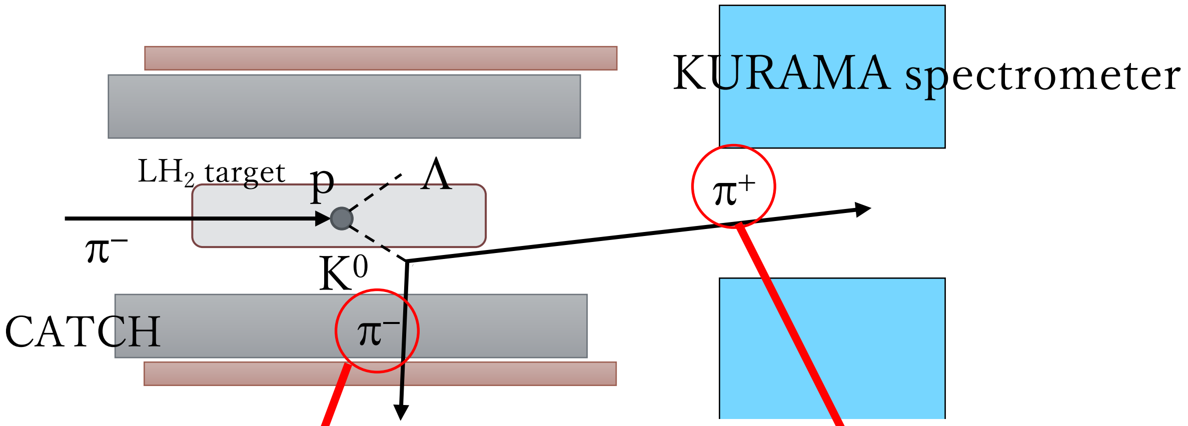

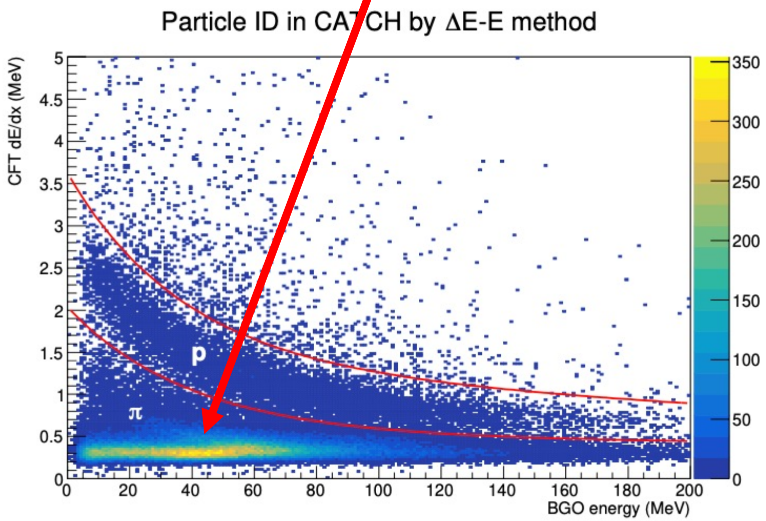

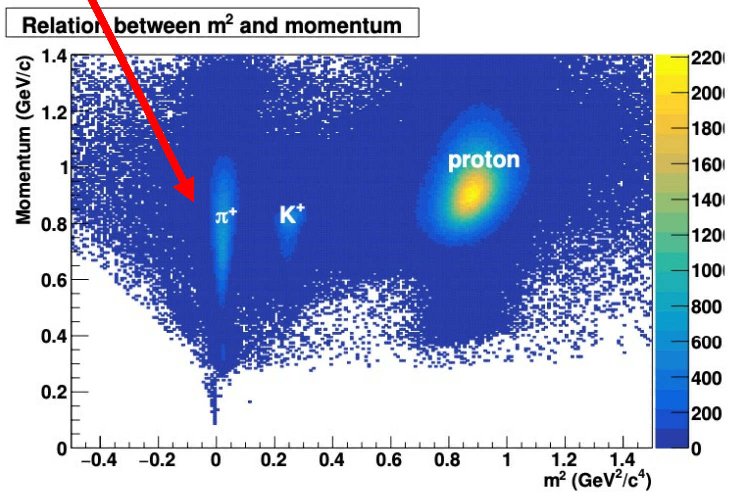

Missing mass ($\pi^- p \rightarrow K^0 X$ reaction)

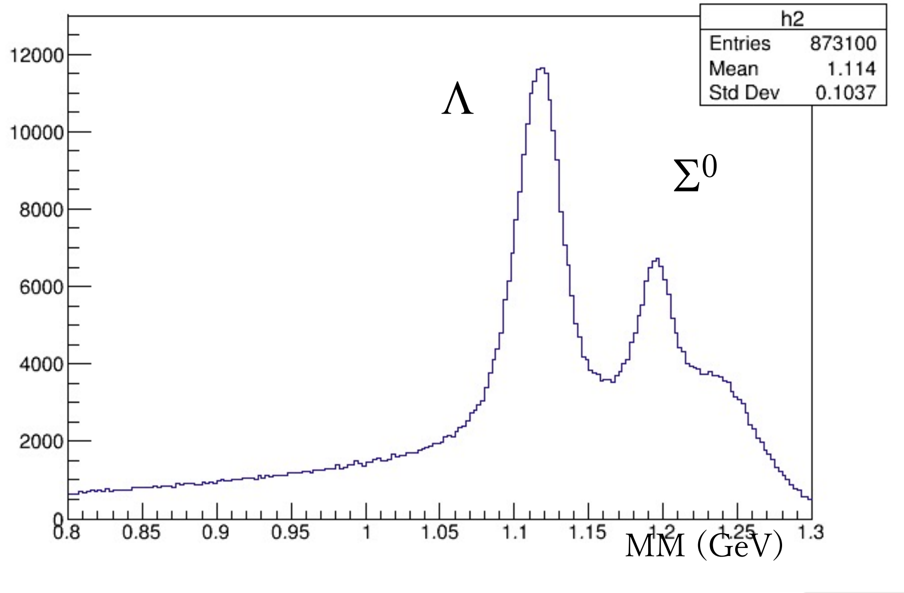

We could establish Λ production method for proton target !

Future upgrade is considered to measure π^- momentum to clean up the background

Feasibility study in E40 byproduct data (Λp scattering)

By-product data in E40
(Σ^-p scattering)

From ~250k Λ beam

Kinematical consistency
for scattered Λ

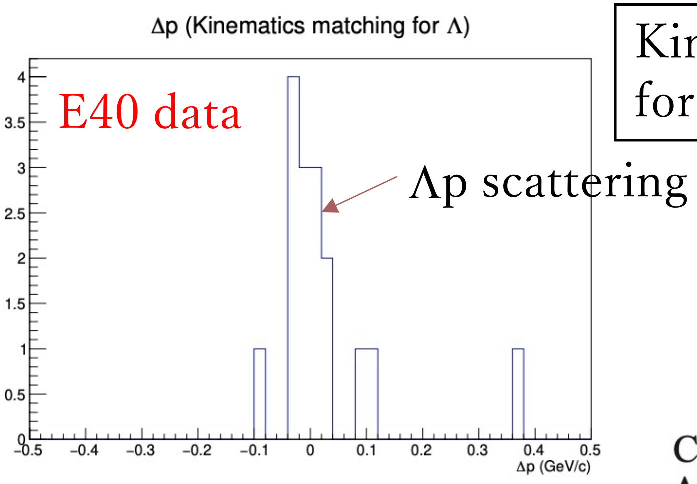

Kinematical consistency
for recoil proton

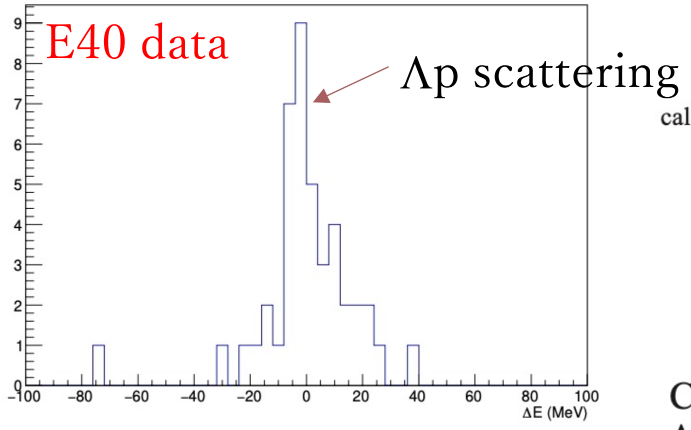

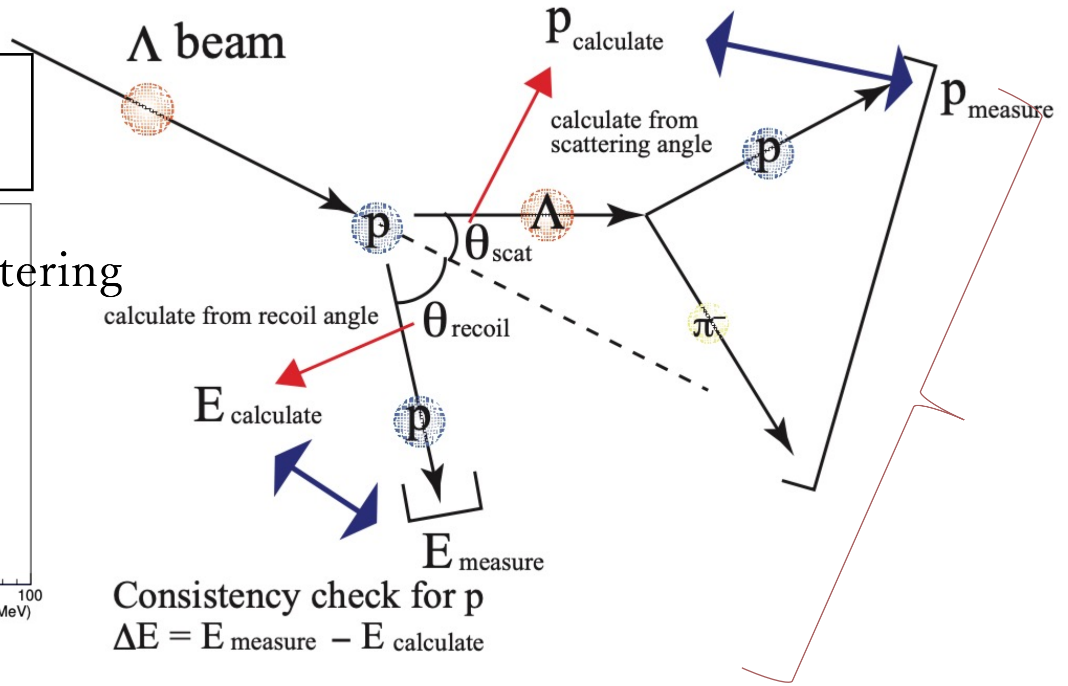

Both p and Λ are detected

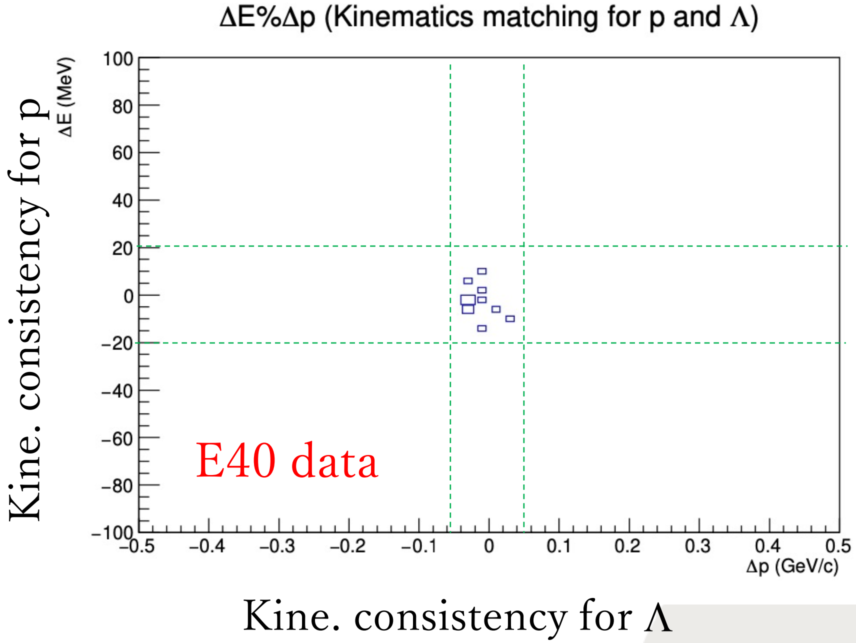

Λp scattering with polarized Λ beam

Simulated results w/ 100M Λ

To suppress B.G. in the Λ production,
we request at least 2 protons for scattering analysis

→ Angular acceptance is limited

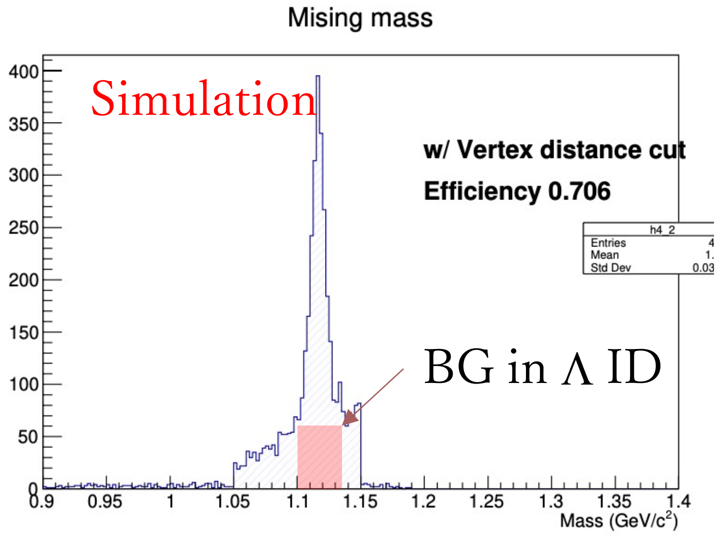

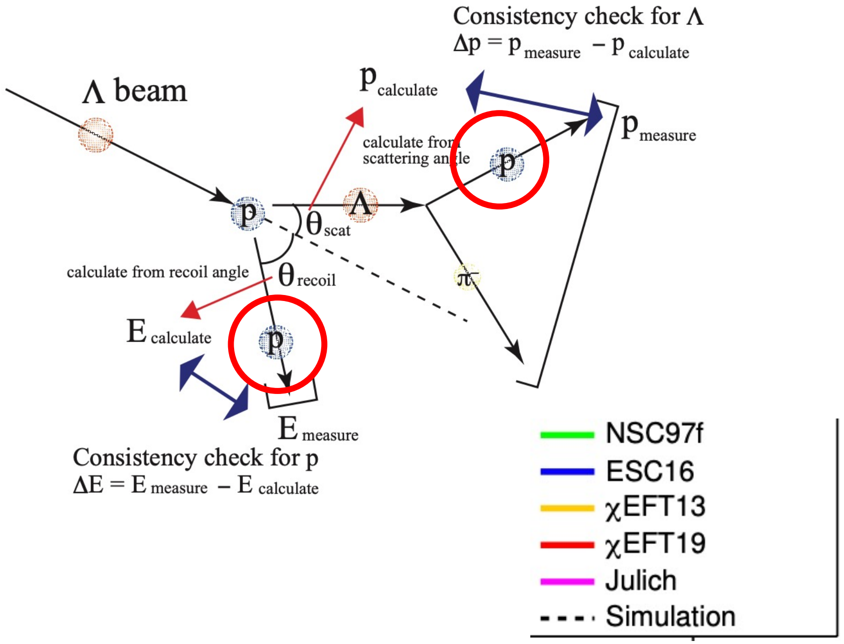

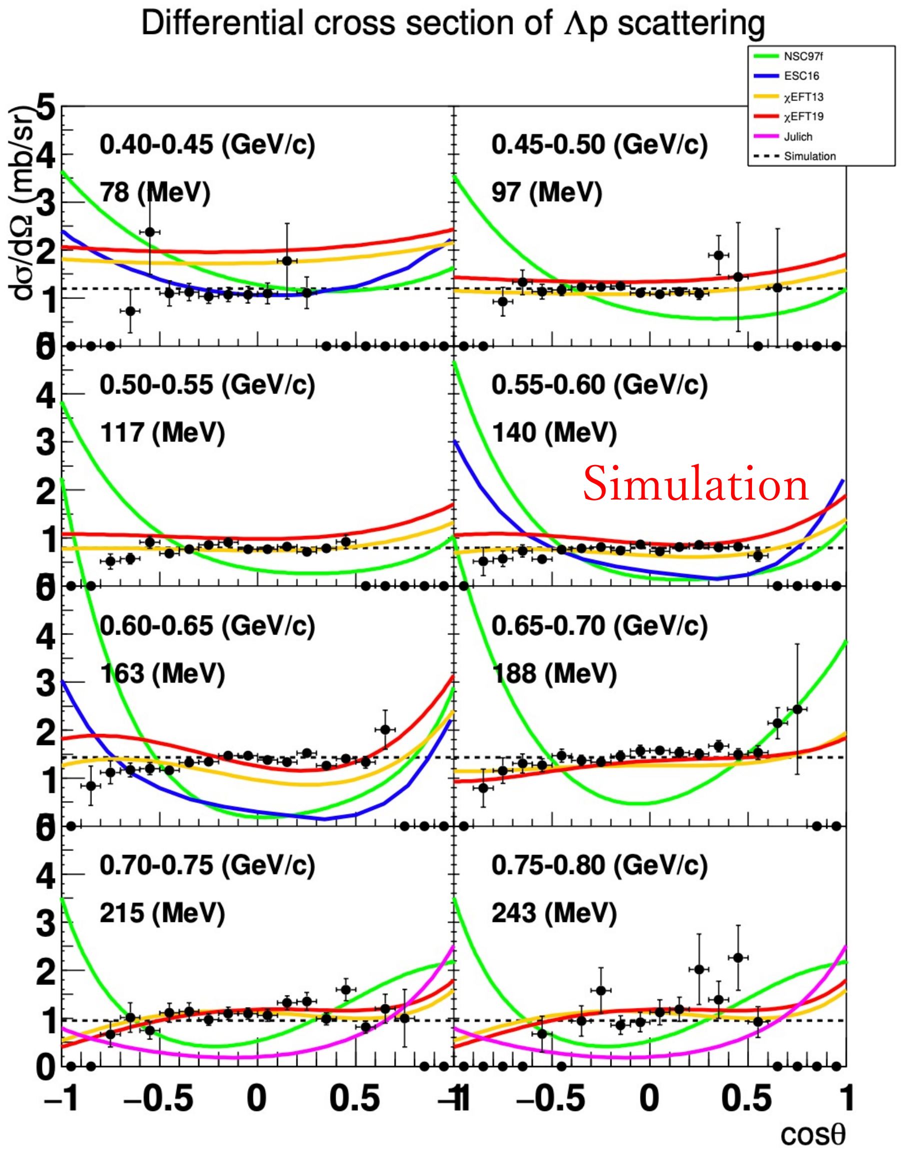

- ✓ Selection of model (chiral EFT, Nijmegen, Julich) is possible
- ✓ Selection in each model
  - ✓ NSC97f, ESC16 OK
  - ✓ ChiralEFT13, 19 OK

Simulated results w/ 100M Λ

Spin observables in Λp scattering

Analyzing power

Left scattered event Right scattered event

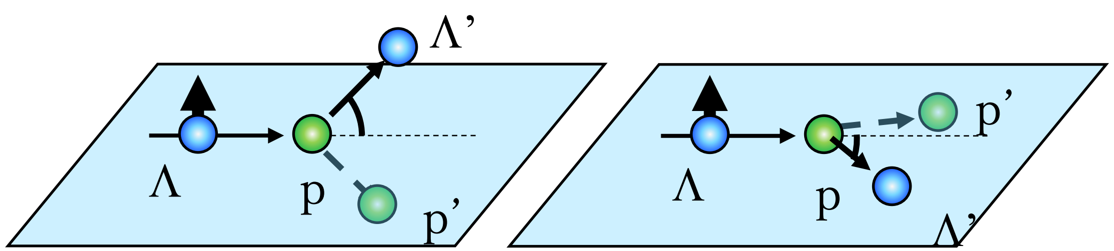

Depolarization (D_y^y)

Change the spin polarization after the Λp scattering

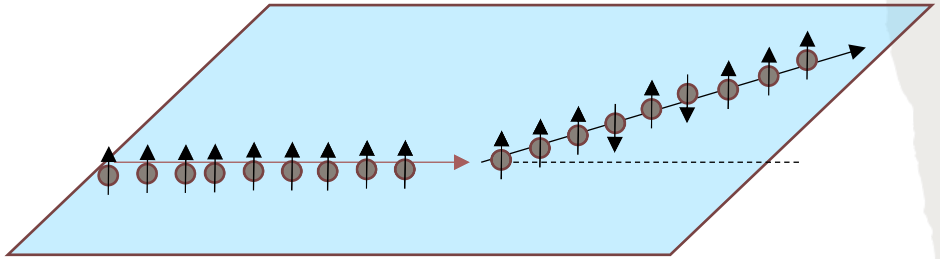

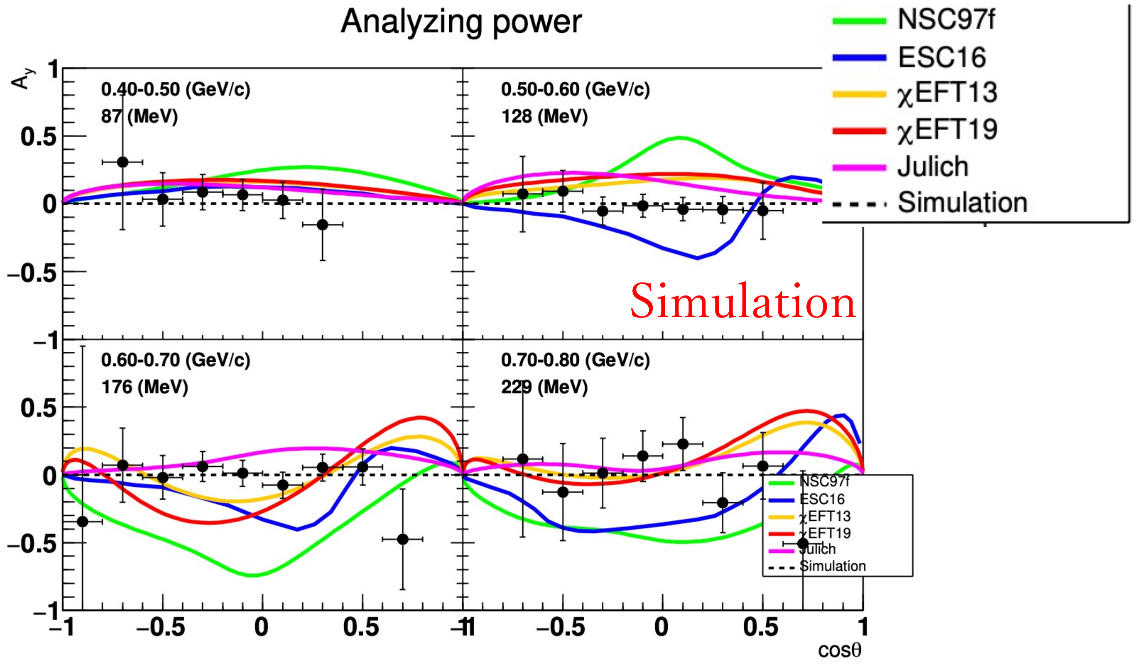

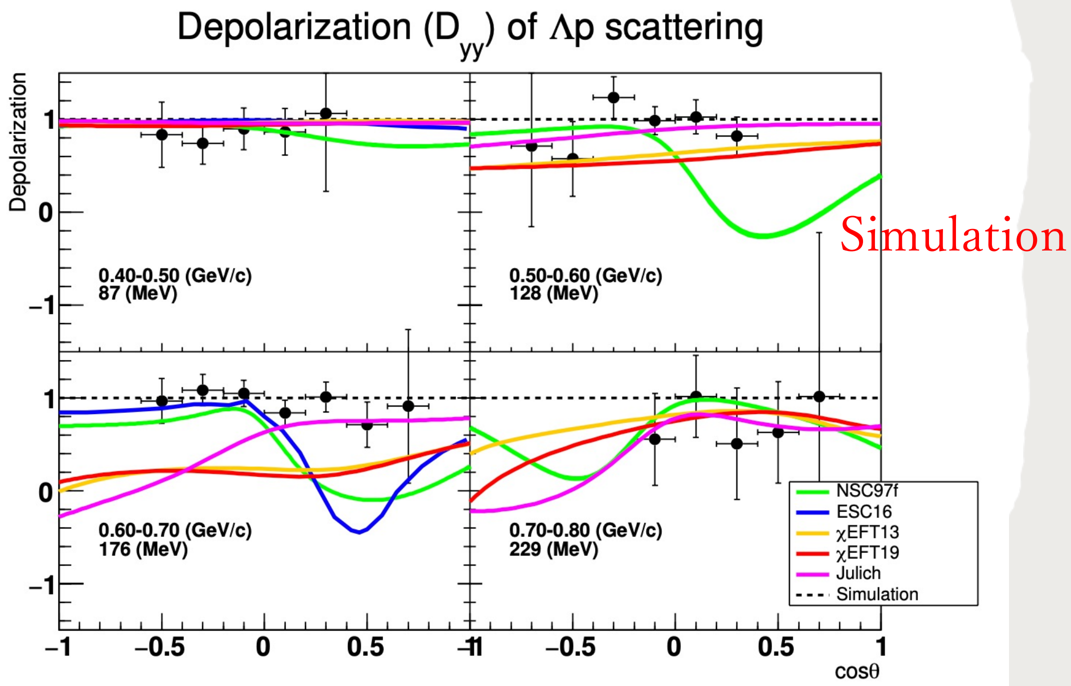

In the middle momentum range (0.5~0.7 GeV/c), 10% level accuracy can be achieved.

We believe that these new scattering data becomes important constraint to determine spin-dependent ΛN interaction

Summary of Λp scattering experiment

- BB interactions are essential ingredient to understand NS matter

  Both theoretical progresses and experimental progress ! Now is a time to make effort to establish the realistic BB interaction in collaboration with theory and experiment.

- Experimental method of YN scattering is established

  Systematic measurement of Σp scattering was performed at J-PARC

  Λp scattering experiment is also feasible.

- There are large uncertainties in the P- and higher waves in ΛN interaction

  Measurement of differential observables ($d\sigma/d\Omega$, spin observables) are important

- New project to measure $d\sigma/d\Omega$ and spin observables of Λp scattering at K1.1 beam line

  Λp scattering with ~100% polarized Λ beam

  p_Λ : 0.4 ~ 0.8 GeV/c (Threshold region of ΣN channel)

  30-days beam time : 50 M Λ beam → $d\sigma/d\Omega$ and $A_y(\Lambda)$ measurements

  +30-days beam time : total 100 M Λ beam → D_{yy} and precice $d\sigma/d\Omega$ and $A_y(\Lambda)$

Thank you for your attention

We need closer collaboration with theorists and experimentalists in the world.

Please give us your comments and suggestion in any time.

Chiral EFT

Underlying chiral symmetry in QCD

Power counting feature to improve calculation systematically by going to higher order

Multi baryon force appear naturally and automatically in a consistent implementation of the framework

YN interaction at NLO

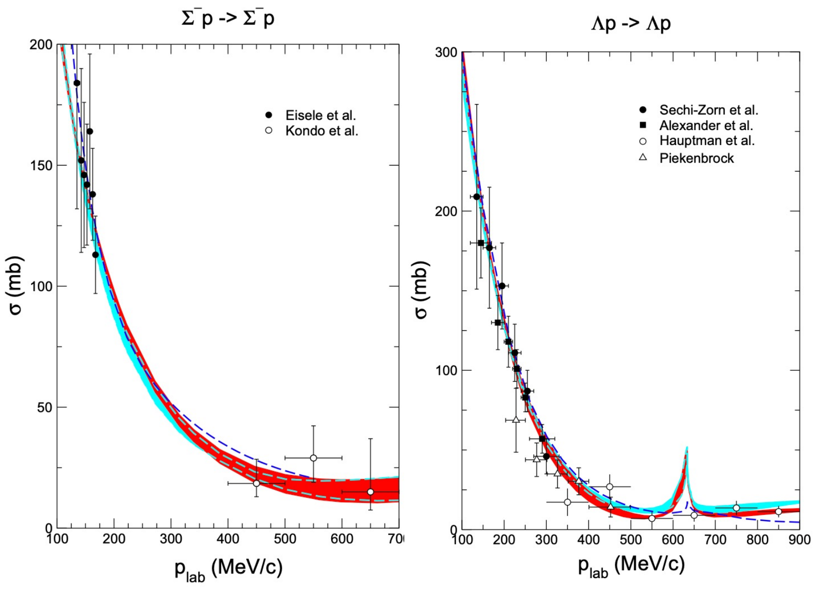

J. Haidenbauer et al., Eur. Phys. J. A (2020) 56:91

J. Haidenbauer et al., Nucl. Phys. A 915 (2013) 24

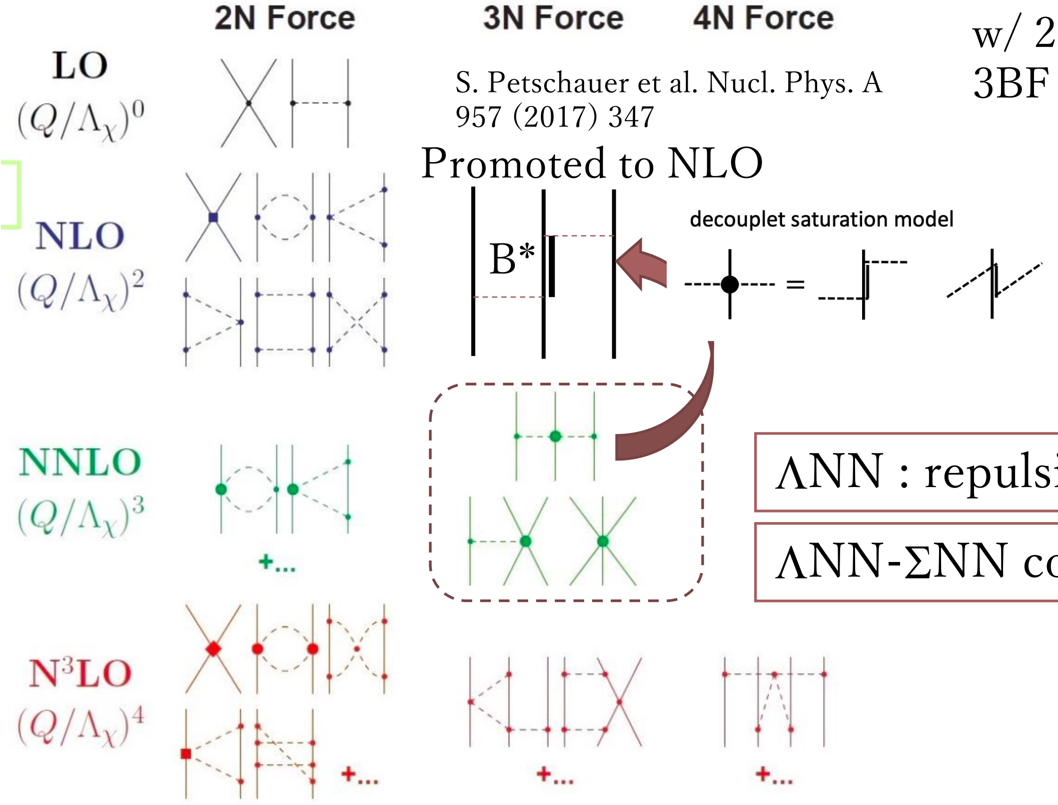

S. Petschauer et al. Nucl. Phys. A 957 (2017) 347

Promoted to NLO

From slide by M. Kohno

Density-dependent effective potential w/ 2π-exchange ΛNN and ΛNN-ΣNN 3BF

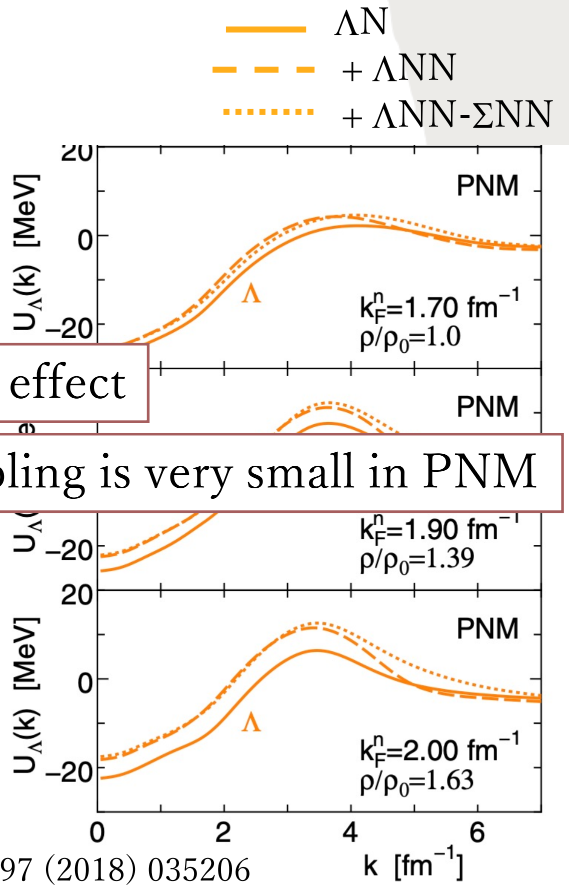

ΛNN : repulsive effect

ΛNN-ΣNN coupling is very small in PNM

M. Kohno, Phys. Rev. C 97 (2018) 035206

Chiral EFT toward NNLO

Two body YN force

Num of LEC

Constrained from YN scattering data (bubble chamber) and NN data

S wave : 5

S wave + S-D transition : 8

Not yet determined well

Λp, Σp scattering data at J-PARC can constrain

P wave : 10

NO LEC

Chiral EFT can be extended to NNLO if YN scattering data are accurate enough.

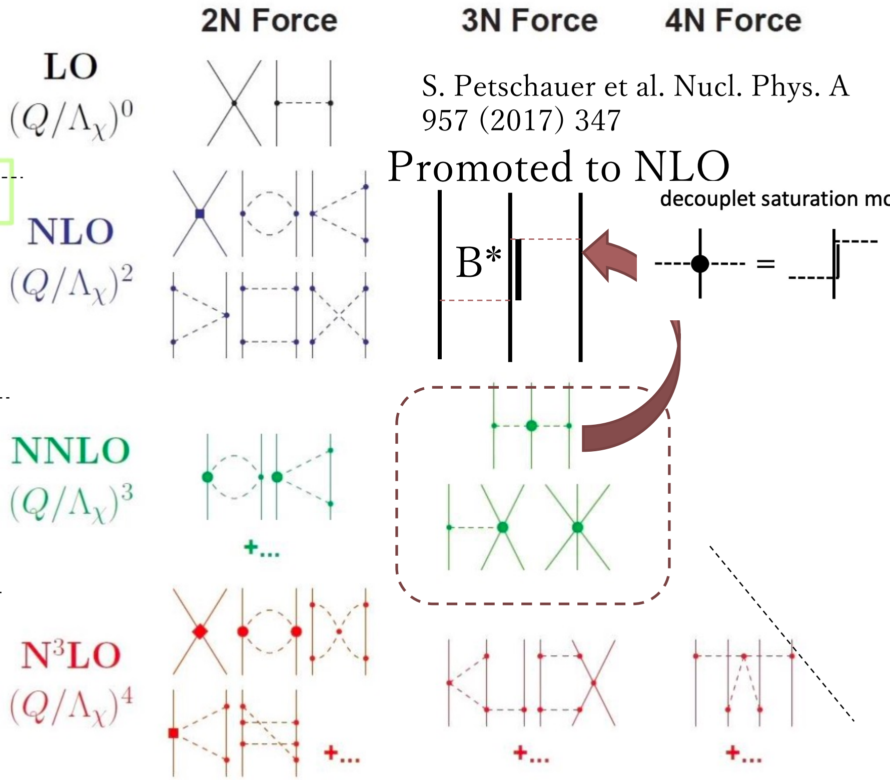

Three body YNN force

Num of LEC in decuplet saturation model

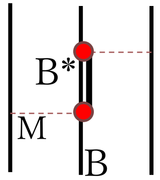

B*-B-M coupling : 2

can be determined theoretically.

2π-exchange ΛNN force is already studied.

B*-B-B-B coupling : 2

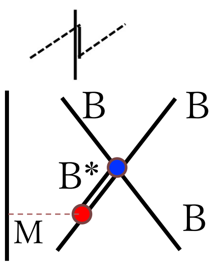

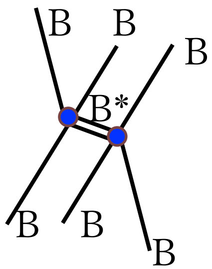

These two LECs should be determined from experiment from

- binding energy $^4_\Lambda$He (0^+ and 1^+ states)
- Λd scattering

These 3BF should be considered for calculation of neutron star matter in future

In near future, chiral EFT can be extended to

- NNLO for two body YN w/ accurate YN scattering data
- NLO for three-body YNN w/ Λd scattering or few-body hypernuclear binding energies

U_Λ dependence for M-R relation

Y. Yamamoto et al.
PRC90, 045805 (2014)

Calculation with ESC model + 3 different 3BF

Λ single particle potential

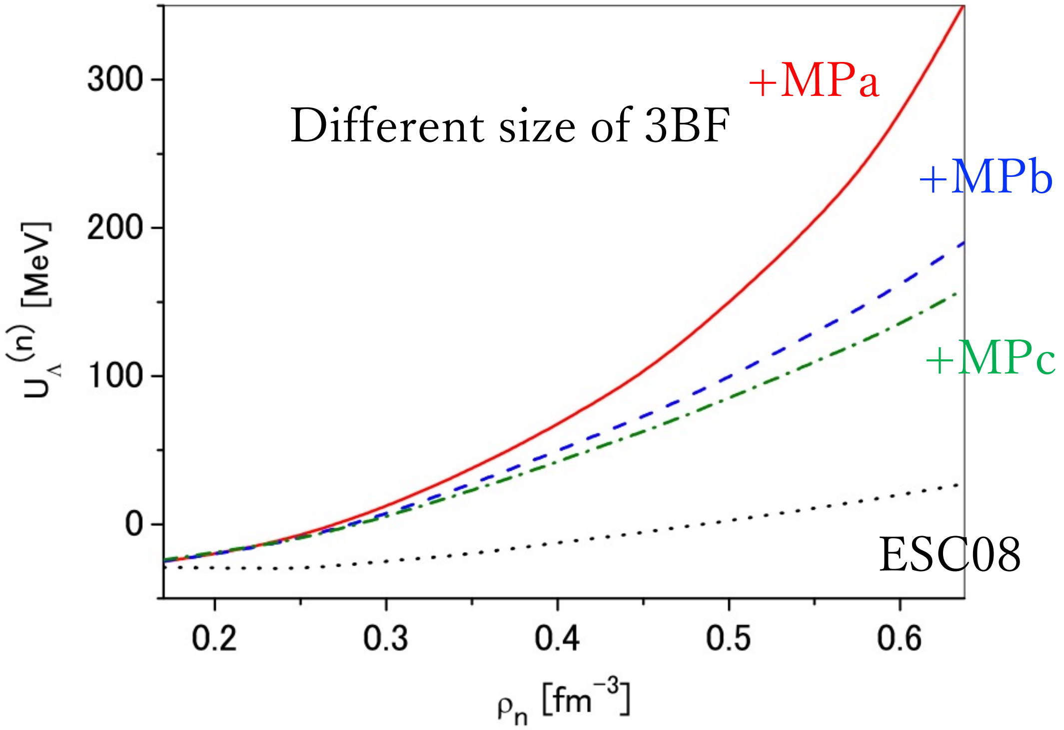

M-R curve

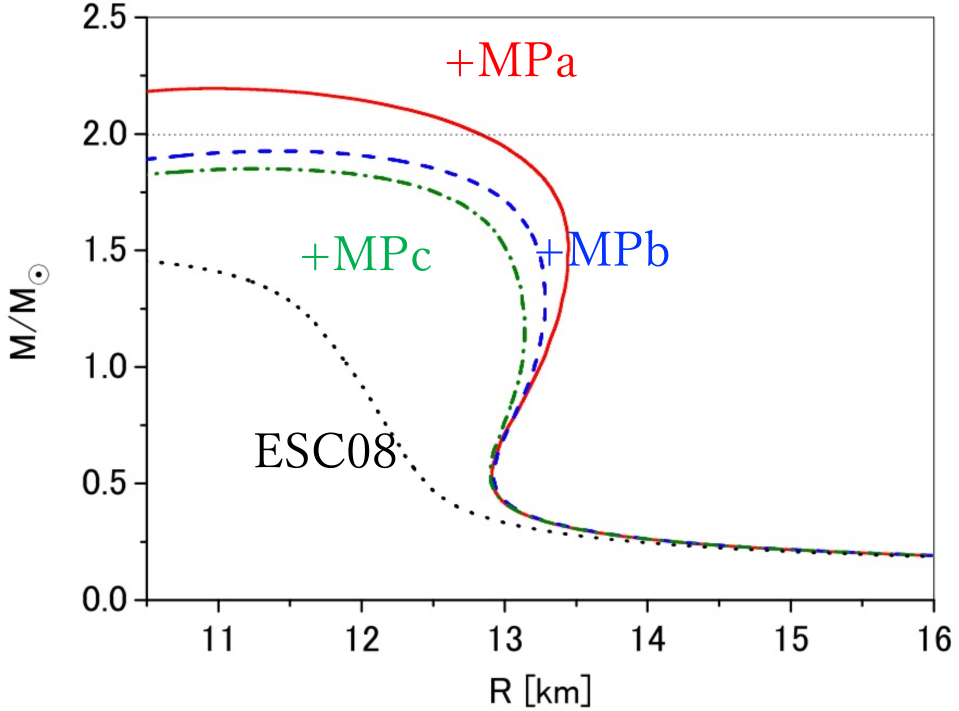

Density dependence of ΛNN 3BF is roughly quadratic ($\propto \rho^2$).

ΛNN strength at normal nuclear density (ρ_0) becomes 9~16 times more effect at 3~4 ρ_0 region.

Precise determination of binding energy is very important.

ΛN interaction and its uncertainty

Isaka et al. pointed out that choice of two-body ΛN interaction has large effect of theoretical calculation

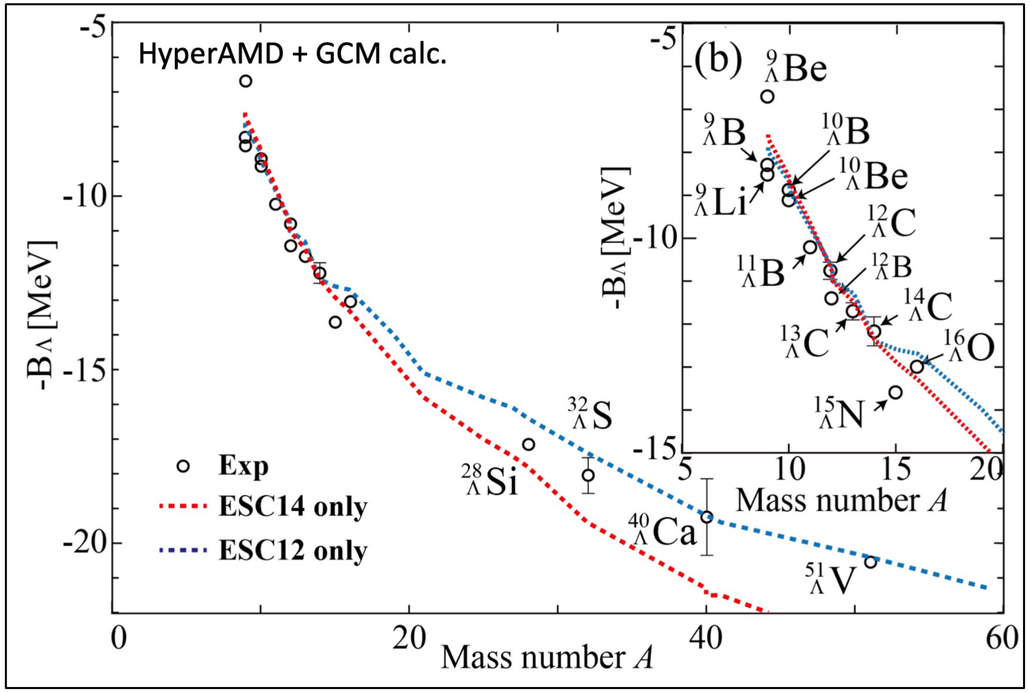

M. Isaka et al., Phys. Rev. C 95, 044308 (2017)

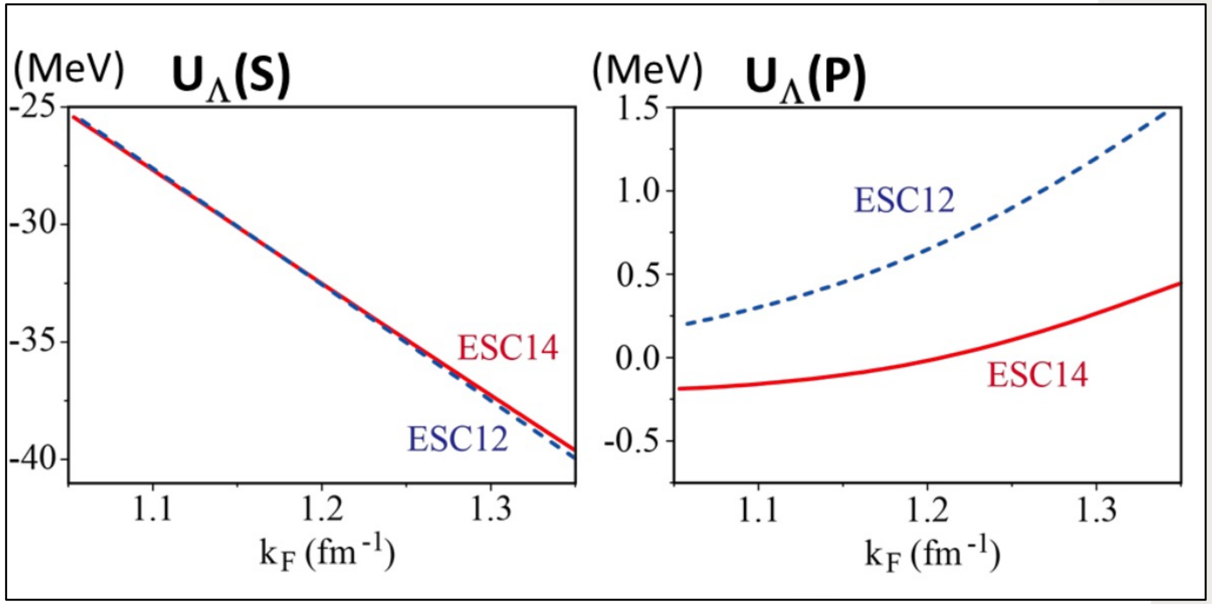

Large P-wave uncertainty of Potential

ESC12 can explain $-B_\Lambda$ w/o ΛNN repulsive int.

ESC14 need ΛNN repulsive int.

Uncertainty in the theoretical microscopic many-body calculation based on realistic NN interactions

Pure neutron matter

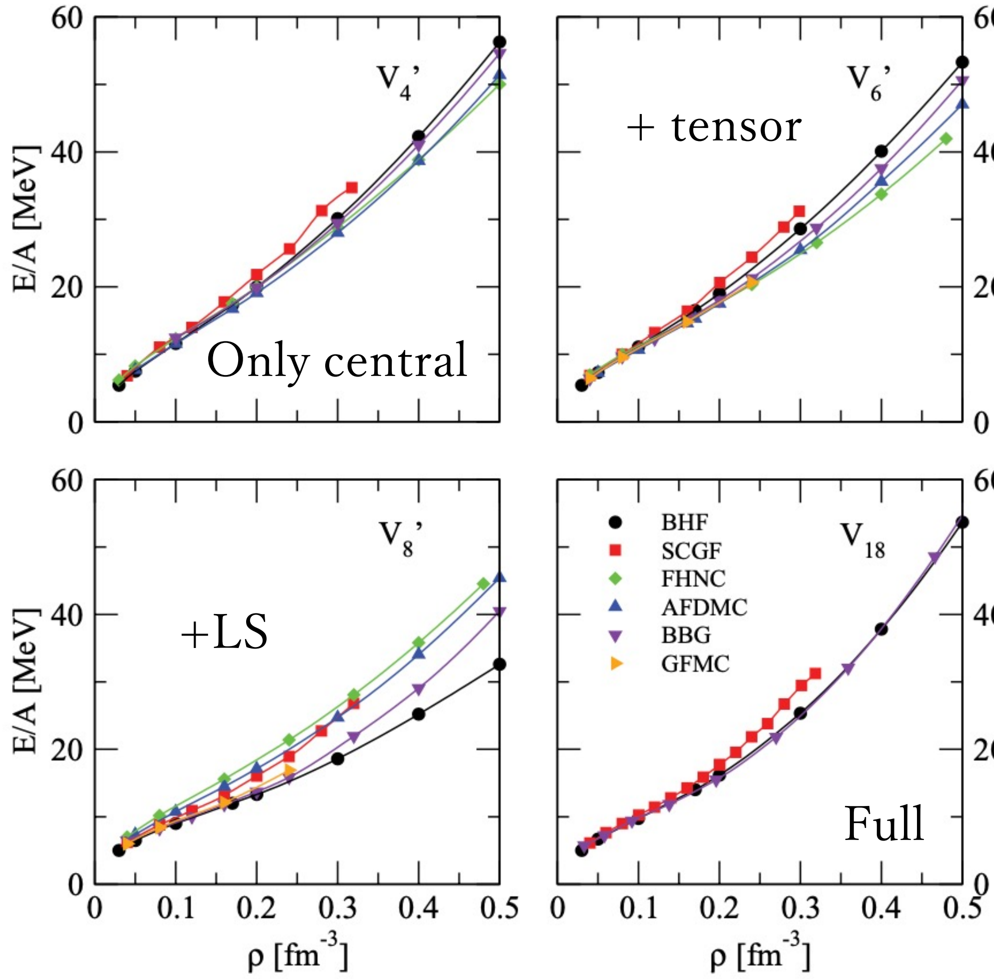

Symmetric nuclear matter

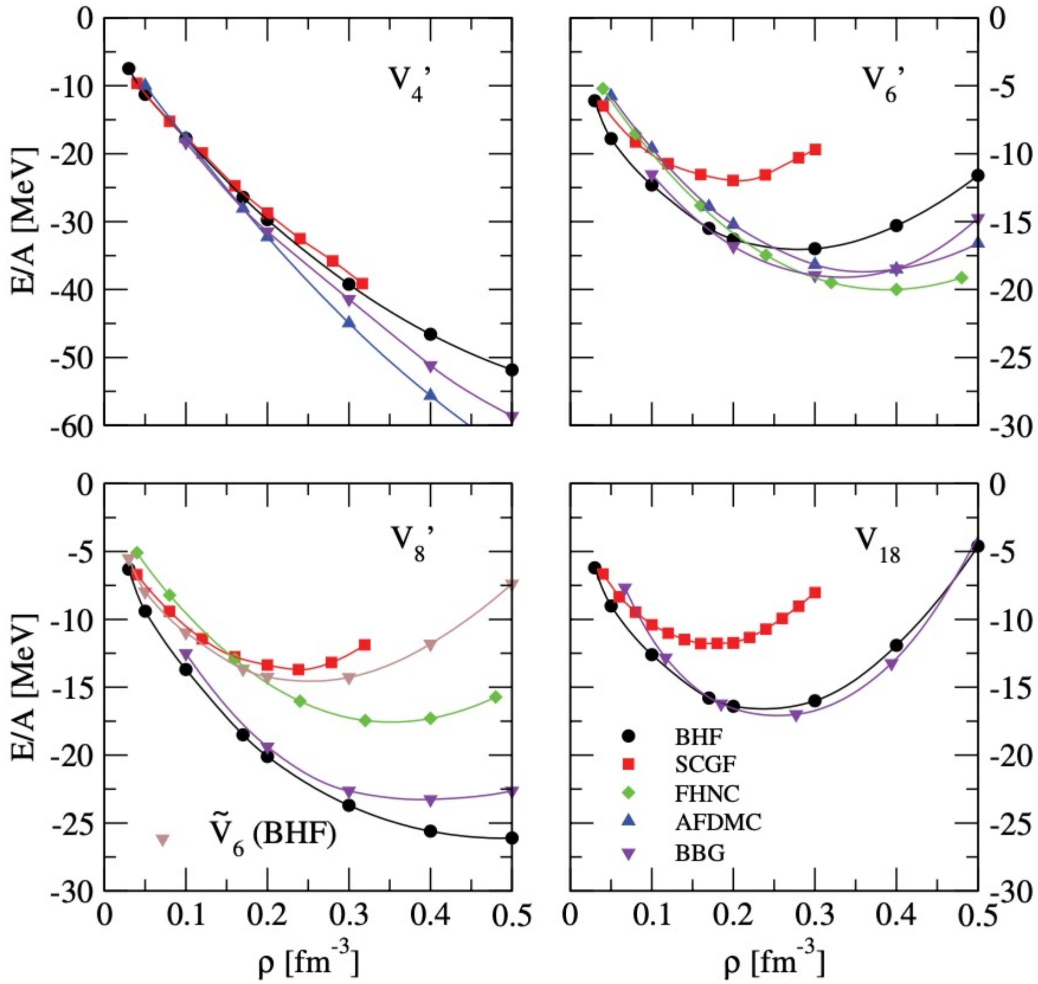

EOS with Quark-Hadron Crossover

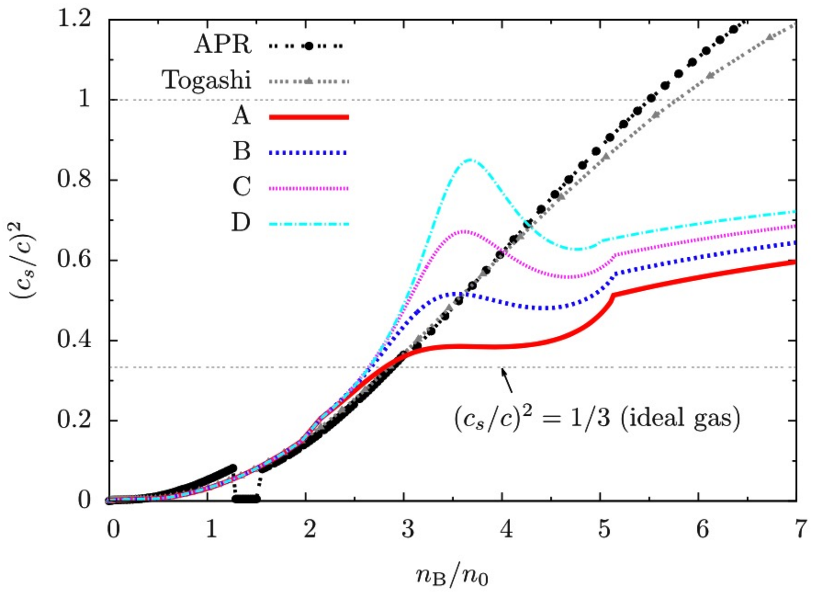

Diquark channel in quark-quark

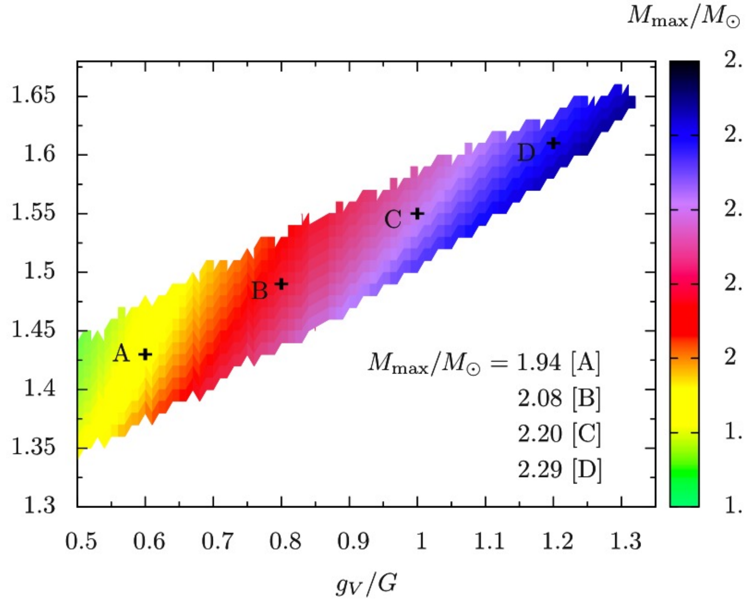

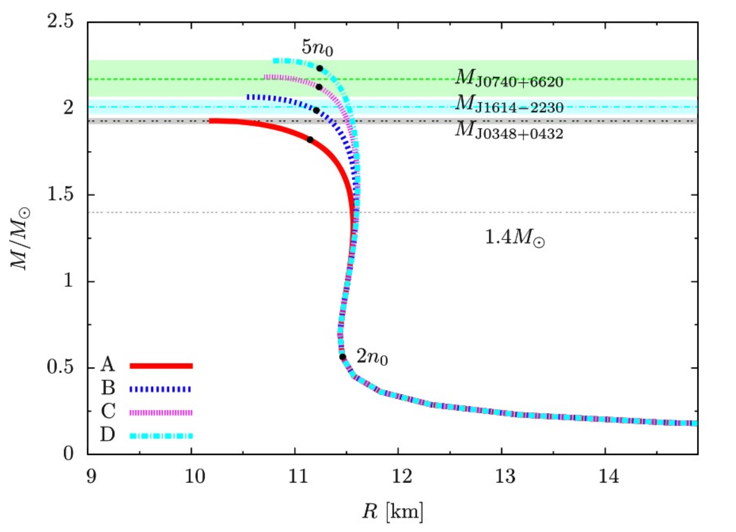

Vector channel in quark-quark

Repulsive force in vector channel is necessary for supporting heavy neutron star

QHC :

$2n_0$ < Baryonic model

Cross over

$5.5n_0$ > Quark phase

Λ hyperon appear at 0.42 fm^{-3} in Togashi EOS

Interpolation region from baryon to quark

Hyperon interaction is necessary to get better description at this region

Uncertainty of ΛN interaction in the present BB int. model

Energy spectra of $^{13}_{\Lambda}$C, $^{16}_{\Lambda}$O, $^{28}_{\Lambda}$Si, $^{51}_{\Lambda}$V, $^{89}_{\Lambda}$Y, $^{139}_{\Lambda}$La, $^{208}_{\Lambda}$Pb

with ESC16 model

M.M. Nagels et al. Phys. Rev. C99, 044003 (2019)

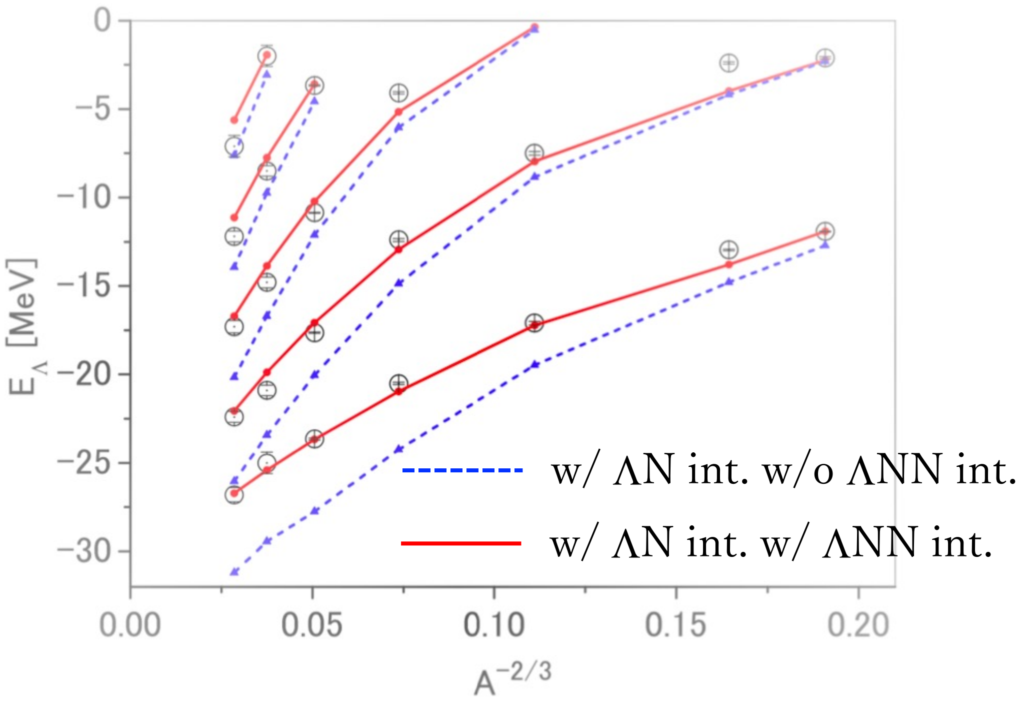

with ESC08 model

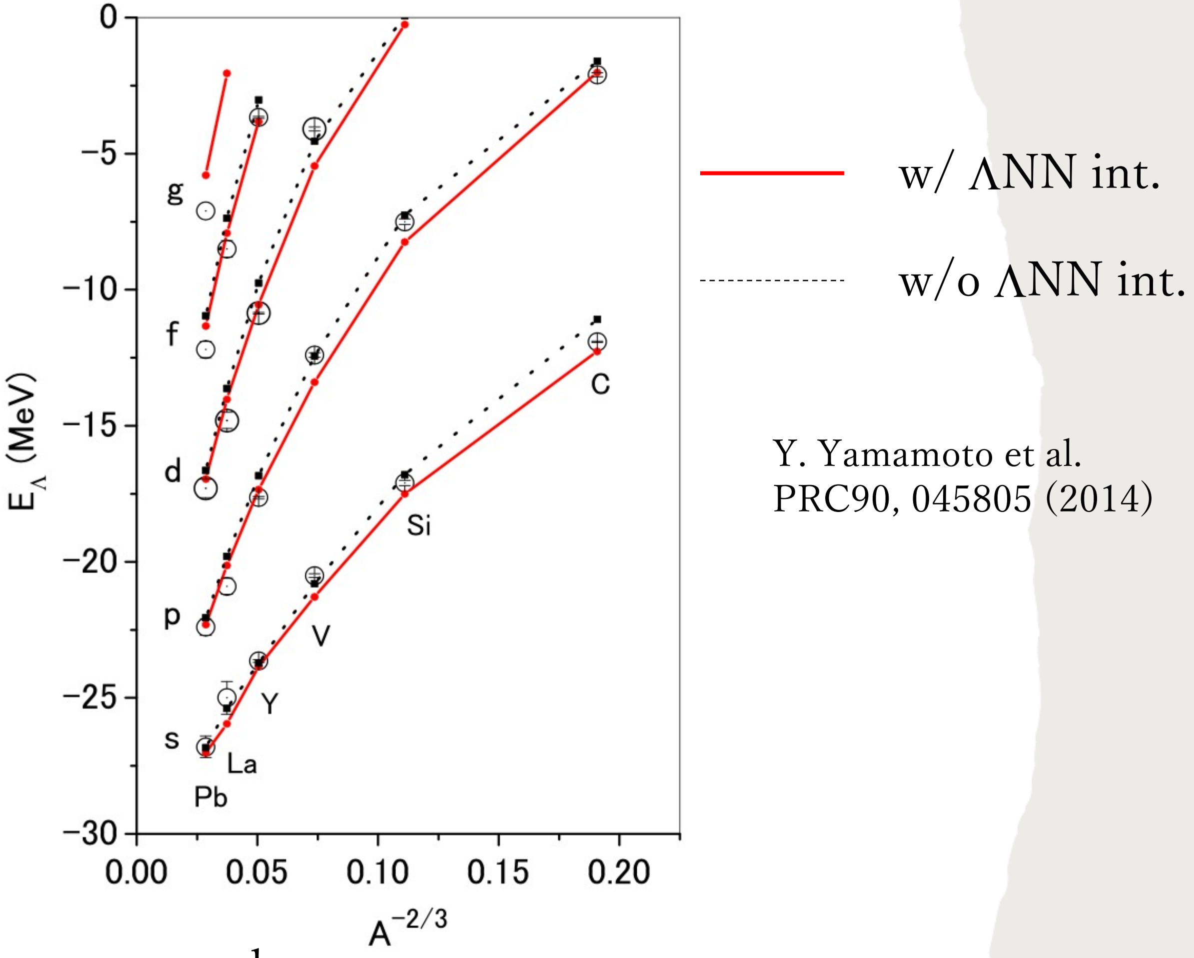

Y. Yamamoto et al.
PRC90, 045805 (2014)

This calculation depends on two-body ΛN interaction very much.

← Owing to Large uncertainty in P-wave ΛN potential

Baryon-baryon interaction model's picture

There exists various theoretical models based on its own fundamental degree of freedom.

Boson exchange picture

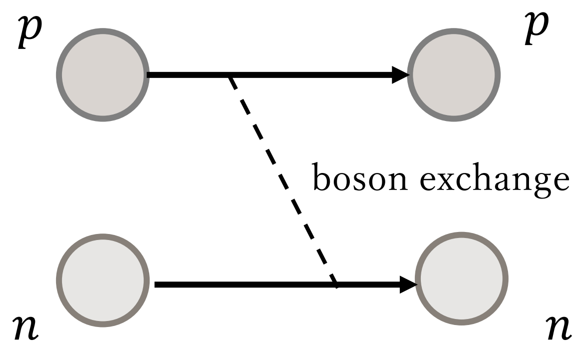

Nijmegen model

Quark based model with effective QCD

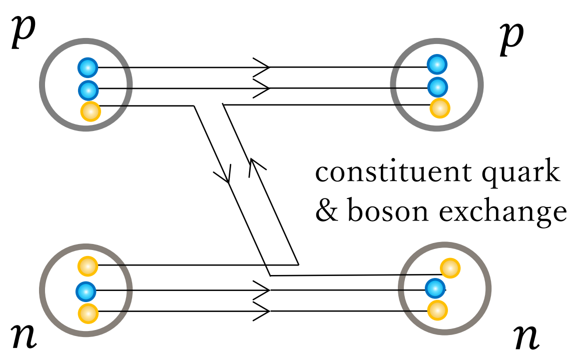

Quark Cluster model

Quantum Chromo Dynamics (QCD)

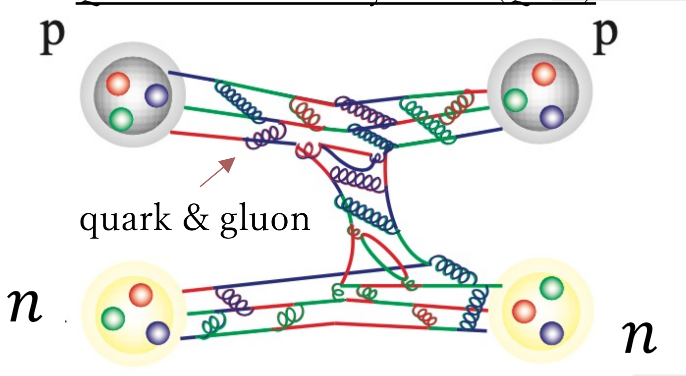

Lattice QCD

Chiral EFT

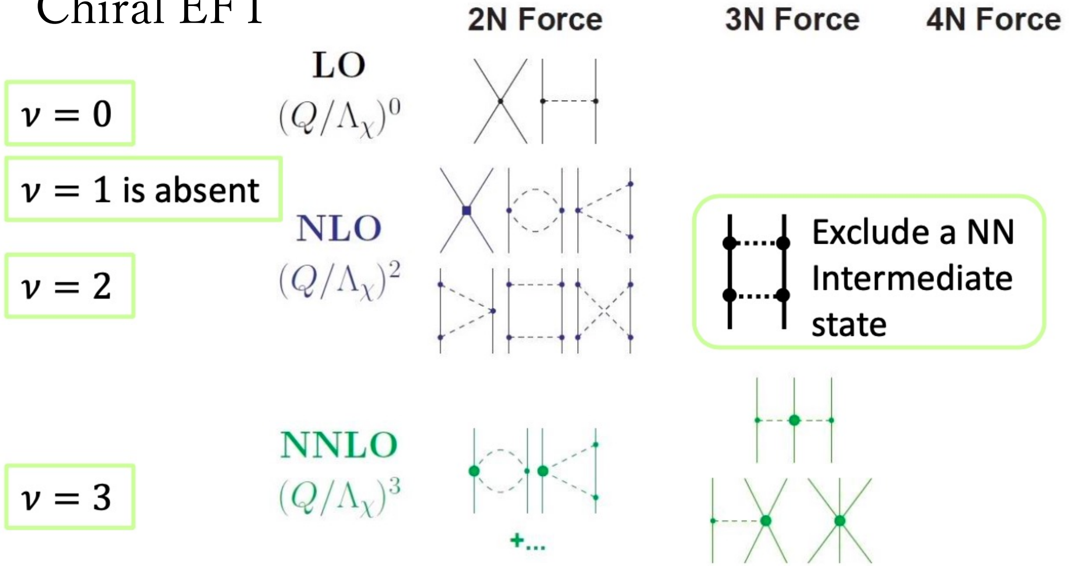

Experimental situation

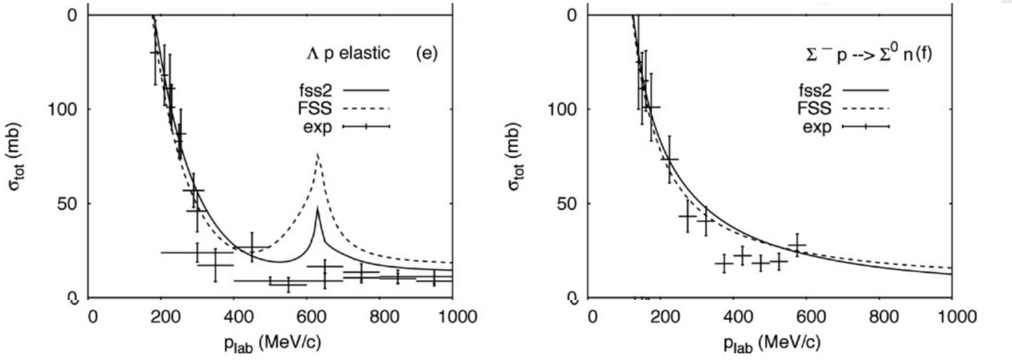

Experimental task is to provide good quality two-body scattering data to impose constraints on these theories to improve them.

Nijmegen model

Widely used interaction in hypernuclear physics

Nijmegen potential + G-matrix calculation is powerful method to study hypernuclei and neutron star

$^{16}O+^{16}O$ elastic scattering at E/A=70 MeV

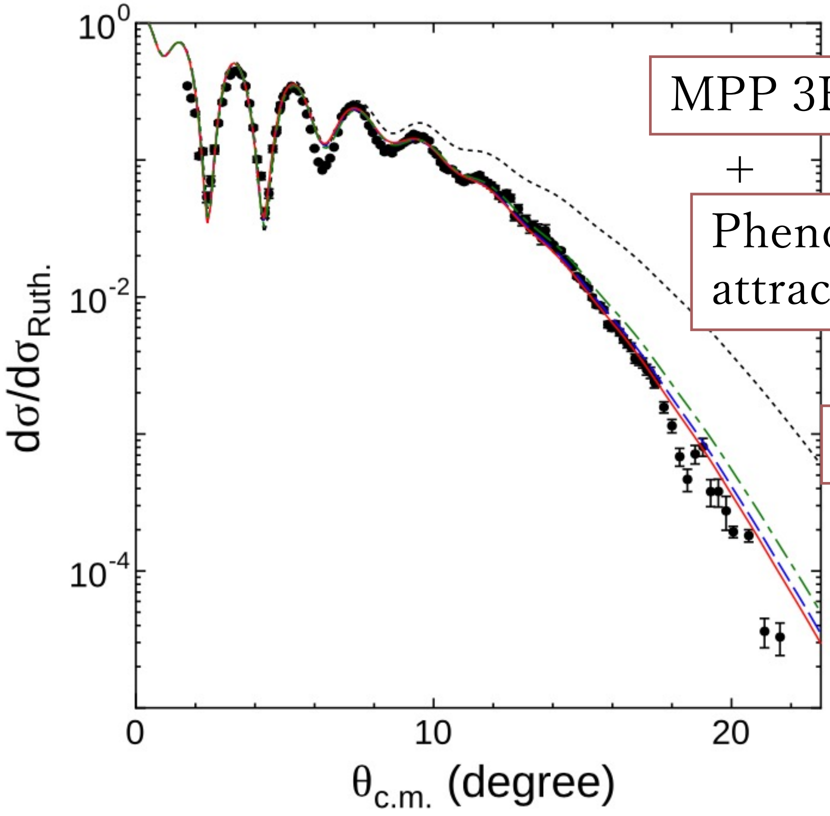

MPP 3B repulsive force

+

Phenomenological 3B attractive force

+

ESC YN model

Yamamoto et al. Phys. Rev. C 90 (2014) 045805

M. M. Nagels et al., Phys. Rev. C 99 (2019) 04403

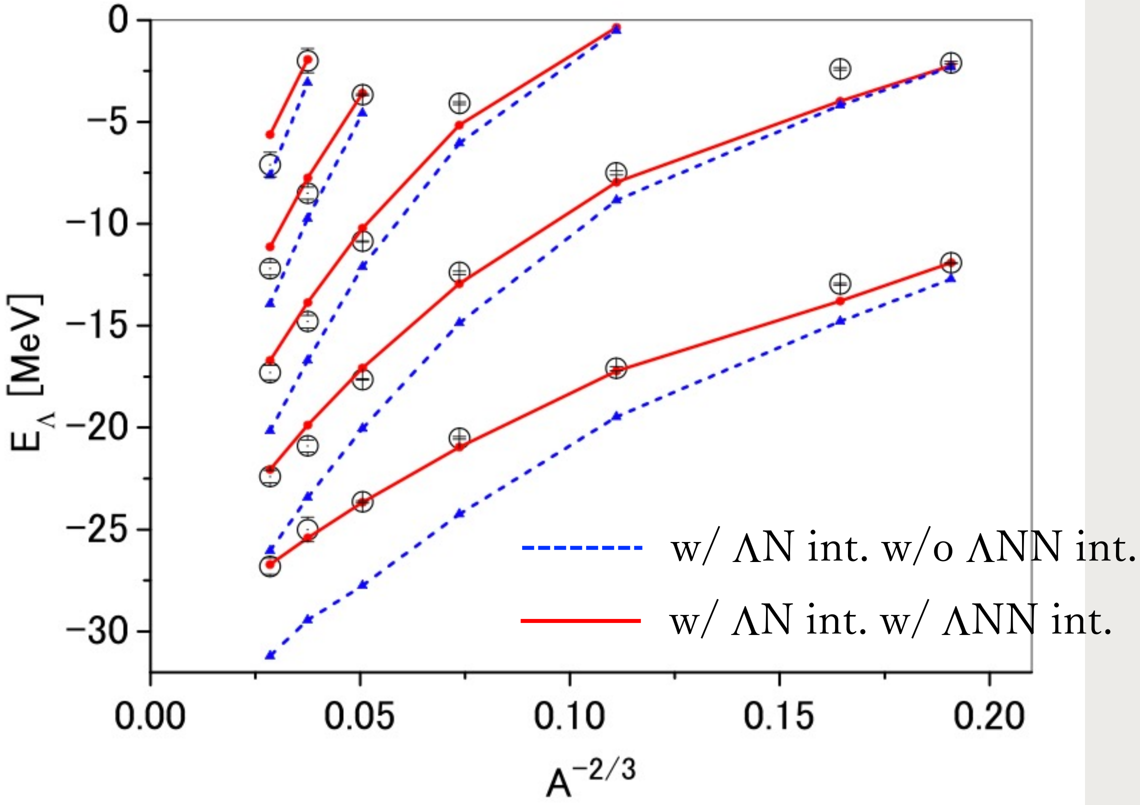

Triggered HIHR/K1.1 project

Lattice QCD

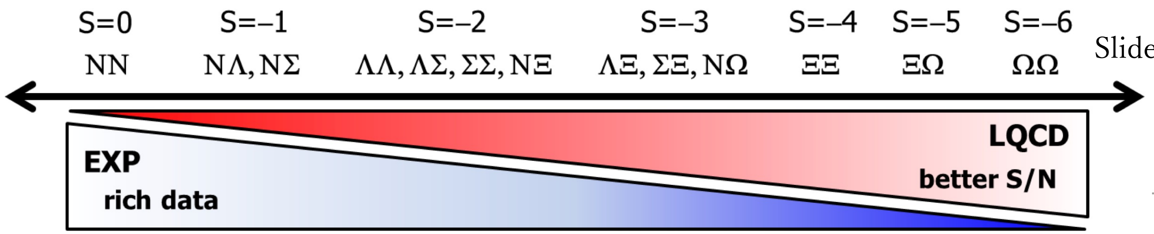

Slide from Doi-san

K. Sasaki et al., Nucl. Phys. A 998 (2020) 121737

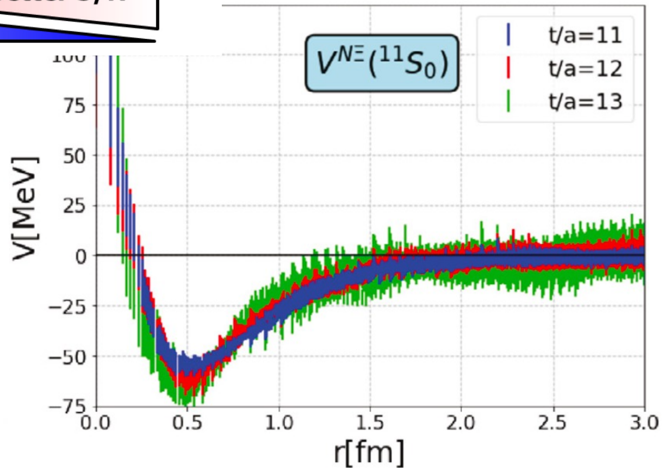

ALICE Collaboration, Nature 588 (2020) 232

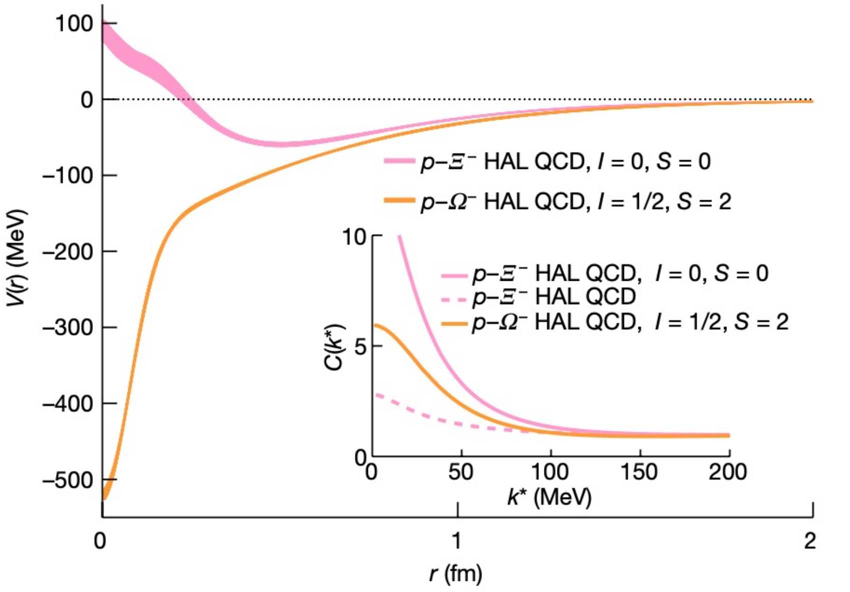

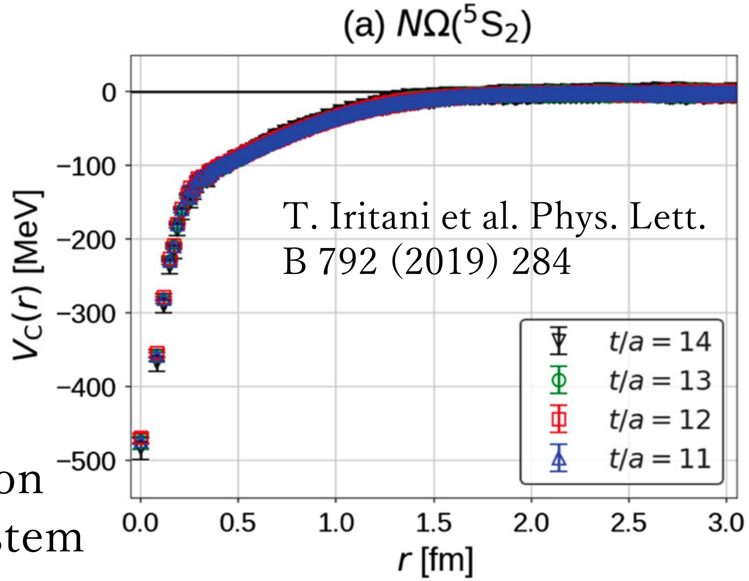

T. Iritani et al. Phys. Lett. B 792 (2019) 284

Attractive potential w/ NO Pauli exclusion
Decay suppression to ΛΞ, ΣΞ for S=2 system

Lattice QCD

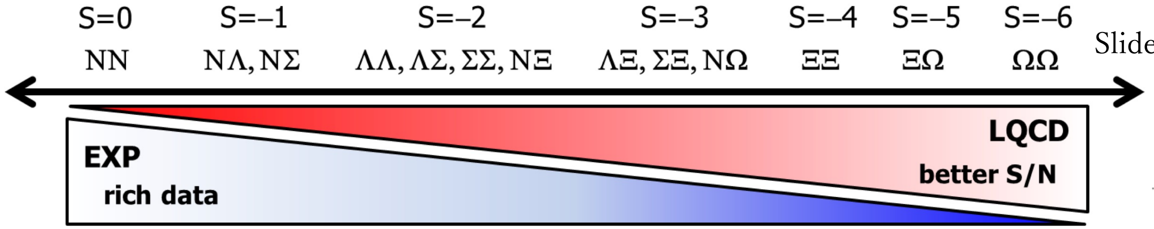

Slide from Doi-san

S=-1 system
Theoretical improvement with Misner's method (T. Miyamoto et al. Phys.Rev. D 101 (2020) 074514)are ongoing.

P-wave, LS-force, 3-body forces will be studied in Fugaku computer

Attractive potential w/ NO Pauli exclusion
Decay suppression to ΛΞ, ΣΞ for S=2 system

K. Sasaki et al., Nucl. Phys. A 998 (2020) 121737

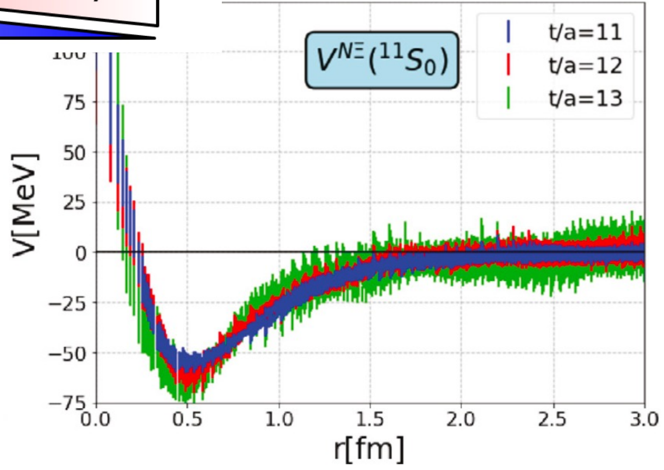

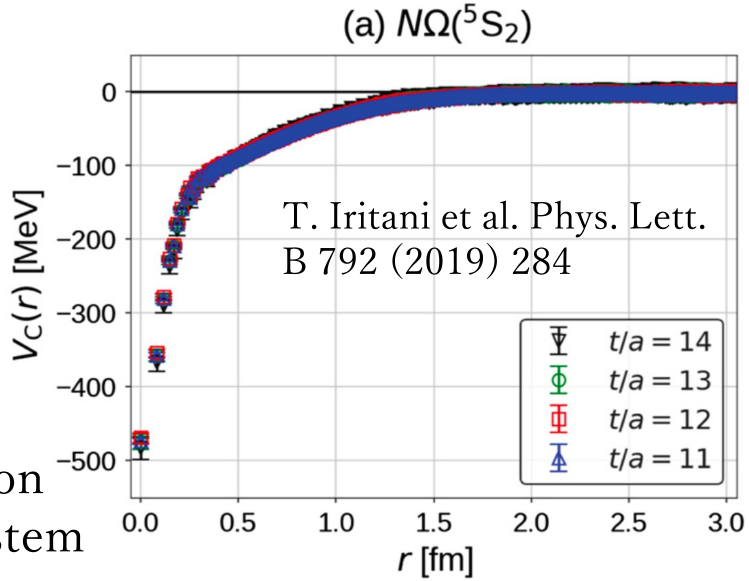

T. Iritani et al. Phys. Lett. B 792 (2019) 284

ALICE Collaboration, Nature 588 (2020) 232

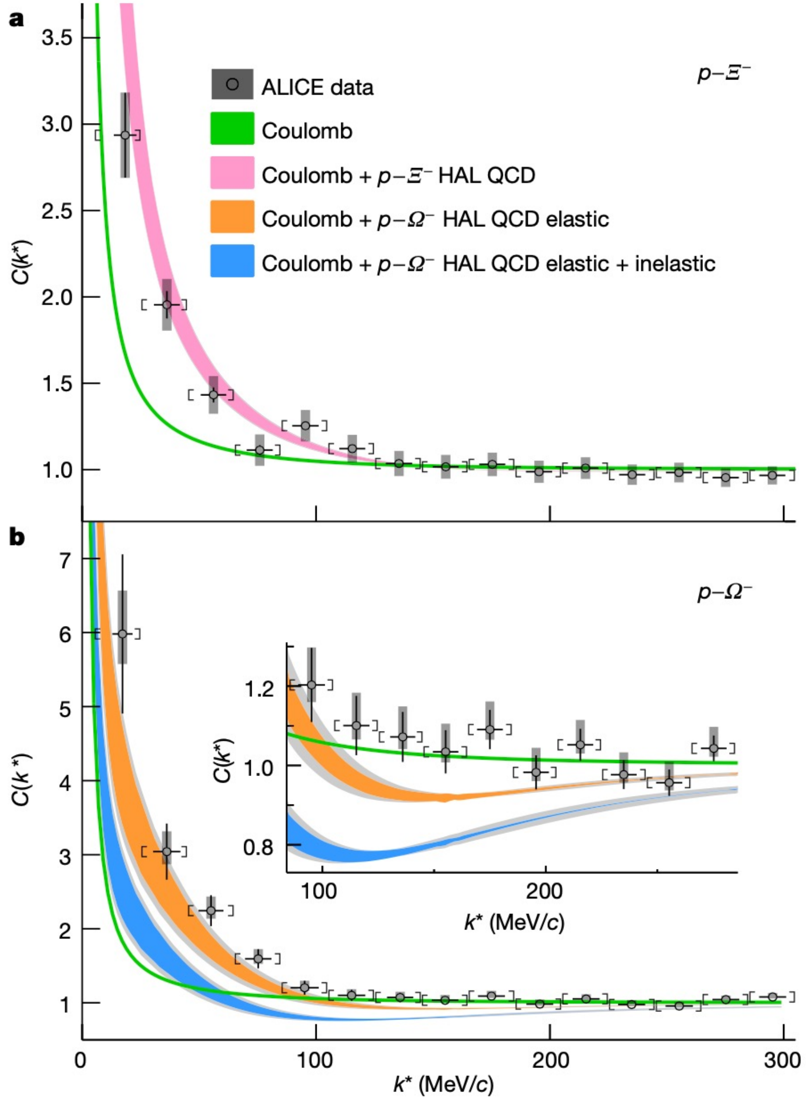

Chiral EFT

- Underlying chiral symmetry in QCD
- Power counting feature to improve calculation systematically by going to higher order
- Multi baryon force appear naturally and automatically in a consistent implementation of the framework

YN interaction at NLO

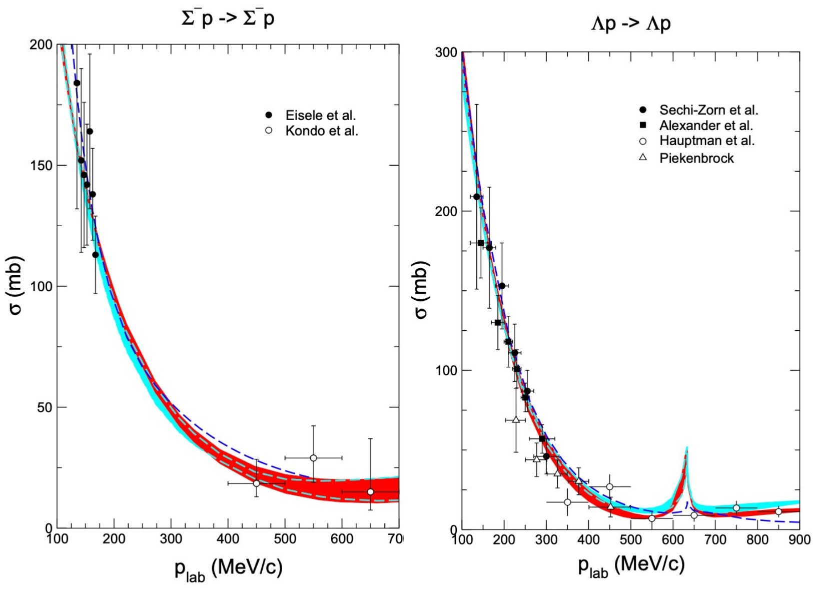

J. Haidenbauer et al., Eur. Phys. J. A (2020) 56:91

J. Haidenbauer et al., Nucl. Phys. A 915 (2013) 24

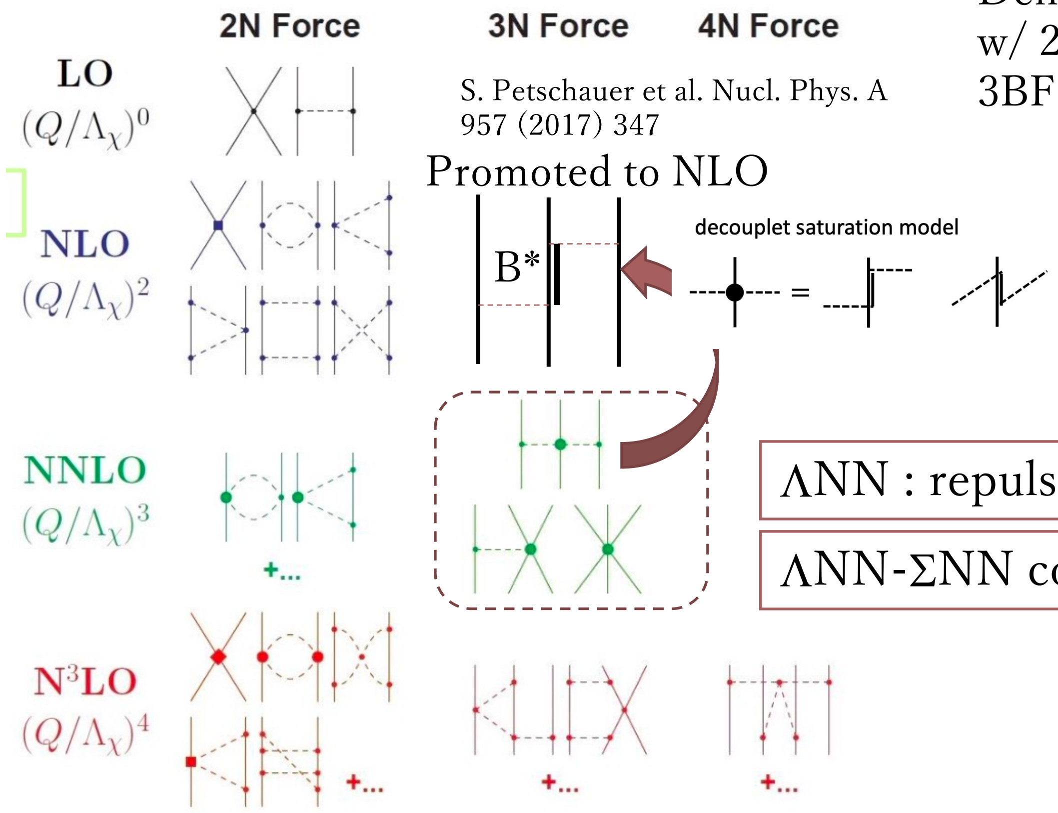

S. Petschauer et al. Nucl. Phys. A 957 (2017) 347

Promoted to NLO

From slide by M. Kohno

Density-dependent effective potential w/ 2π-exchange ΛNN and ΛNN-ΣNN 3BF

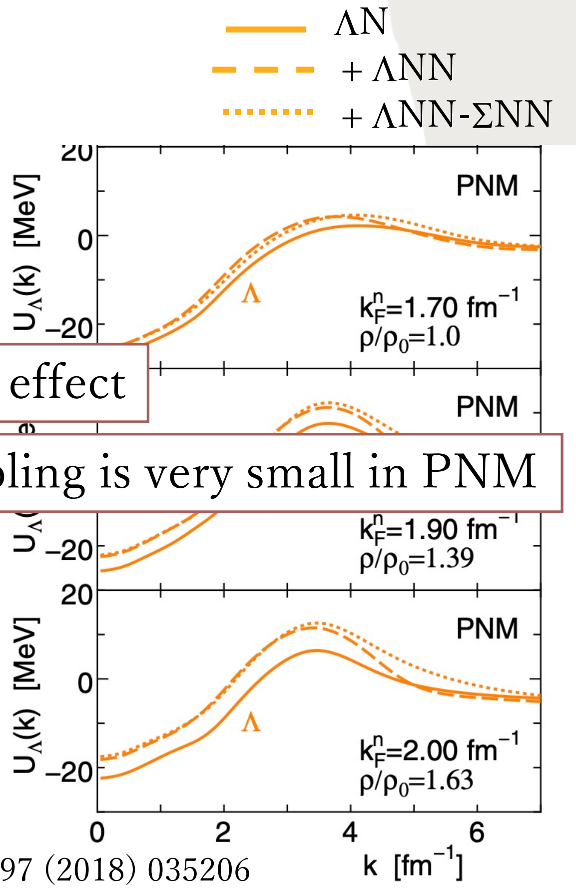

ΛNN : repulsive effect

ΛNN-ΣNN coupling is very small in PNM

M. Kohno, Phys. Rev. C 97 (2018) 035206

Recent experimental progress at J-PARC

Two successive two-body reactions

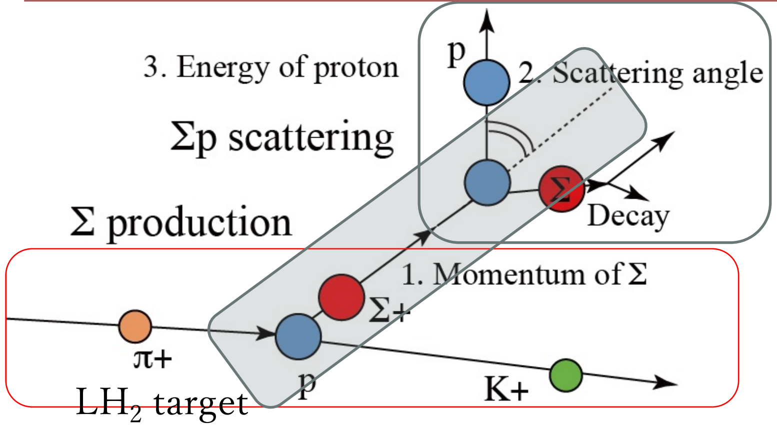

Detection of Σp scattering event by CATCH detector

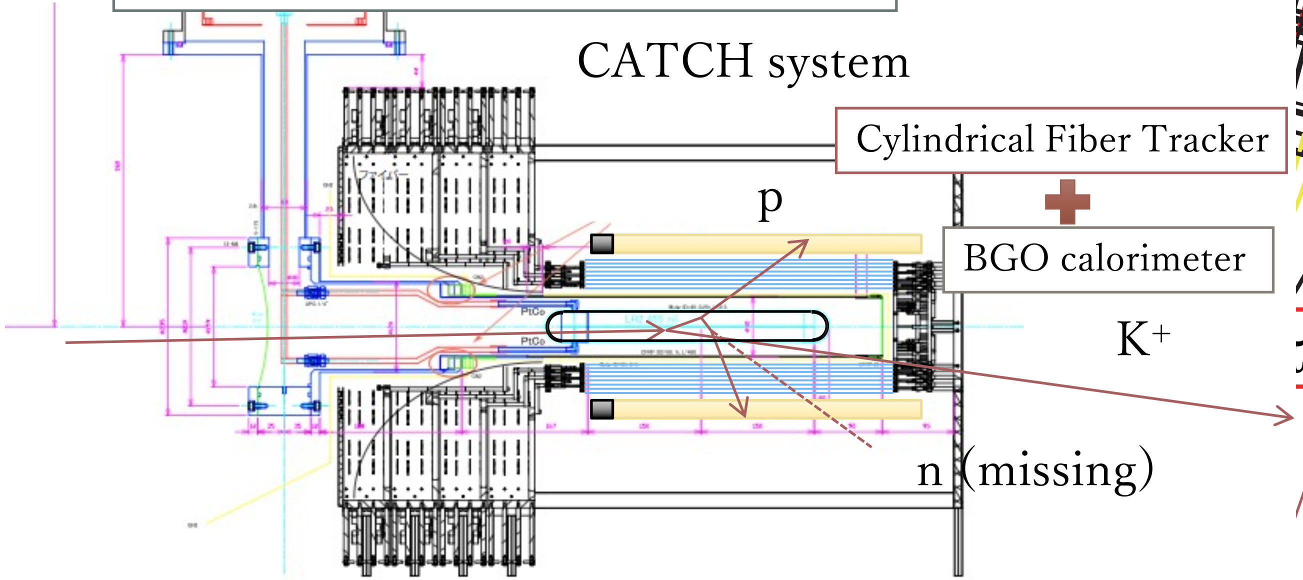

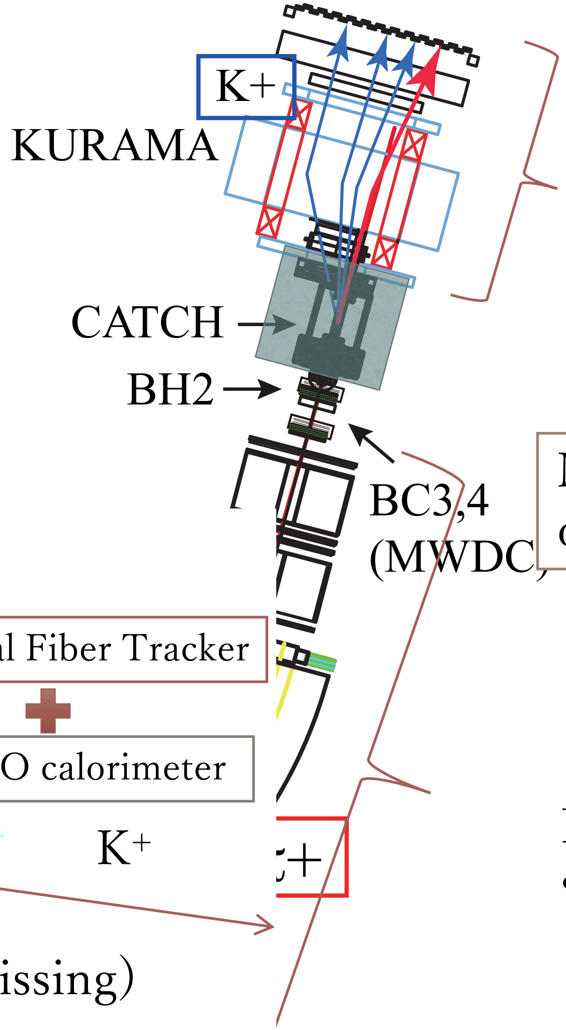

KURAMA spectrometer

- Identification of K$^+$
- Momentum analysis

Momentum reconstruction of Σ beam

Beamline spectrometer

- Momentum analysis of π beam

J-PARC K1.8 beamline

Recent experimental progress at J-PARC

K. Miwa et al. arXiv:2104.13608

Two successive two-body reactions

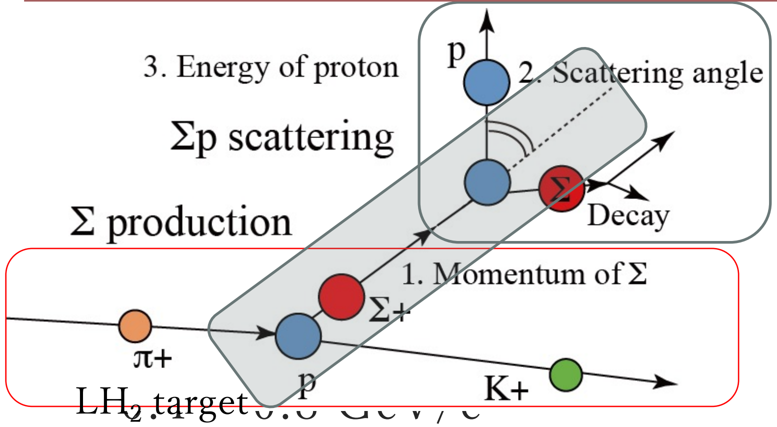

Detection of Σp scattering event by CATCH detector

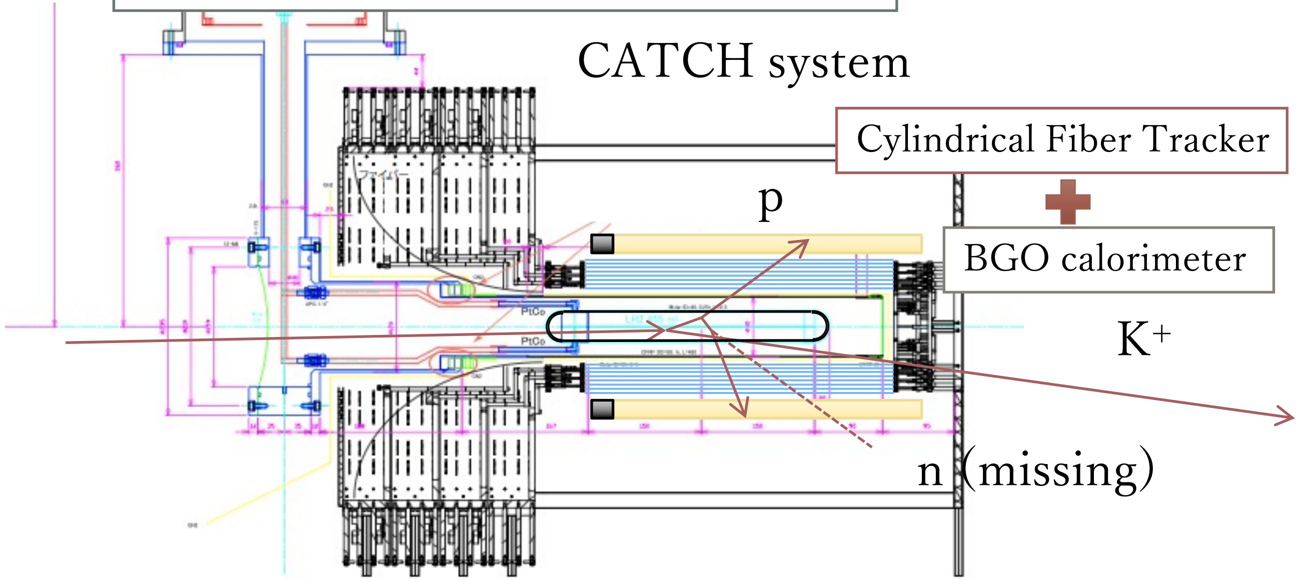

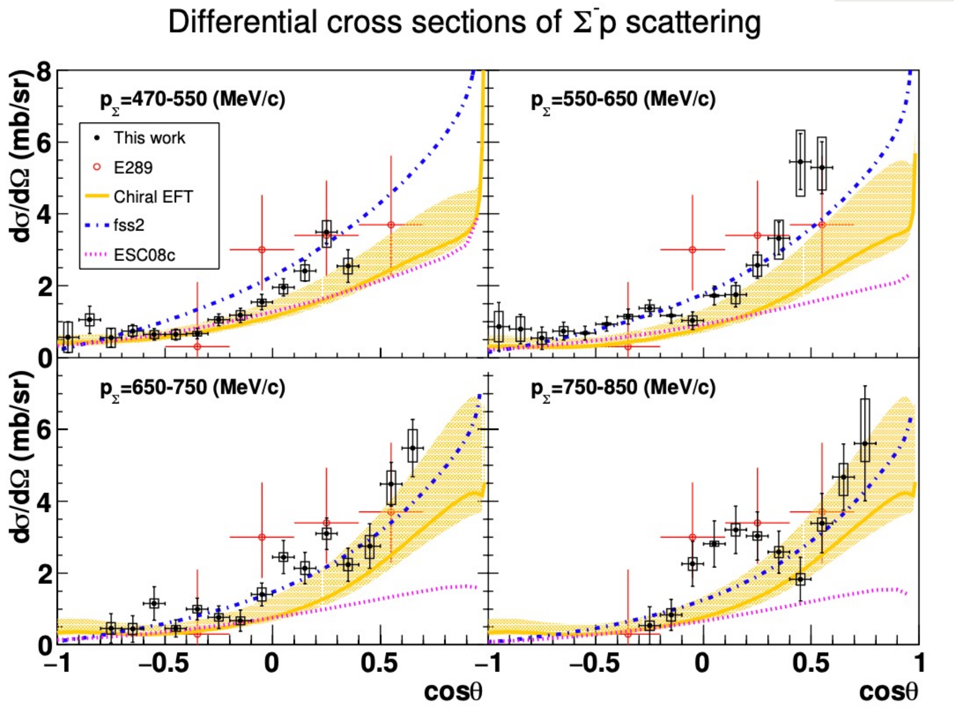

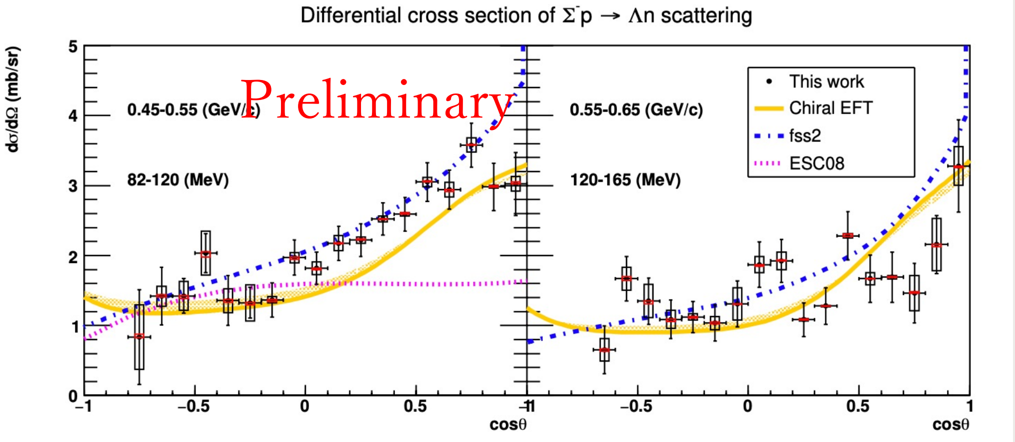

Toward realistic YN interaction(Experimental side)

YN case

2-body scattering data ---▸ Phase shift analysis

Derivation of YN potential

Link between here hopefully soon connected

Small relative-momentum region

S. Acharya et al. Phys. Rev. C 99 024001 (2019)

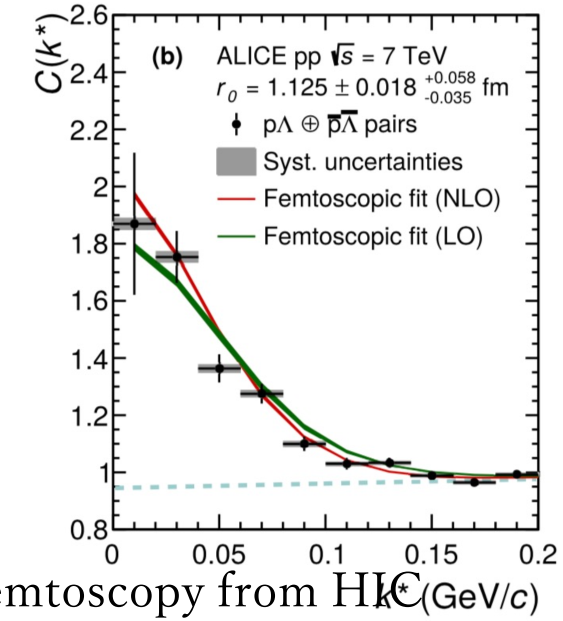

Femtoscopy from HIC

Intermediate energy region

K. Miwa et al. arXiv:2104.13608

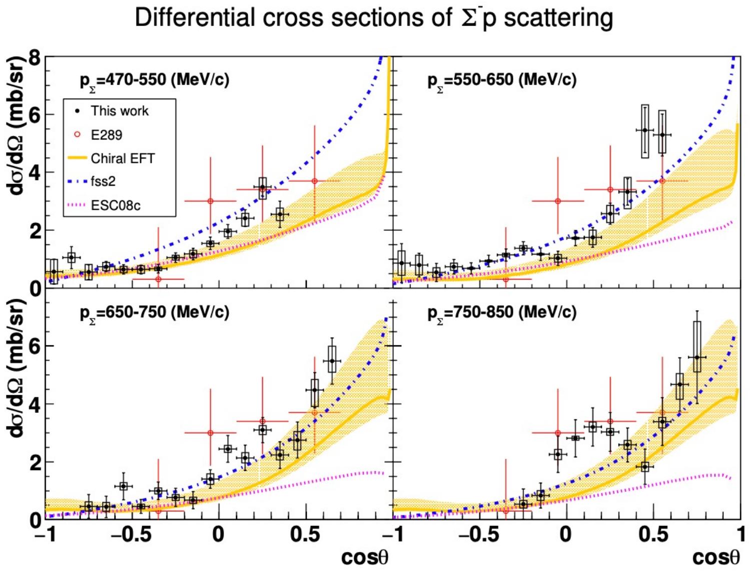

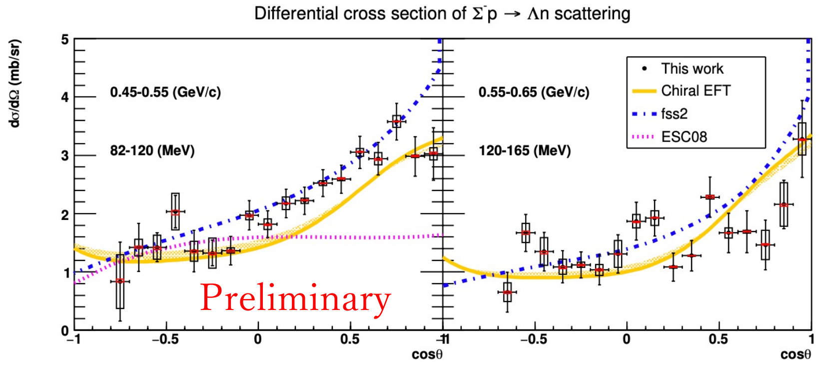

To be submitted soon

Yp scattering experiment at J-PARC

Toward realistic YN interaction(Experimental side)

YN case

2-body scattering data → Phase shift analysis ⇄ Derivation of YN potential

Scattering observable in S=-1 system

Differential information

dσ/dΩ
Spin observables

Contribution for establishing “realistic” YN interaction model

- ✓ Constraint on theoretical model
- ✓ Accurate data to contribute LEC in chiral EFT

Research on Nuclei, Nuclear matter

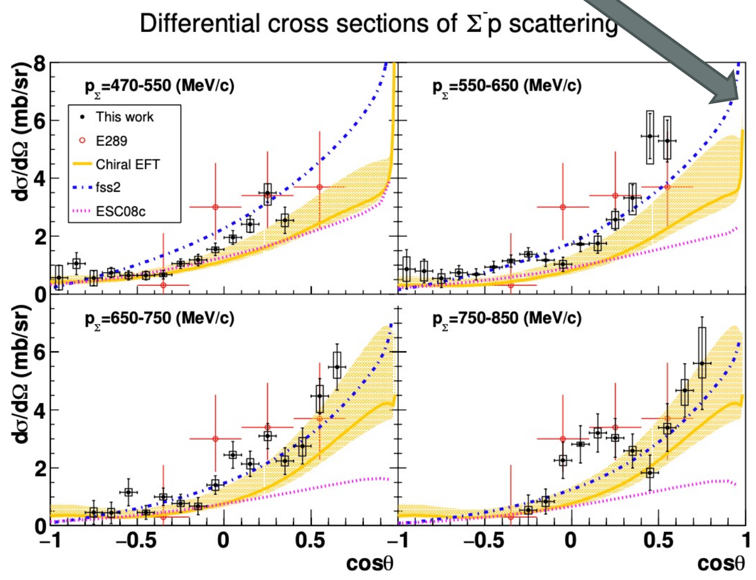

K. Miwa et al. arXiv:2104.13608

Consideration of phase shift analysis in future

Lattice QCD simulation

Potential from Lattice ← QCD

Neutron star and YN interaction

Two-body YN scattering is essential to understand the internal structure of neutron star.

- Interaction at short range
- Basic information to derive 3 body force from hypernuclear structure

Hypernuclear physics based on Realistic YN interaction

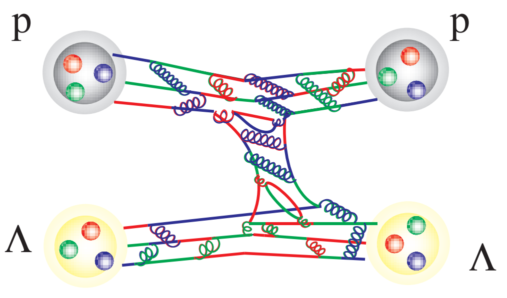

YN scattering experiment
Lattice QCD
Recent theoretical framework

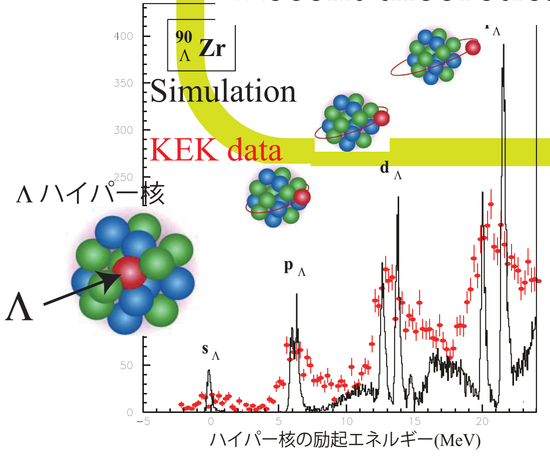

Ultra high-resolution Λ hypernuclear spectroscopy

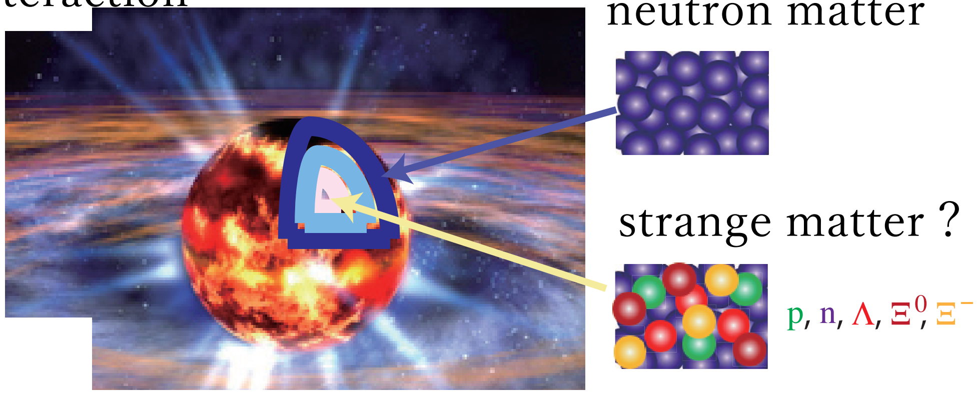

EOS of neutron star

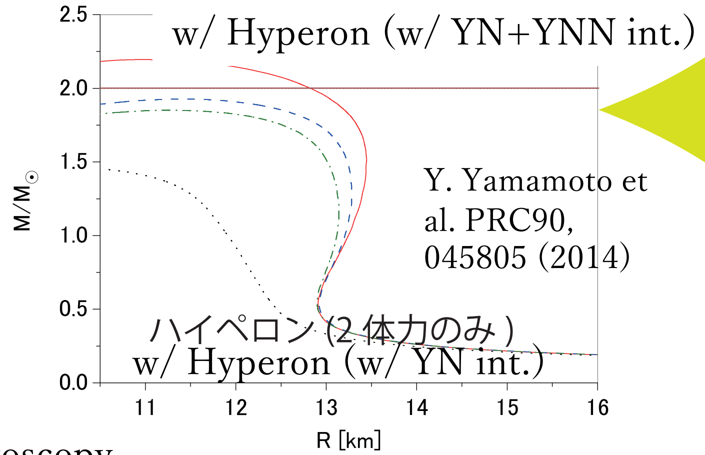

日本物理学会誌より
木内健太、関口雄一郎

Gravitational wave from neutron star merger

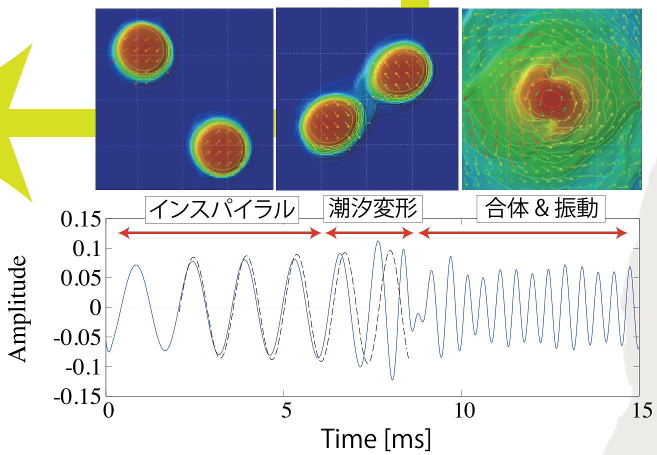

HIHR/K1.1 physics

High resolution Λ hypernuclear spectroscopy with dispersion-matching beam line

ORIGINAL plan

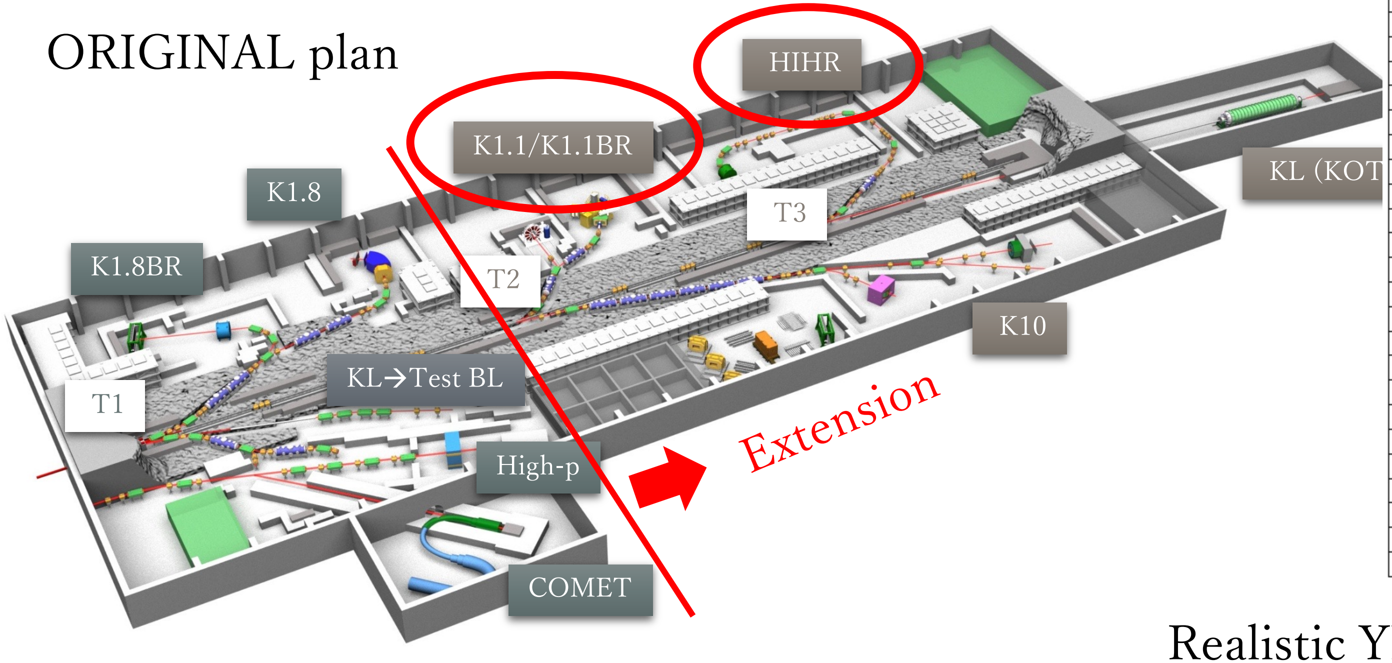

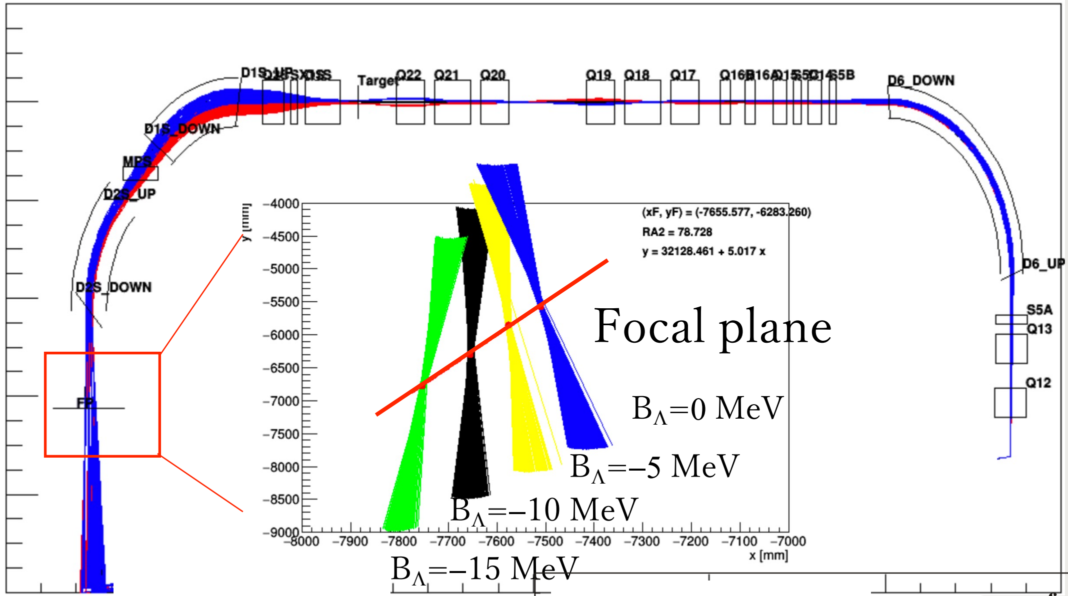

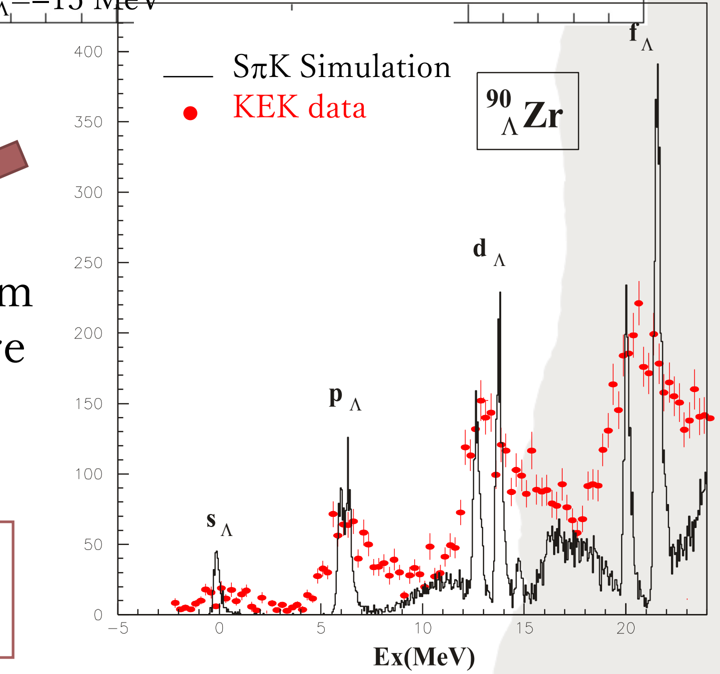

Realistic YN interaction

Λp scattering w/ polarized Λ

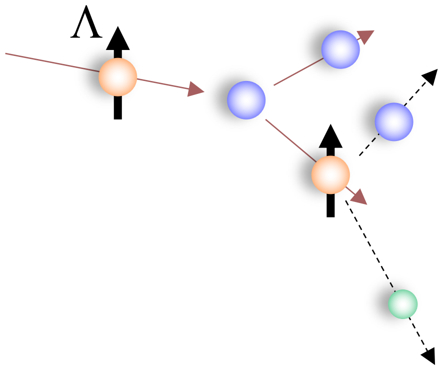

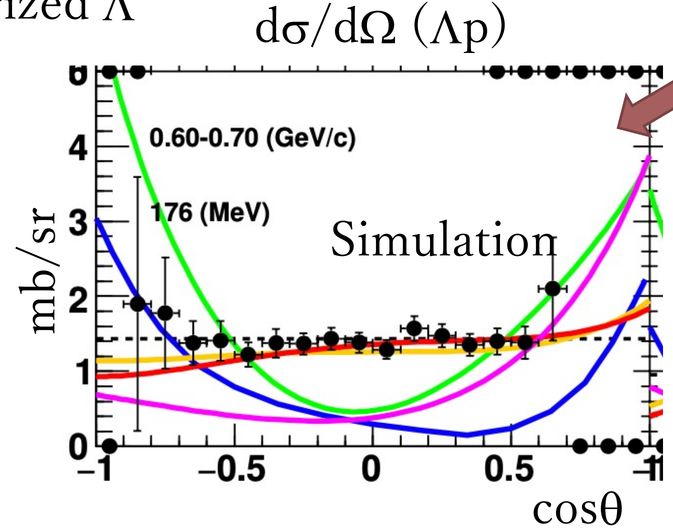

ΛNN information from hypernuclear structure

Attack hyperon puzzle in neutron star

Λ binding energy and ΛNN interaction

Energy spectra of $^{13}_{\Lambda}C$, $^{16}_{\Lambda}O$, $^{28}_{\Lambda}Si$, $^{51}_{\Lambda}V$, $^{89}_{\Lambda}Y$, $^{139}_{\Lambda}La$, $^{208}_{\Lambda}Pb$ with ESC16 model

M.M. Nagels et al. Phys. Rev. C99, 044003 (2019)

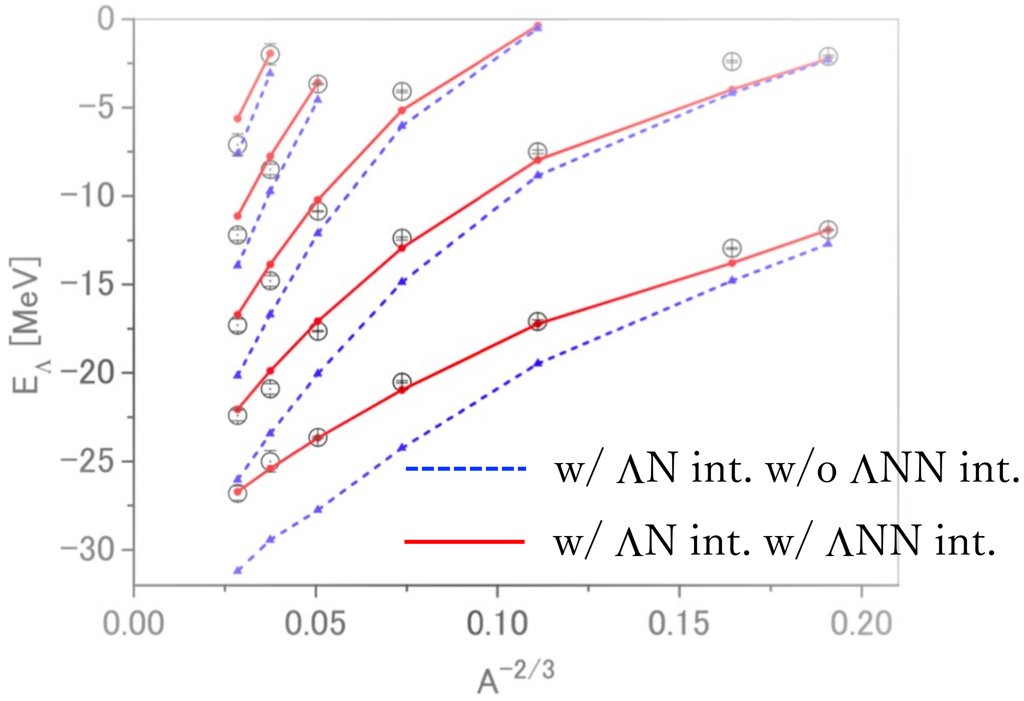

ESC16 need ΛNN repulsive interaction to explain Λ hypernuclear bounding energy

Λ hypernuclei with chiral YN potential

J. Haidenbauer, I. Vidana, Eur. Phys. J. A (2020) 56:55

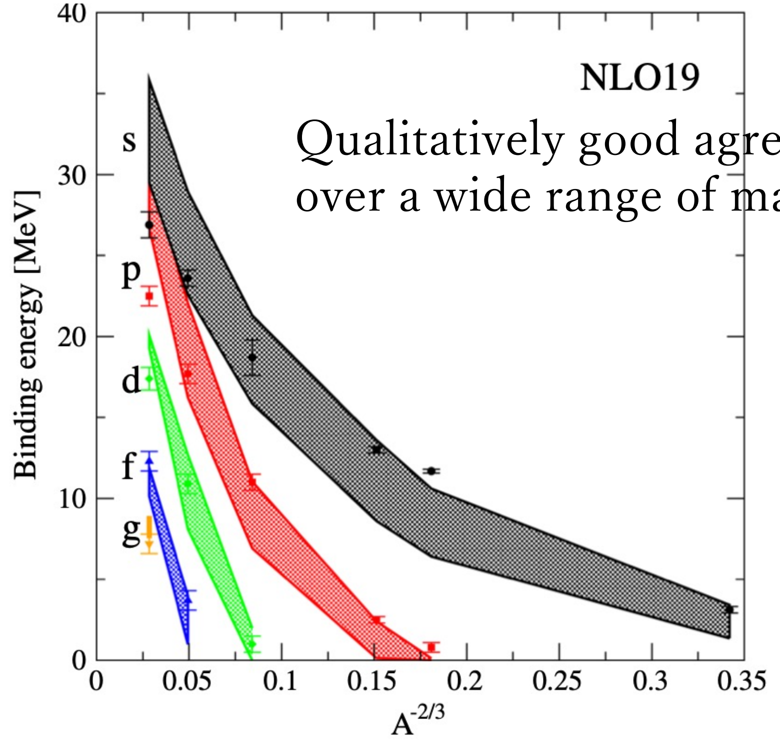

Qualitatively good agreement with data over a wide range of mass number

Sizable cutoff dependence
→ Would be reduced at higher order and after inclusion of 3BF

Λ binding energy and ΛNN interaction

Energy spectra of $^{13}_{\Lambda}$C, $^{16}_{\Lambda}$O, $^{28}_{\Lambda}$Si, $^{51}_{\Lambda}$V, $^{89}_{\Lambda}$Y, $^{139}_{\Lambda}$La, $^{208}_{\Lambda}$Pb with ESC16 model

M.M. Nagels et al. Phys. Rev. C99, 044003 (2019)

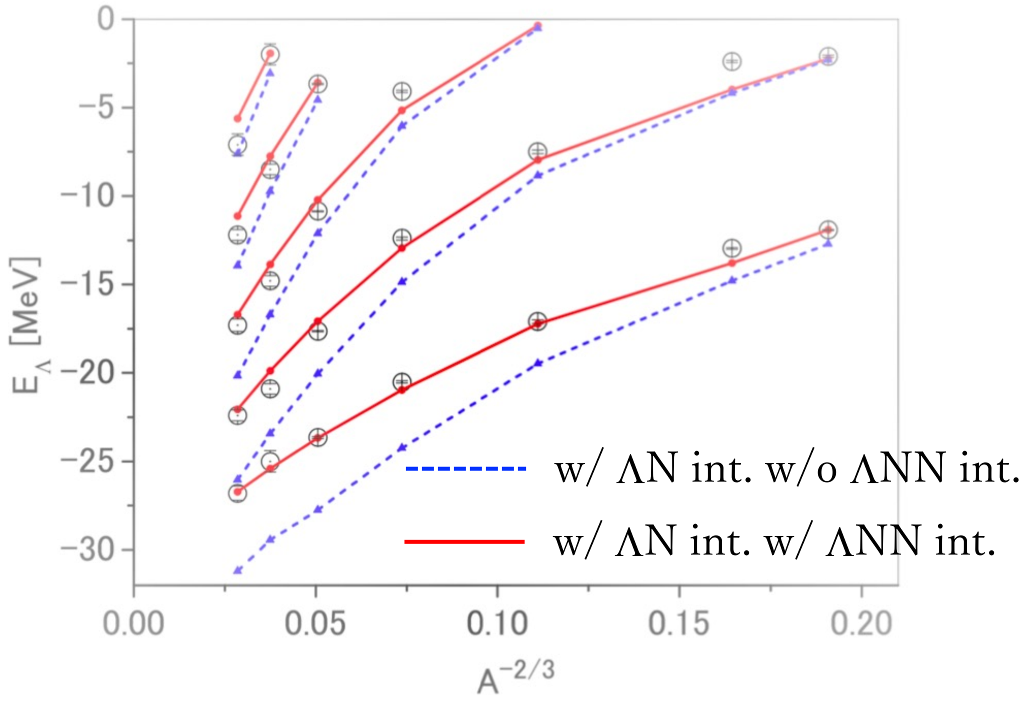

Essential measurement to derive ΛNN int.

ESC16 need ΛNN repulsive interaction to explain Λ hypernuclear bounding energy

Isaka et al. pointed out that choice of two-body ΛN interaction has large effect of theoretical calculation

M. Isaka et al., Phys. Rev. C 95, 044308 (2017)

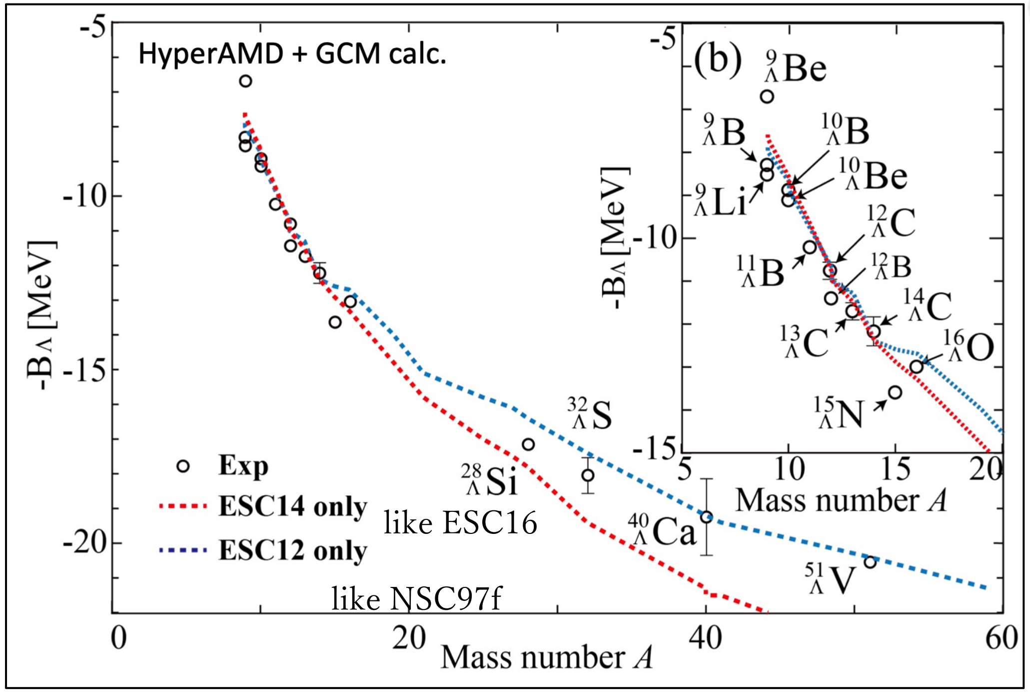

ESC12 (similar with NSC97f) can explain $-B_\Lambda$ w/o ΛNN repulsive int.

ESC14 (similar with ESC16) need ΛNN repulsive int.

ΛN interaction and its uncertainty

Energy spectra of $^{13}_{\Lambda}$C, $^{16}_{\Lambda}$O, $^{28}_{\Lambda}$Si, $^{51}_{\Lambda}$V, $^{89}_{\Lambda}$Y, $^{139}_{\Lambda}$La, $^{208}_{\Lambda}$Pb with ESC16 model

M.M. Nagels et al. Phys. Rev. C99, 044003 (2019)

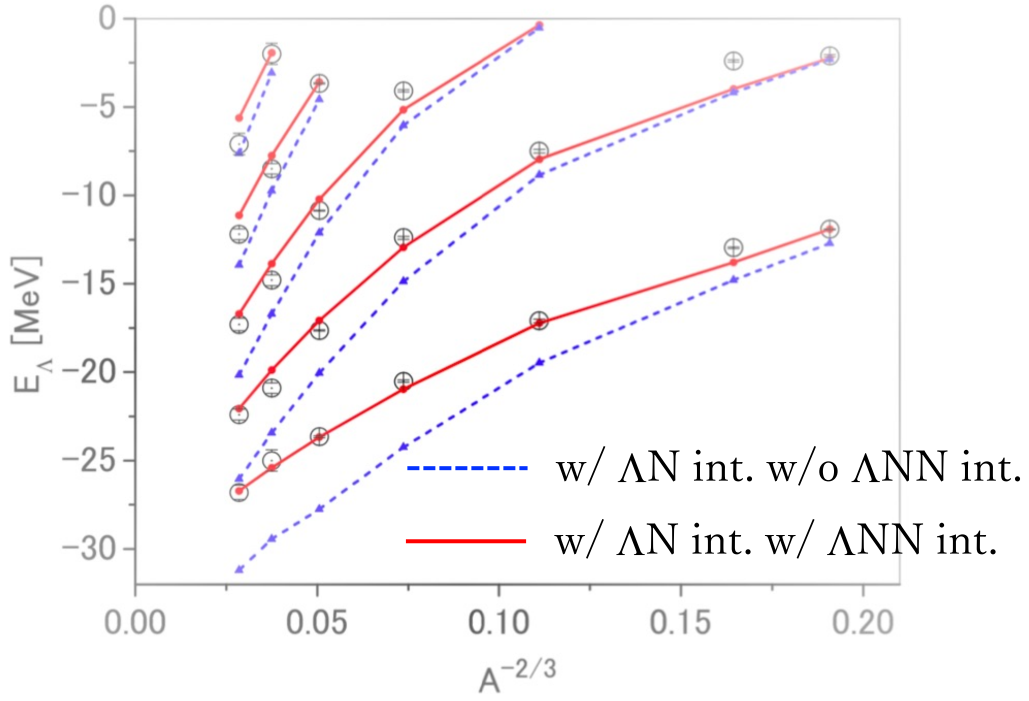

Essential measurement to derive ΛNN int.

Isaka et al. pointed out that choice of two-body ΛN interaction has large effect of theoretical calculation

M. Isaka et al., Phys. Rev. C 95, 044308 (2017)

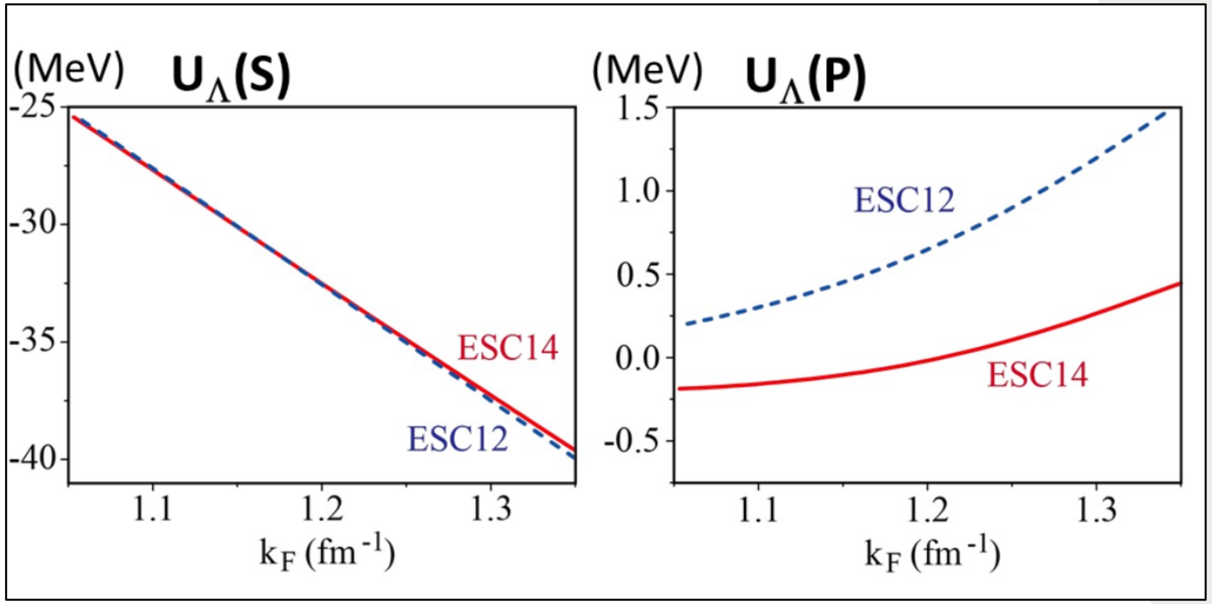

Large P-wave uncertainty of Potential

ESC12 can explain $-B_\Lambda$ w/o ΛNN repulsive int.

ESC14 need ΛNN repulsive int.

ΛN interaction and its uncertainty

Paper of chiral EFT J. Haidenbauer et al. Eur. Phys. J. A. (2020) 56:91

> allow one to pin down the interaction in the $S = -1$ sector. It should be emphasized that the aspects discussed above apply only to the interaction in the S waves. Since there are practically no data for differential observables, it is impossible to fix the YN contact terms in the P-waves. In this case, imple-

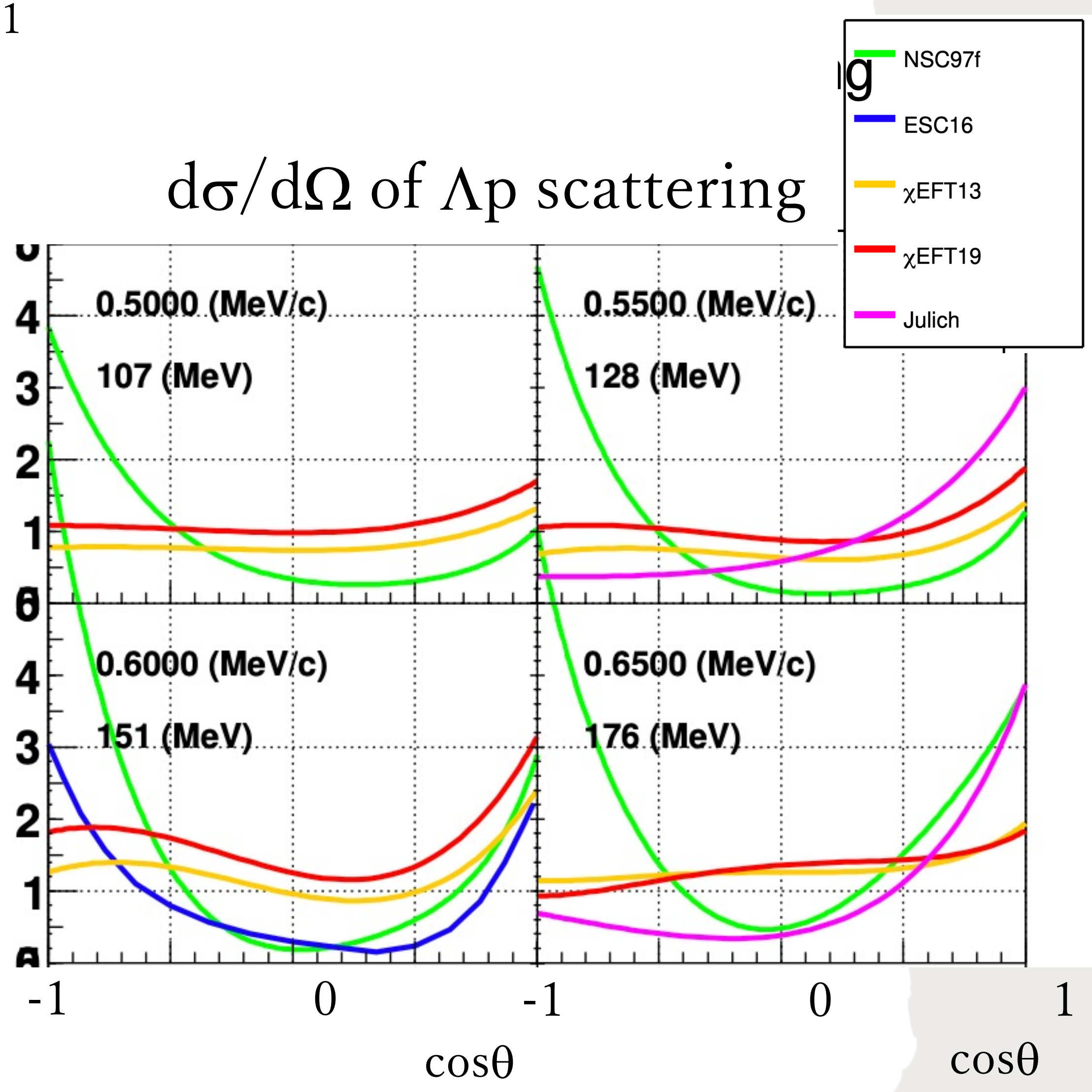

Even for the ΛN interaction, there are large uncertainty in the P-wave interaction.

Total cross section might be similar for each model. However, the angular dependence is very different.

We need accurate scattering data in the P-wave and higher regions

As many scattering observables as possible to construct realistic YN interaction

Conventional representation of elastic scattering

From S. Ishikawa et al.
PRC 69, 034001 (2004)

Scattering amplitude in $\frac{\vec{1}}{2}+\frac{\vec{1}}{2}\rightarrow\frac{\vec{1}}{2}+\frac{\vec{1}}{2}$ scattering : → 4 x 4 matrix

→ 6 components from the restriction of parity conservation and time-reversal invariance

spin-independent spin-spin symmetric LS (ΔS=0) anti-symmetric LS (ΔS=1) Tensor

T matrix

$$\boldsymbol{M} = V_{\mathrm{c}} + V_{\sigma}(\boldsymbol{s}_a\cdot\boldsymbol{s}_b) + V_{\mathrm{SLS}}(\boldsymbol{s}_a+\boldsymbol{s}_b)\cdot\boldsymbol{L} + V_{\mathrm{ALS}}(\boldsymbol{s}_a-\boldsymbol{s}_b)\cdot\boldsymbol{L} + V_{\mathrm{T}}([\boldsymbol{s}_a\otimes\boldsymbol{s}_b]^{(2)}\cdot\boldsymbol{Y}_2(\hat{\boldsymbol{r}})),$$

Scalar amplitude

$U_\alpha \equiv <\boldsymbol{k}_f|V_c|\boldsymbol{k}_i>, U_\beta \equiv <\boldsymbol{k}_f|V_\sigma|\boldsymbol{k}_i>$

Vector amplitude

$S_{ALS} \equiv <\boldsymbol{k}_f|V_{ALS}L_1|\boldsymbol{k}_i>, S_{ALS} \equiv <\boldsymbol{k}_f|V_{SLS}L_1|\boldsymbol{k}_i>$

Tensor amplitude

$T_j = \frac{1}{2}<\boldsymbol{k}_f|V_T Y_{2j-1}|\boldsymbol{k}_i>$

<u>We are going to measure following observables.</u>

Differential cross section

$$\left(\frac{d\sigma}{d\Omega}\right) = \frac{1}{4}\mathrm{Tr}(MM^\dagger) = |U_\alpha|^2 + \frac{3}{16}|U_\beta|^2 + \frac{1}{2}(|S_{SLS}|^2 + |S_{ALS}|^2) + \frac{1}{4}|T_1|^2 + \frac{1}{2}(|T_2|^2 + |T_3|^2).$$

Analyzing power (Polarization)

$$A_y(Y) = -\frac{1}{\sqrt{2}\sigma(\theta)}\mathrm{Im}\left\{(U_\alpha + \frac{1}{4}U_\beta)^* S_{SLS} + (U_\alpha - \frac{1}{4}U_\beta)^* S_{ALS} - \frac{1}{2}T_\alpha^*(-S_{ALS} + S_{SLS})\right\},$$

Depolarization

$$D_y^y = \frac{1}{\sigma(\theta)}\mathrm{Re}\left\{\frac{1}{2\sqrt{3}}\left(U_0 + \frac{1}{\sqrt{3}}U_1\right)^* U_1 + \frac{1}{2}\left(U_0 - \frac{1}{\sqrt{3}}U_1\right)^*\left(\frac{1}{\sqrt{6}}T_1 + T_3\right) - S_1^* S_2 + \frac{1}{2}|S_3|^2 - \frac{1}{\sqrt{6}}T_1^*\left(\frac{1}{\sqrt{6}}T_1 - T_3\right) - \frac{1}{2}|T_2|^2\right\}.$$

Number of observables is still limited to determine each component separately.
But many observables contribute to impose constraints on YN theoretical models.

Analyzing power

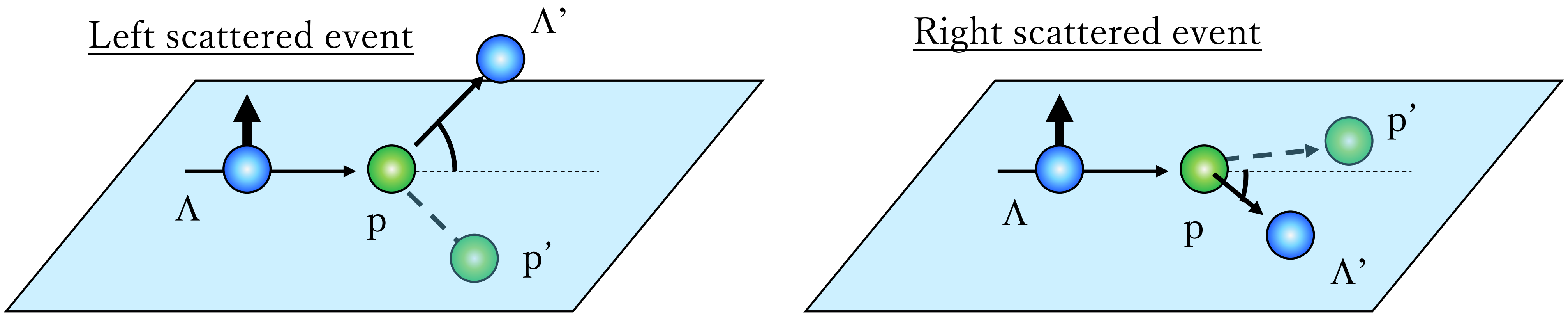

We will measure dσ/dΩ for left and right scatted event separately

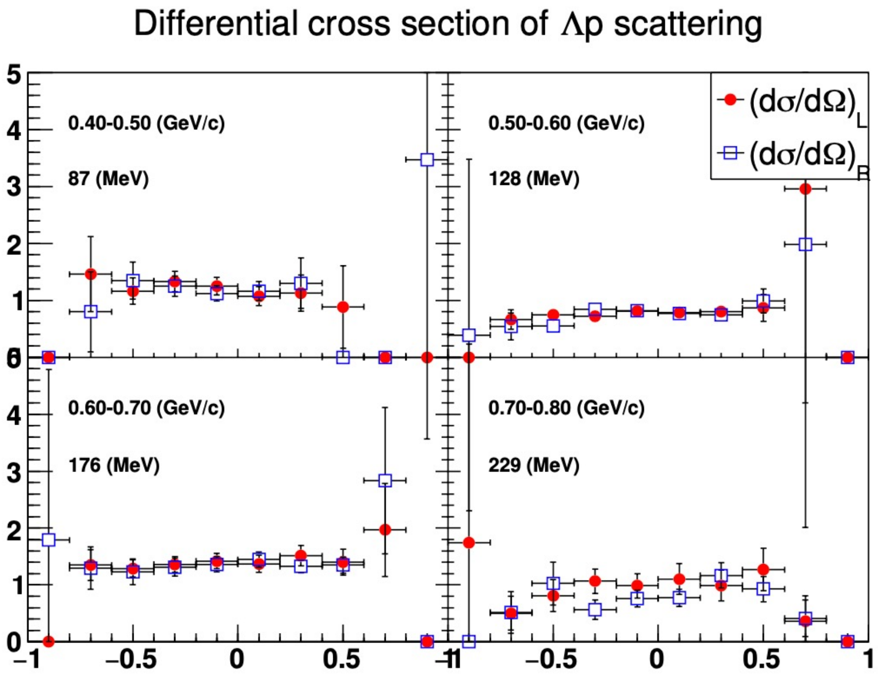

$$A_y(\theta) = \frac{\pi}{2P_\Lambda}\frac{\left(\frac{d\sigma}{d\Omega}\right)_L - \left(\frac{d\sigma}{d\Omega}\right)_R}{\left(\frac{d\sigma}{d\Omega}\right)_L + \left(\frac{d\sigma}{d\Omega}\right)_R}$$

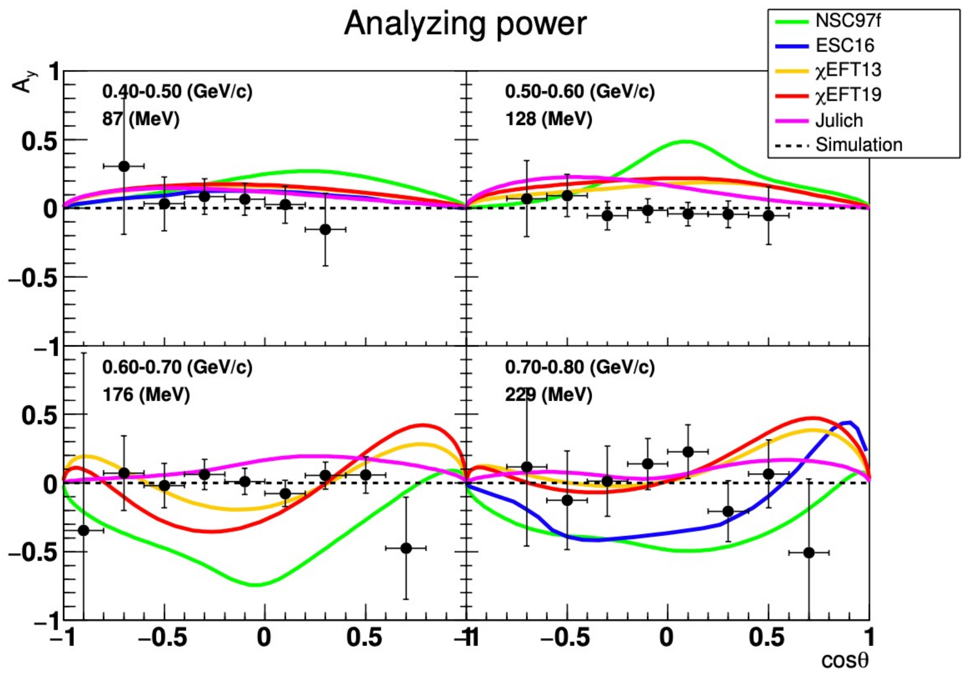

Up/Down asymmetry for depolarization measurement

Spin polarization in the final state

$$P_{scat} = \frac{2}{\alpha}\frac{N_U - N_D}{N_U + N_D} = \frac{P + D_y^y P_{beam}}{1 + PP_{beam}}$$

P_{beam} : Polarization of beam

$$P_{beam} = P(\phi = 0) \times \cos\phi$$

P : Induced polarization by the unpolarized beam

D_y^y : Depolarization

U/D asymmetry of detector is important

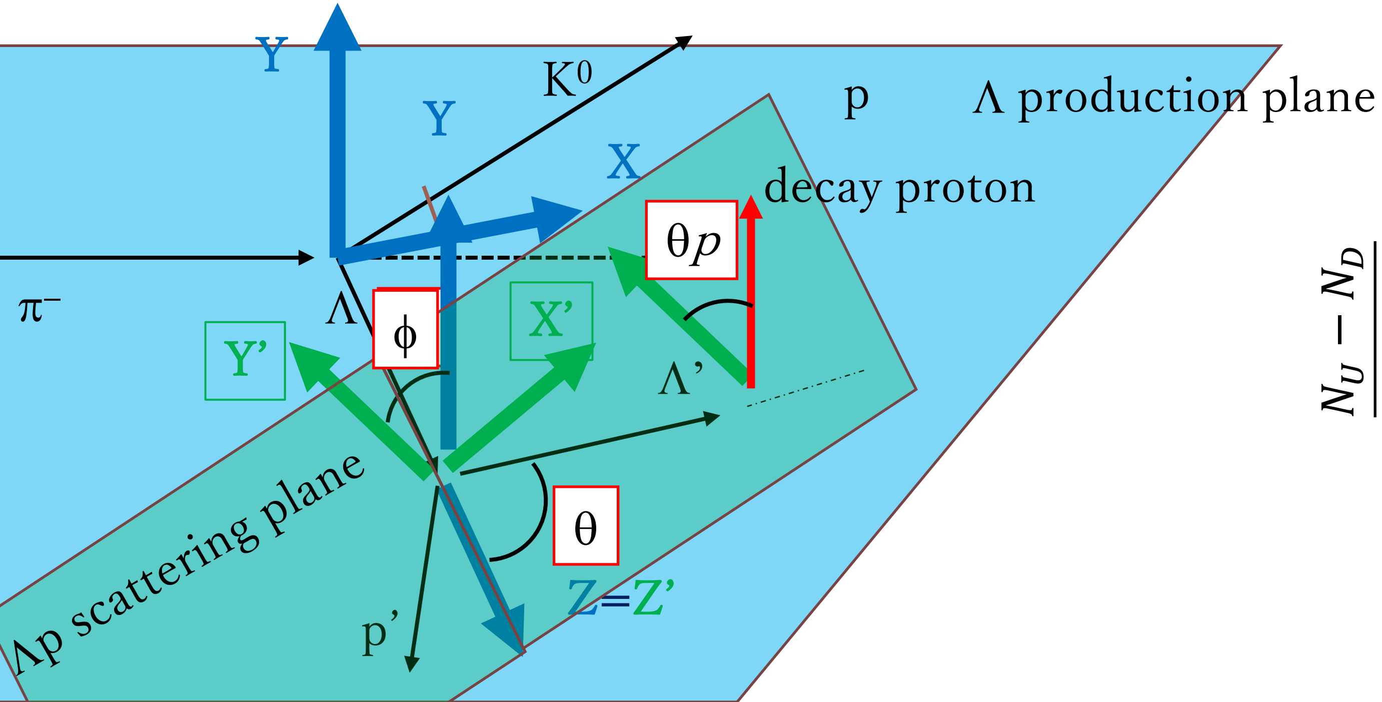

No polarization case ($P_{beam} = 0, P = 0$)
for symmetry study of detector

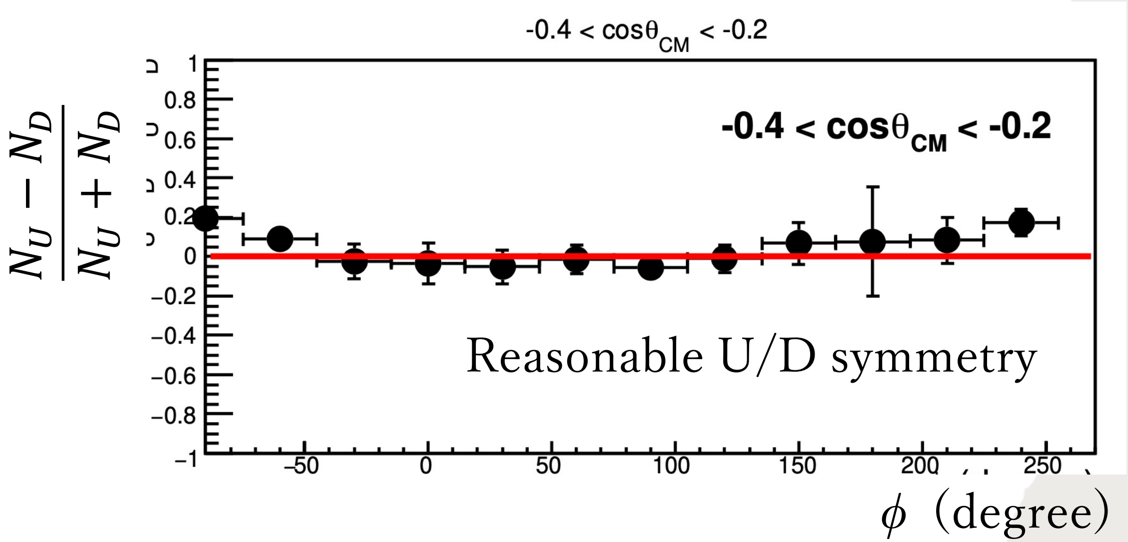

Up/Down asymmetry for depolarization measurement

Spin polarization in the final state

$$P_{scat} = \frac{2}{\alpha}\frac{N_U - N_D}{N_U + N_D} = \frac{P + D_y^y P_{beam}}{1 + P P_{beam}}$$

P_{beam} : Polarization of beam

$$P_{beam} = P(\phi = 0) \times \cos\phi$$

P : Induced polarization by the unpolarized beam

D_y^y : Depolarization

U/D asymmetry of detector is important

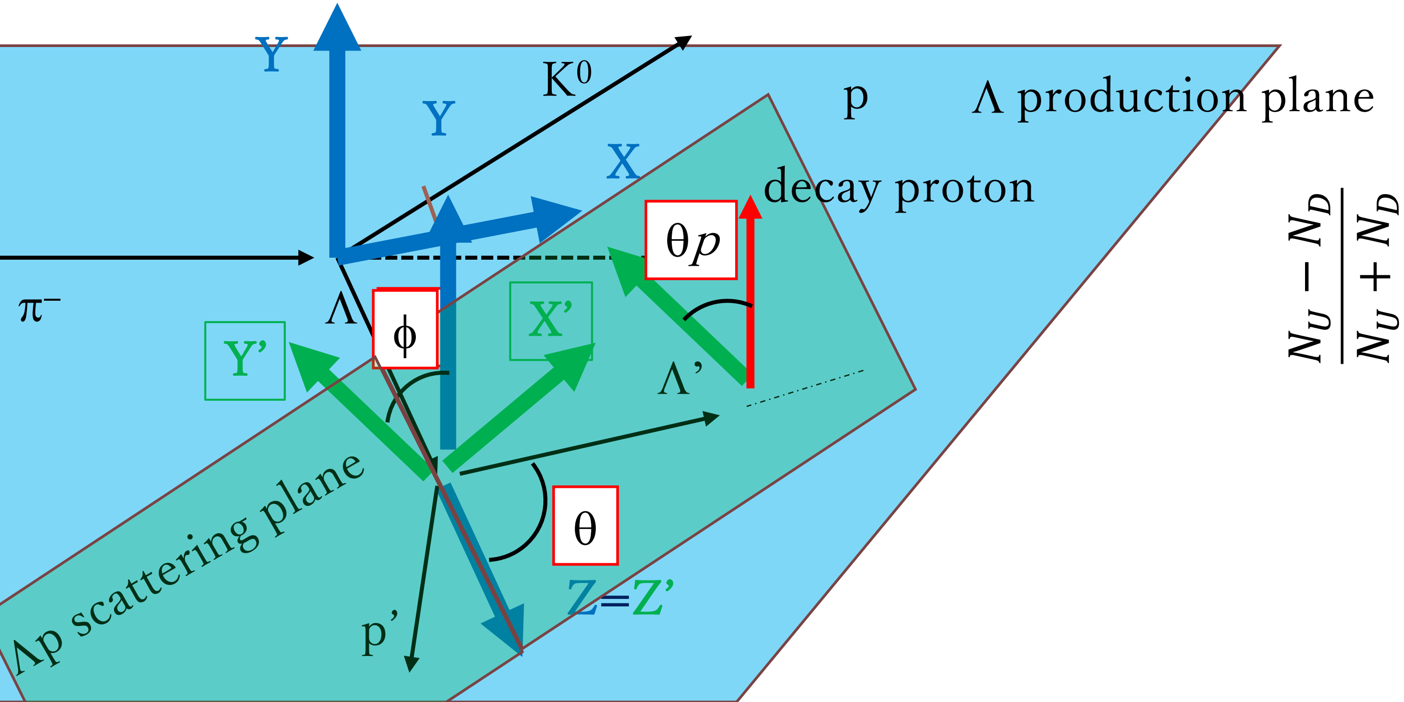

Polarized case

Polarization case $(P_{beam} = 1, P = 0, D_y^y = 1)$

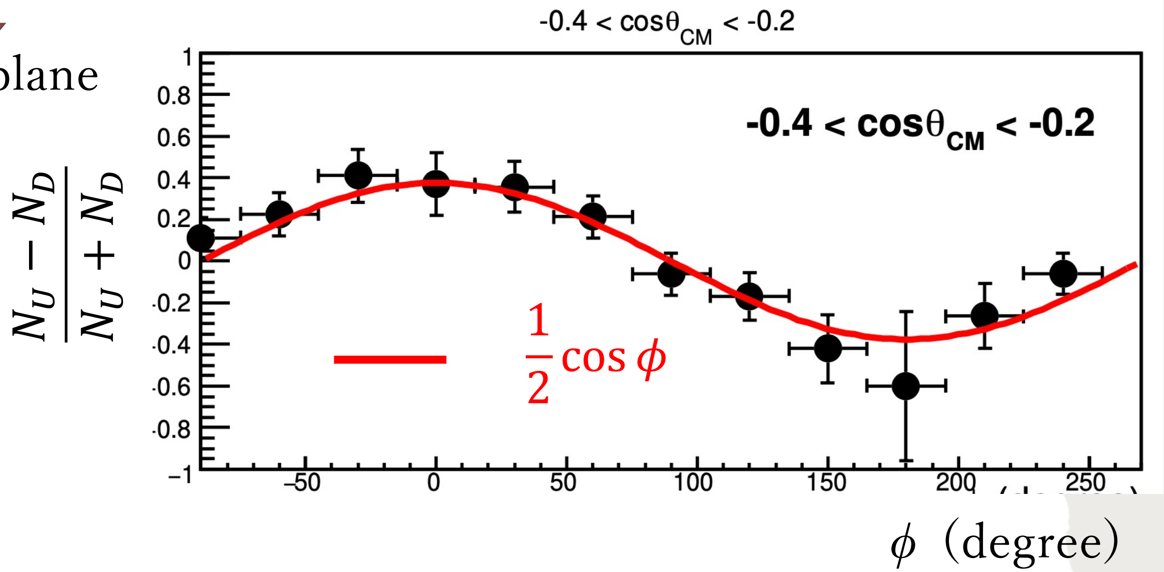

ϕ dependence of U/D asymmetry can be observed

Up/Down asymmetry for depolarization measurement

Spin polarization in the final state

$$P_{scat} = \frac{2}{\alpha}\frac{N_U - N_D}{N_U + N_D} = \frac{P + D_y^y P_{beam}}{1 + P P_{beam}}$$

P_{beam} : Polarization of beam

$$P_{beam} = P(\phi = 0) \times \cos\phi$$

P : Induced polarization by the unpolarized beam

D_y^y : Depolarization

U/D asymmetry of detector is important

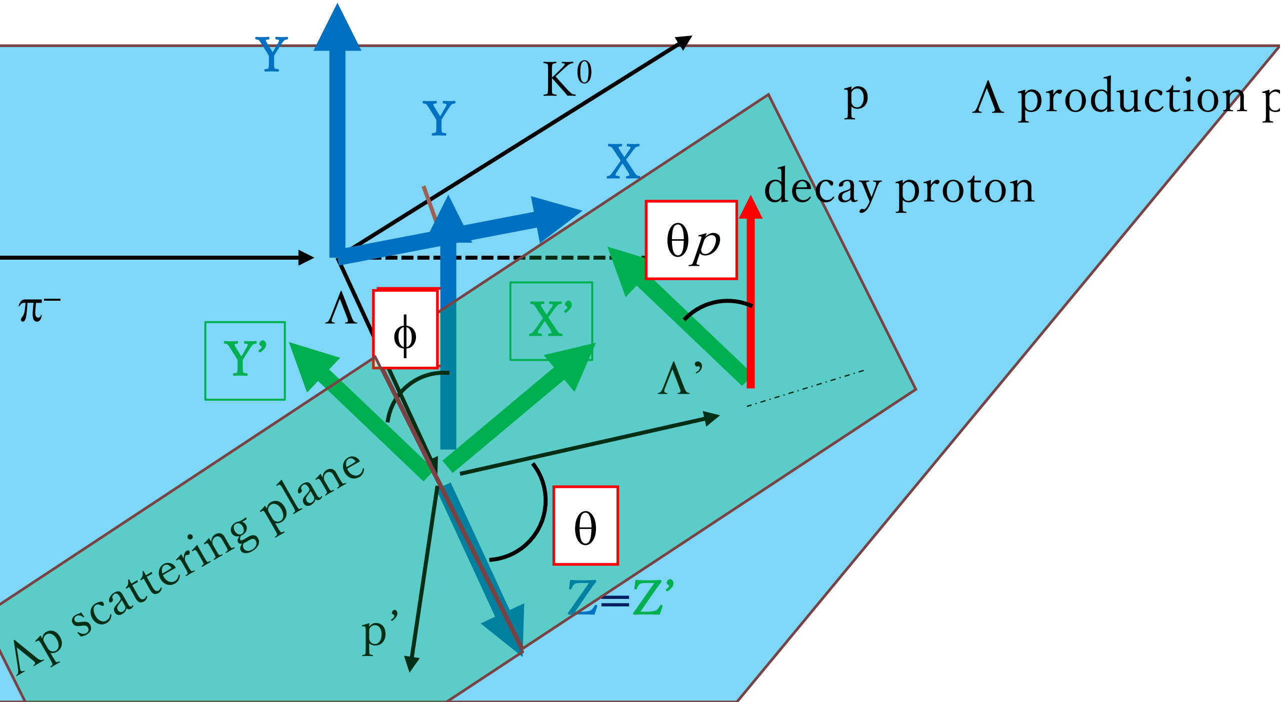

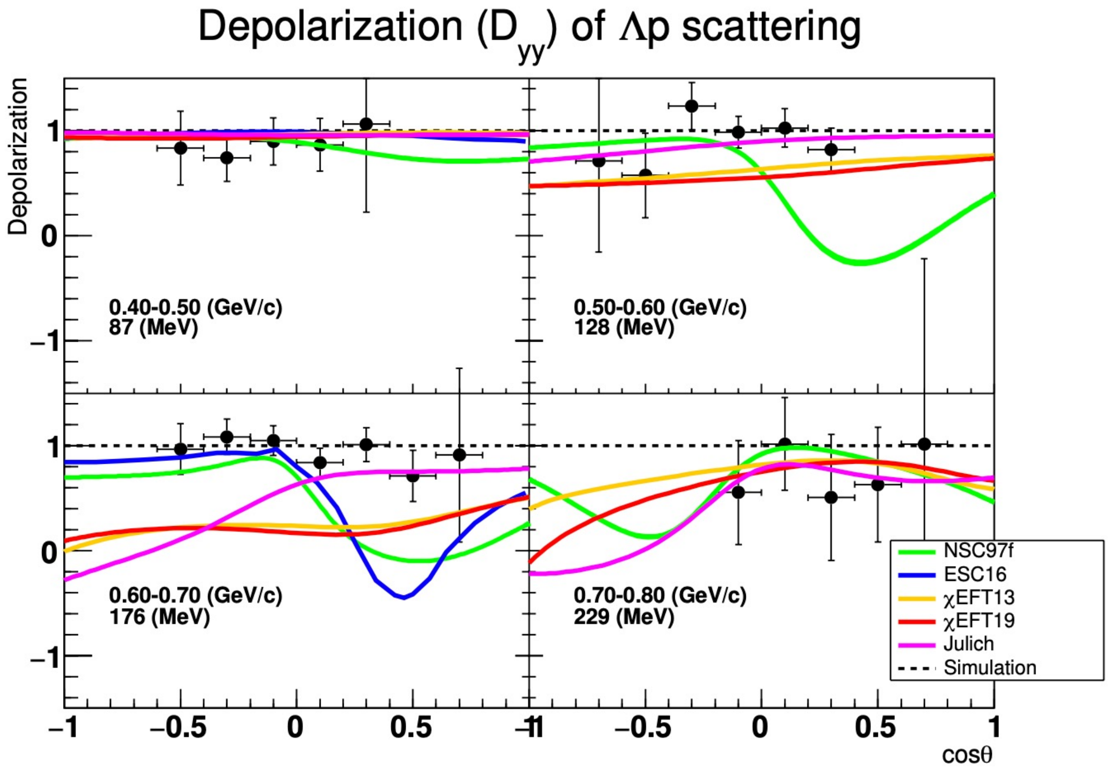

Spin observables in Λp scattering

Simulated results w/ 100M Λ

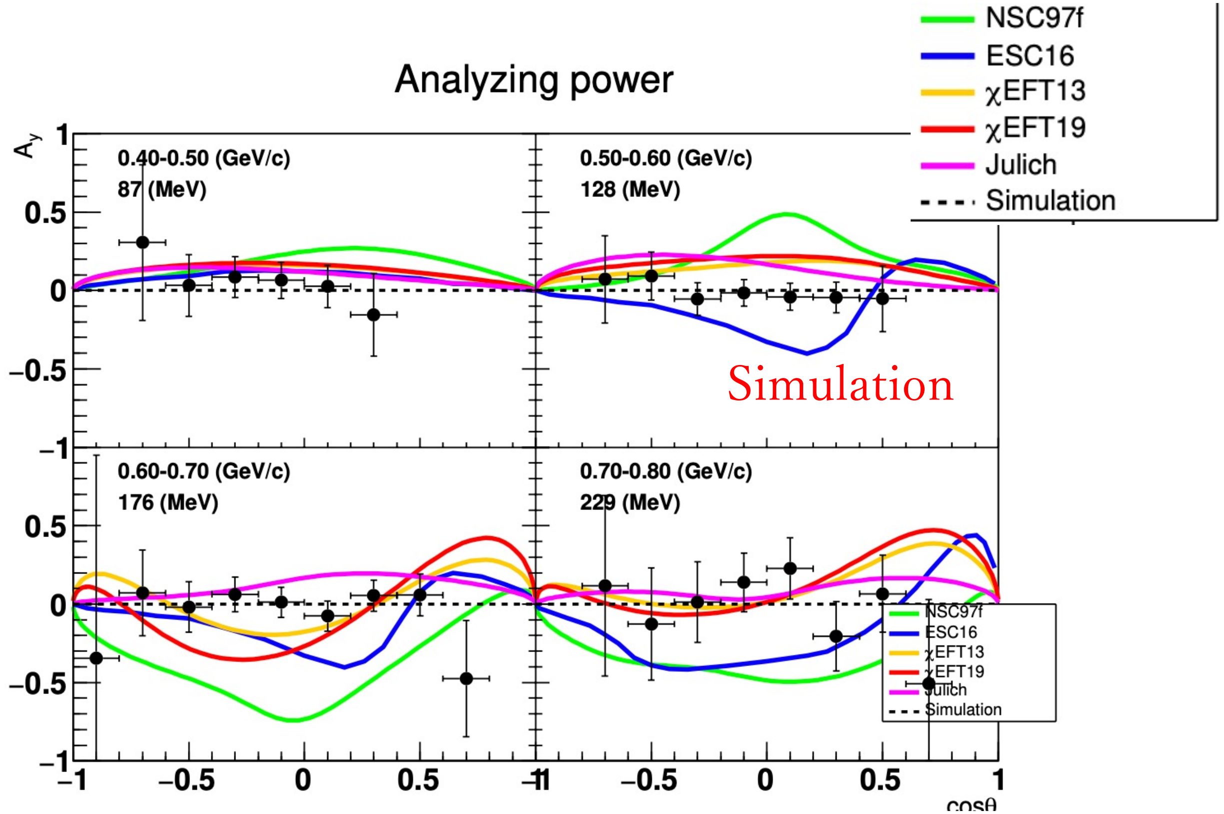

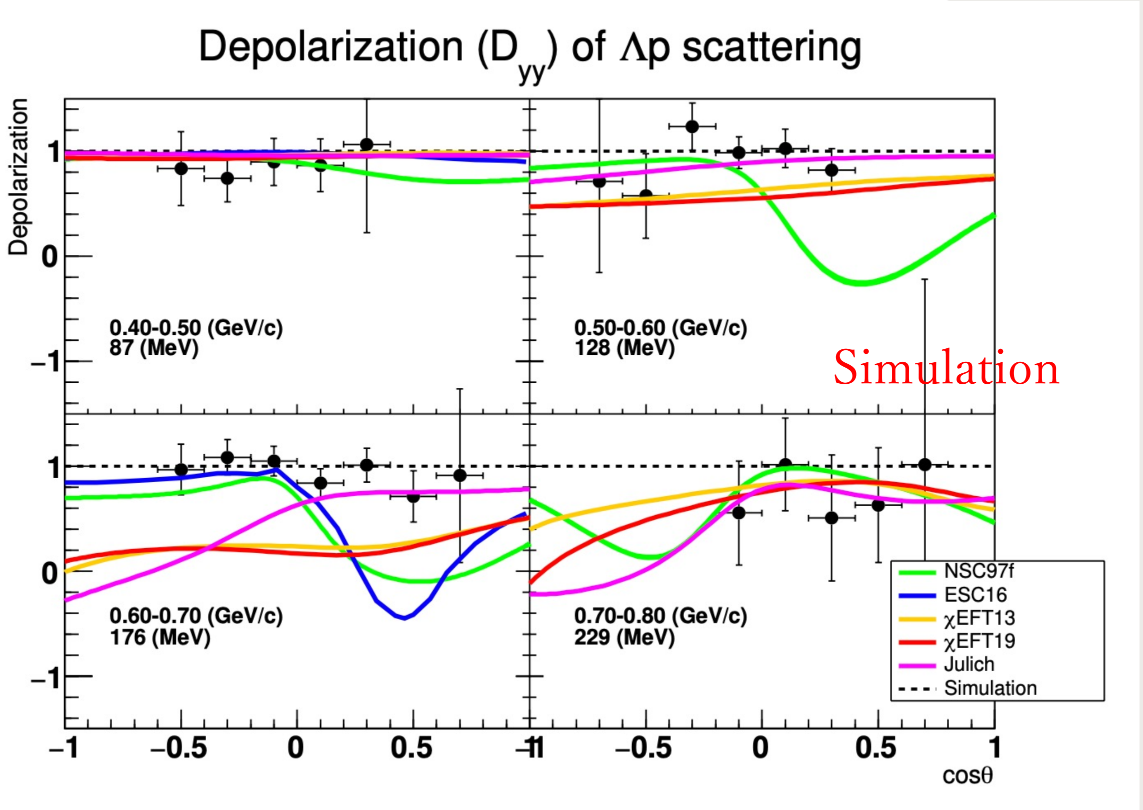

$$A_y(Y) = -\frac{1}{\sqrt{2}\sigma(\theta)}\mathrm{Im}\left\{(U_\alpha + \frac{1}{4}U_\beta)^* S_{SLS} + (U_\alpha - \frac{1}{4}U_\beta)^* S_{ALS} - \frac{1}{2}T_\alpha^*(-S_{ALS} + S_{SLS})\right\},$$

→ Sensitive LS force + ⋯.

$$D_y^y = \frac{1}{\sigma(\theta)}\mathrm{Re}\left\{\frac{1}{2\sqrt{3}}\left(U_0 + \frac{1}{\sqrt{3}}U_1\right)^* U_1 + \frac{1}{2}\left(U_0 - \frac{1}{\sqrt{3}}U_1\right)^*\left(\frac{1}{\sqrt{6}}T_1 + T_3\right) - S_1^* S_2 + \frac{1}{2}|S_3|^2 - \frac{1}{\sqrt{6}}T_1^*\left(\frac{1}{\sqrt{6}}T_1 - T_3\right) - \frac{1}{2}|T_2|^2\right\}.$$

→ Rather sensitive tensor force + ⋯.

In the middle momentum range (0.5~0.7 GeV/c), 10% level accuracy can be achieved.

Toward construction of realistic YN interaction

Even for YN case

We need help of theorist and experience of NN experimentalist.
We are very happy if we make a such collaboration for the phase-shift analysis

Two-body scattering data → Phase-shift analysis

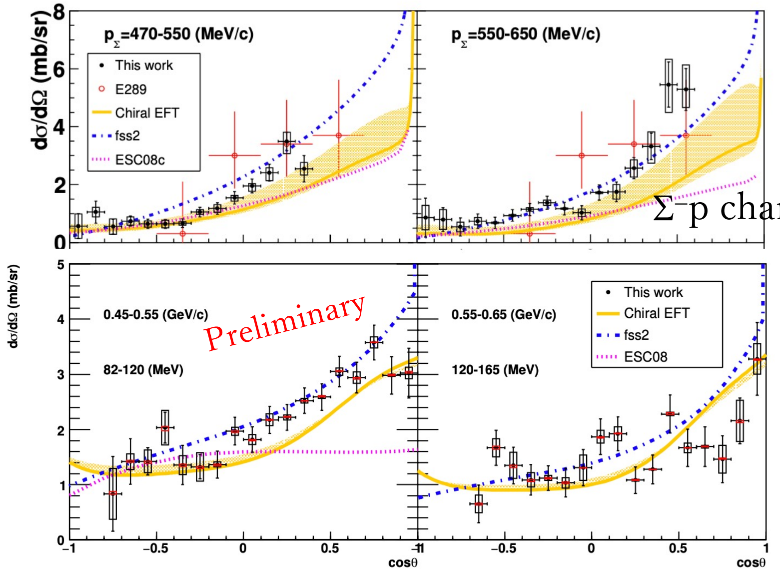

Σ^-p channel

$\Sigma^-p \rightarrow \Lambda n$ channel

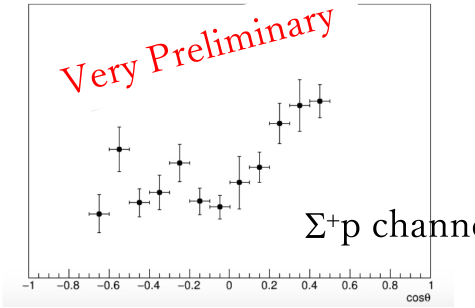

Σ^+p channel

ΣN channel would be available in very near future

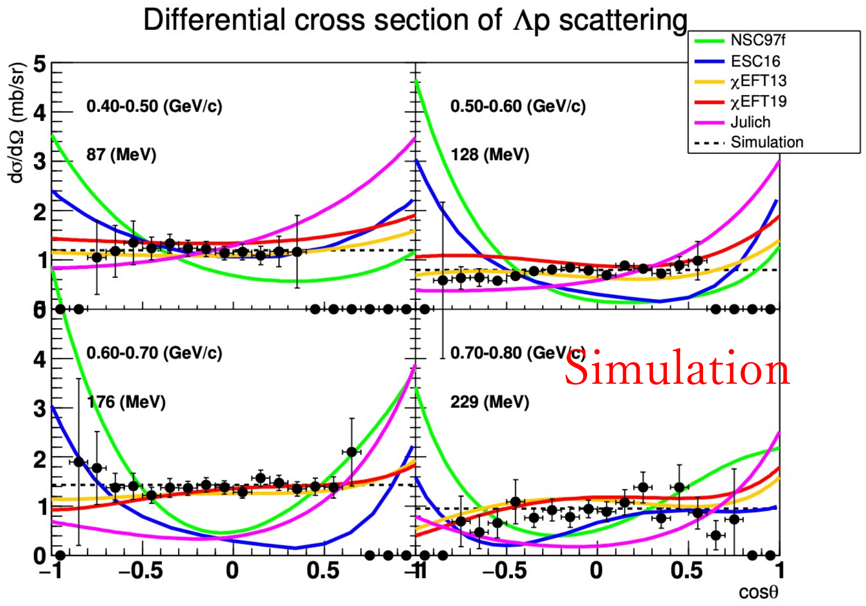

ΛN channel will be measured after hall extension project

Small relative-momentum region

S. Acharya et al. Phys. Rev. C 99 024001 (2019)

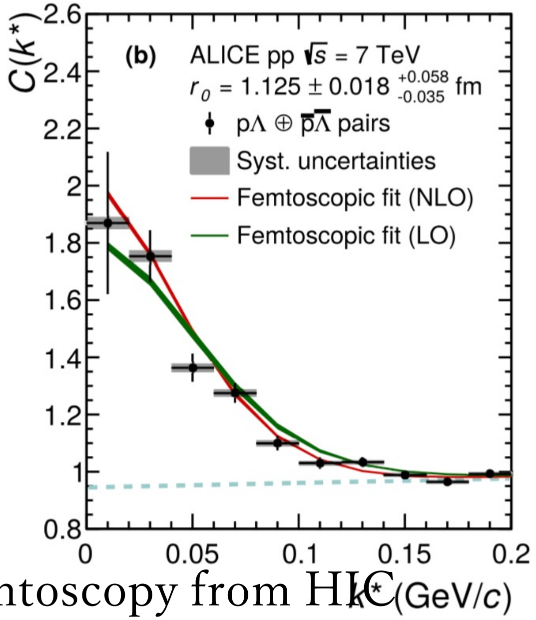

Femtoscopy from HIC

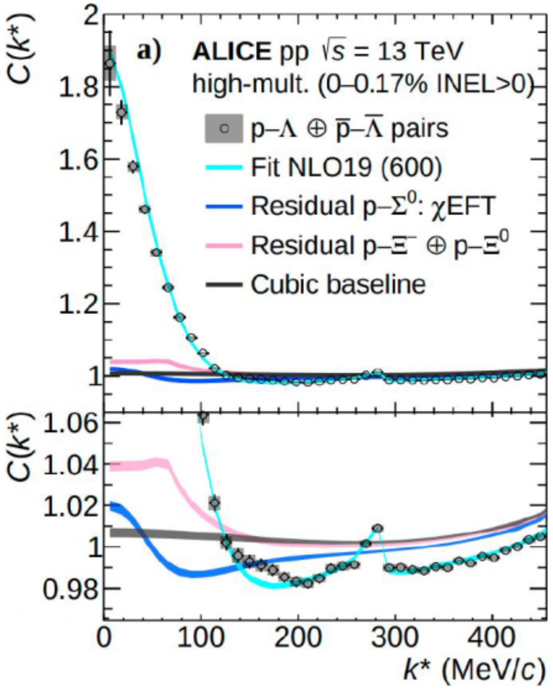

- ✓ High statistics !
- ✓ Correlations for many baryon pairs and baryon-meson pairs !
- ✓ More sensitive for small relative-momentum region (S-wave region)

Intermediate energy region

- ✓ Become feasible !
- ✓ Differential information can be obtained.
- ✓ Spin observables can be measured !
- ✓ More sensitive for intermediate energy region
  - ✓ Hyperon production kinematics
  - ✓ Experimental reason

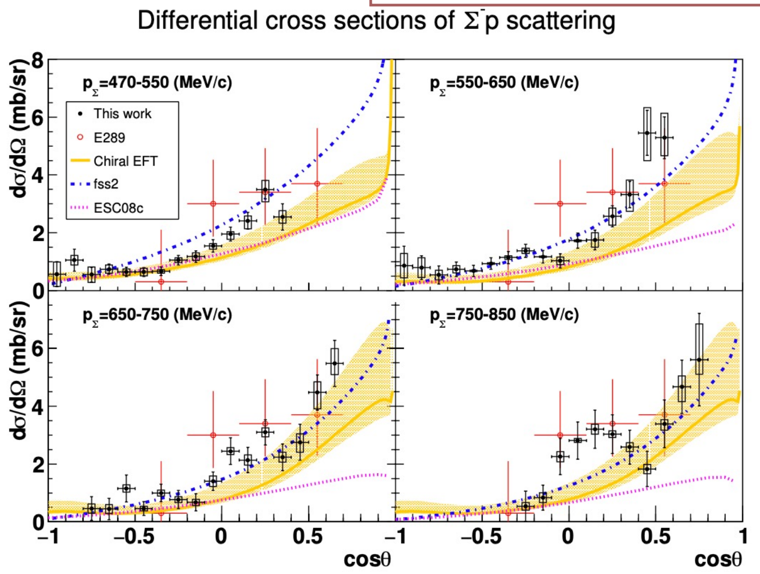

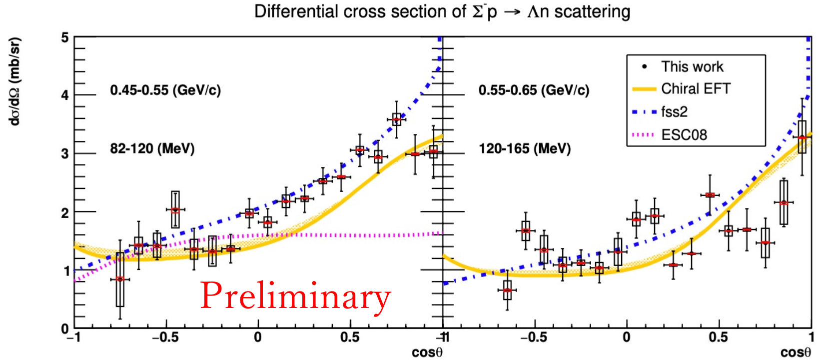

To be submitted soon

Yp scattering experiment at J-PARC

Mass number dependence

Widely used interaction in hypernuclear physics

Nijmegen potential + G-matrix calculation is powerful method to study hypernuclei and neutron star

$^{16}O+^{16}O$ elastic scattering at E/A=70 MeV

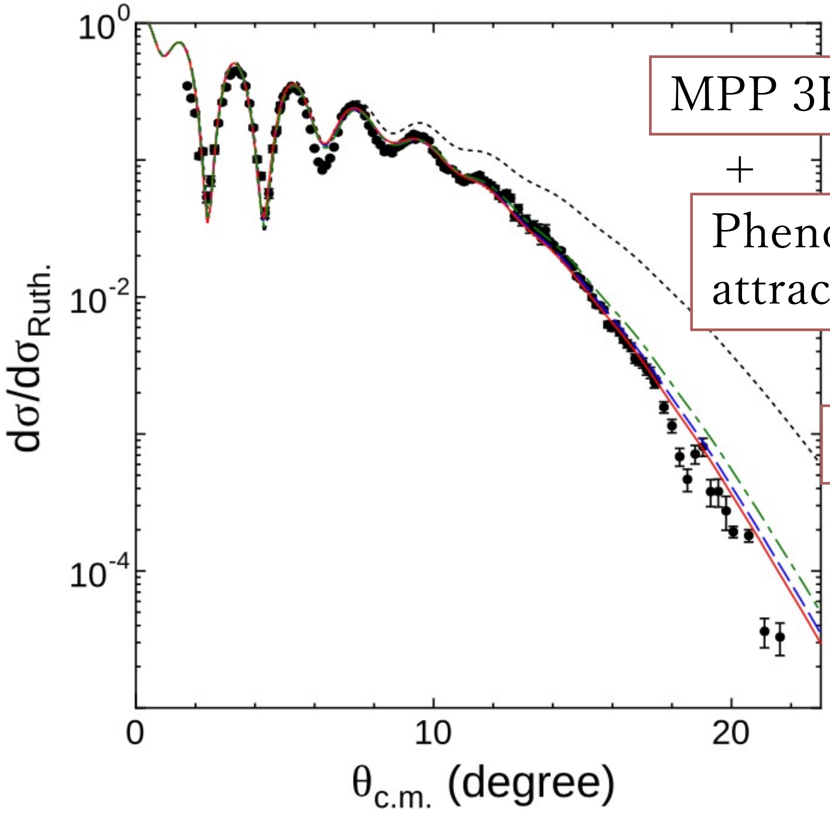

MPP 3B repulsive force

+

Phenomenological 3B attractive force

+

ESC YN model

Yamamoto et al. Phys. Rev. C 90 (2014) 045805

M. M. Nagels et al., Phys. Rev. C 99 (2019) 04403

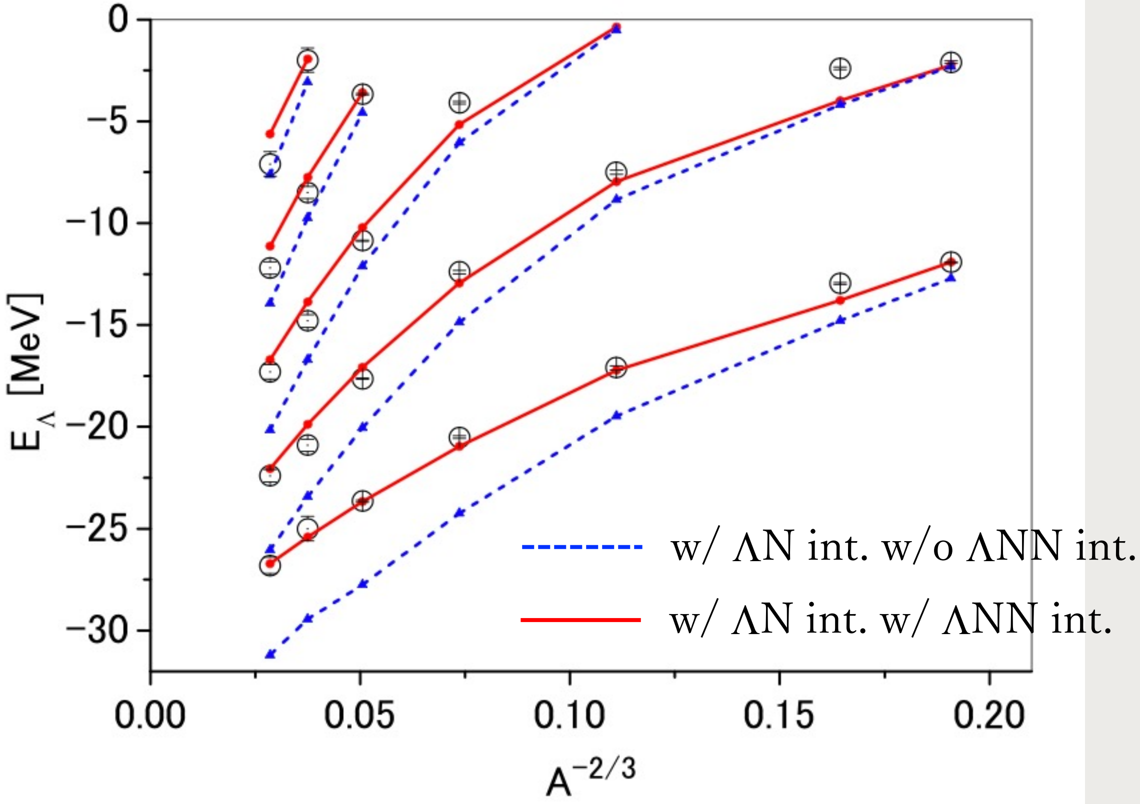

Triggered HIHR/K1.1 project

Neutron star matter and YN/YNN interactions

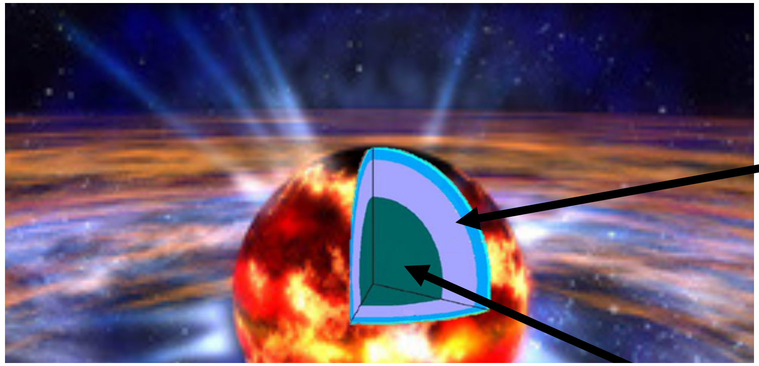

Neutron Matter

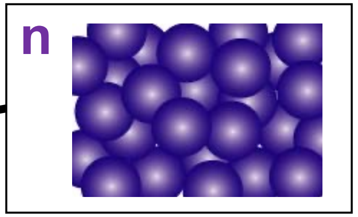

Strange Hadronic Matter

Hyperons should appear

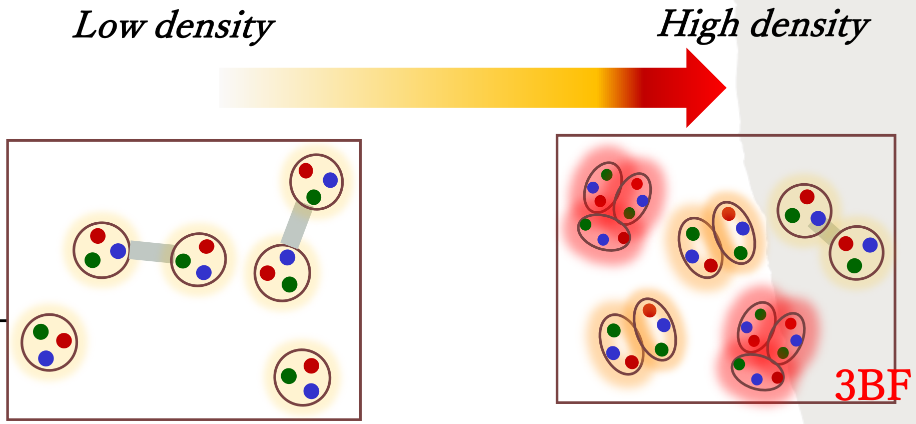

We have to see a tiny fraction of 3BF effect

We need

- Realistic YN interaction model
- Precise Λ binding energy for wide-mass range for density dependence of ΛN interaction → ΛNN interaction

J. Haidenbauer et al., Eur. Phys. J. A (2020) 56:91

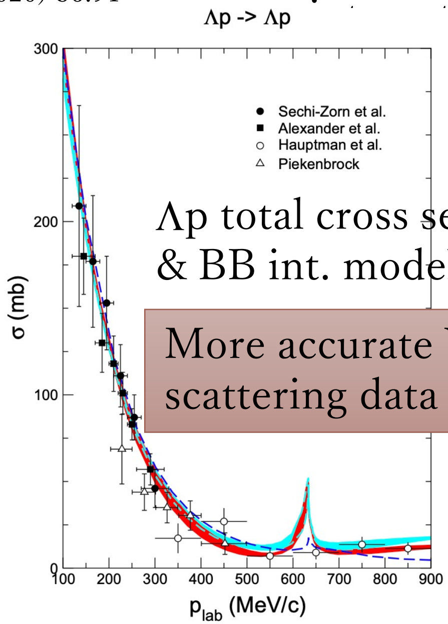

Λp total cross section & BB int. models

More accurate YN scattering data

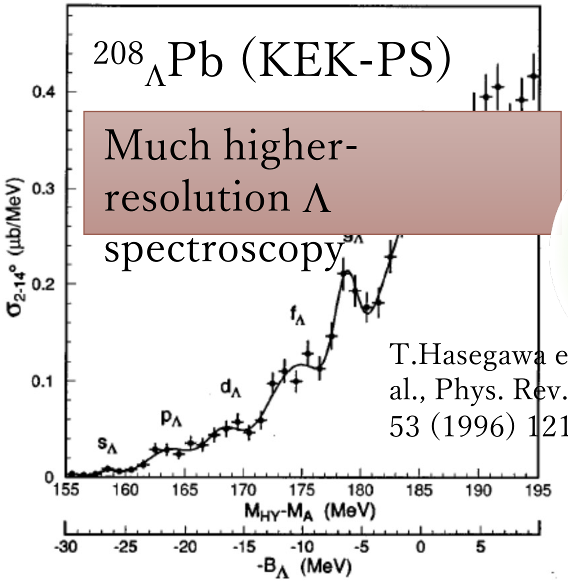

$^{208}{}_{\Lambda}$Pb (KEK-PS)

Much higher-resolution Λ spectroscopy

T.Hasegawa et al., Phys. Rev. C 53 (1996) 1210.

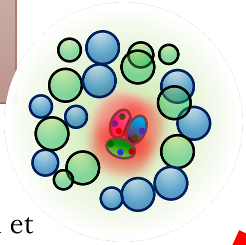

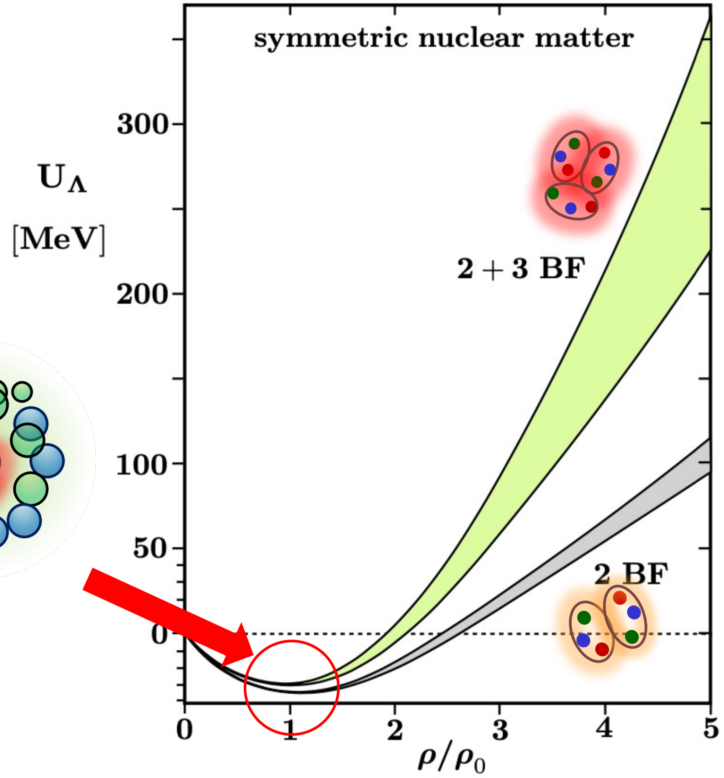

3 BF : Significant repulsive contribution at high density

D. Gerstung et al., Eur. Phys. J. A(2020) 56:175

HIHR/K1.1 physics

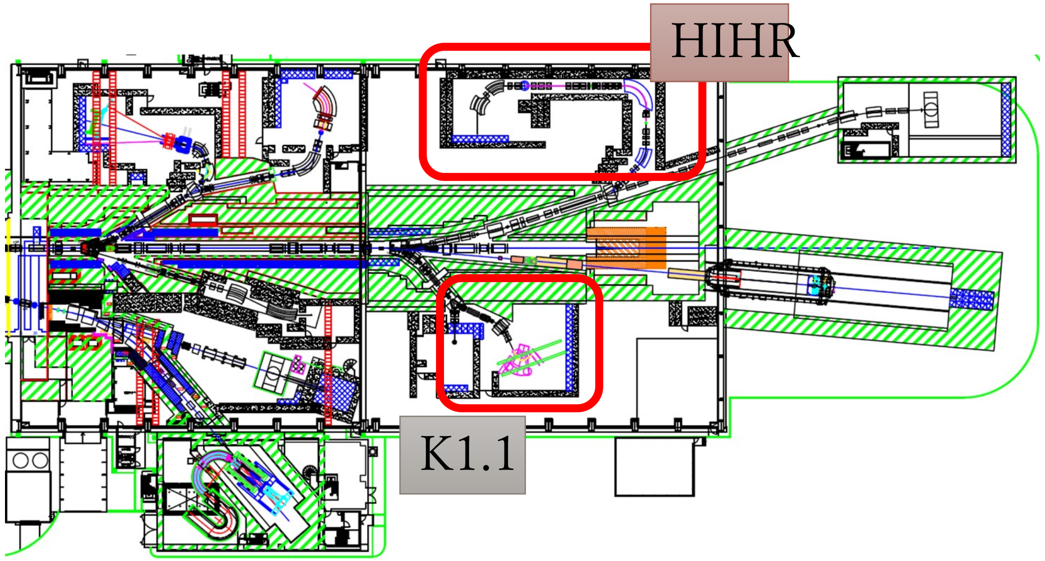

K1.1 beam line

Optimized for S=-1 physics → Suitable to produce polarized Λ

Λp scattering experiment w/ polarized Λ beam

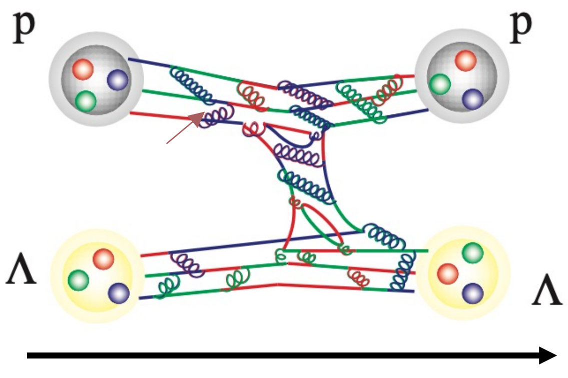

We need accumulation of many YN scattering observables

High-Intensity and High-Resolution beam line

Dispersion-matching beam line → NO need to track beam particles

Potential high-intensity beam at J-PARC can be used

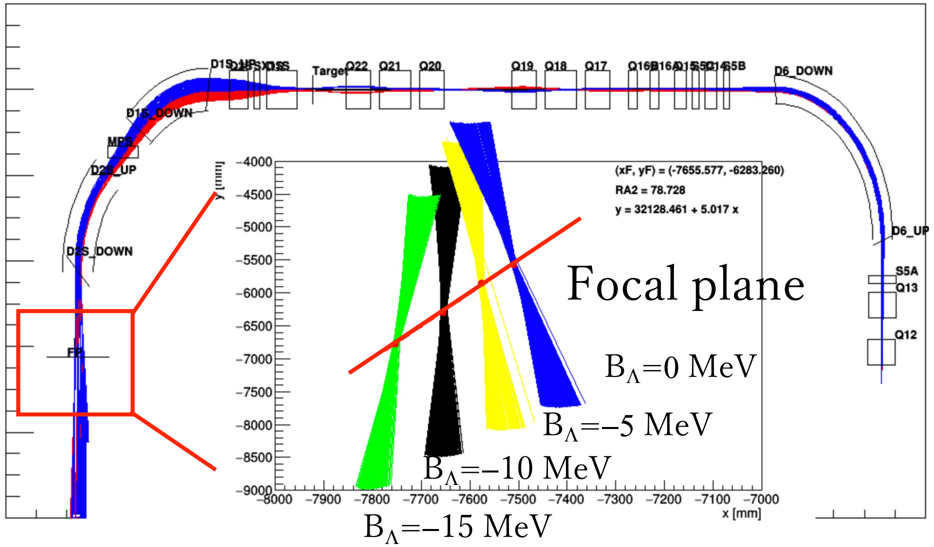

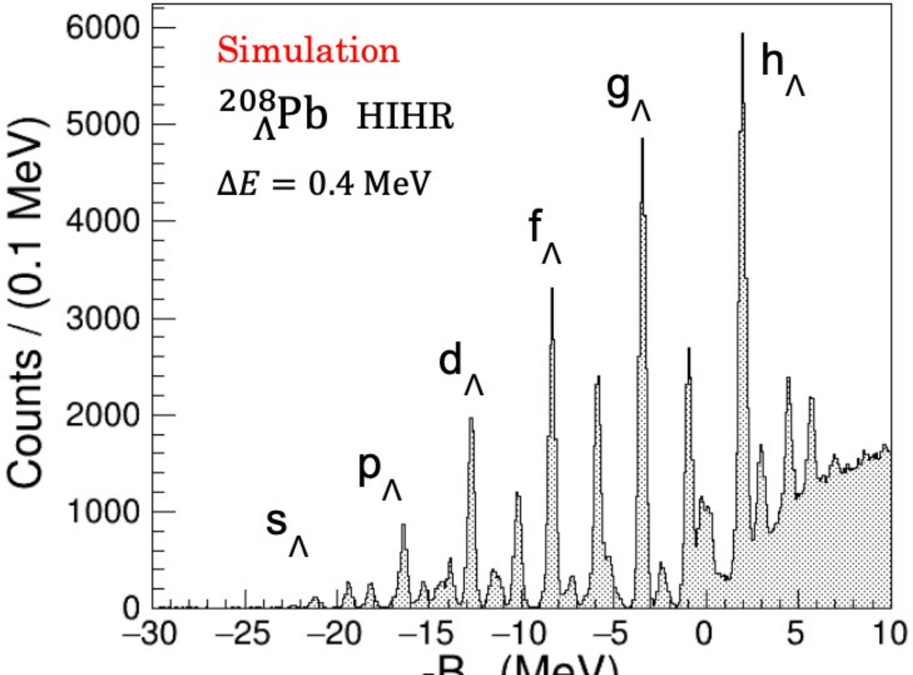

High-resolution Λ hypernuclear spectroscopy at HIHR

ΛNN interaction :
Key of **Hyperon Puzzle**
Small effects to Λ binding energies

Impossible to separate peaks
with a few MeV resolution

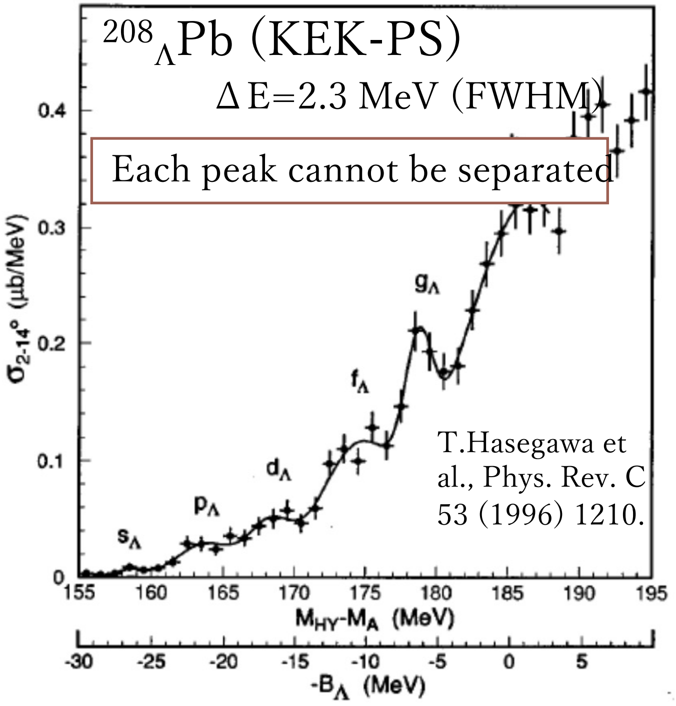

HIHR : Dispersion-matching beam line
→ Realize **high-resolution** spectroscopy **without beam intensity limit**
High intensity π beam of **> 10^8 /pulse**
(**~100 times stronger** than KEK-PS)
- Thin target can be used

→ High resolution and various target opti

Better than 0.4 MeV (FWHM) resolution

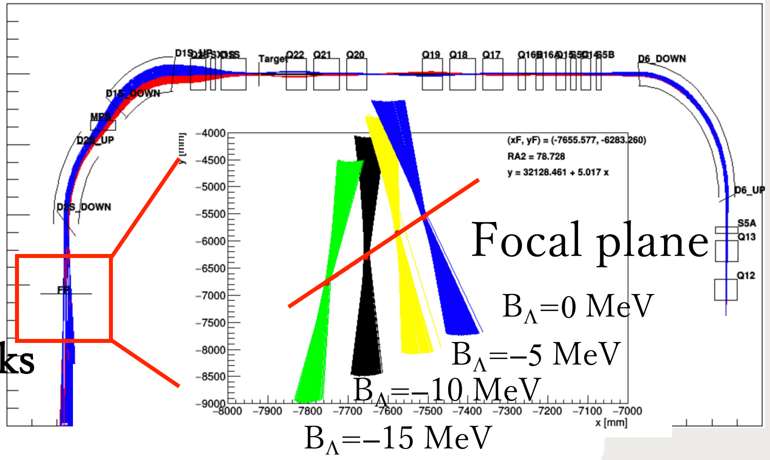

Clear separation **of sub-major as well as major peaks**

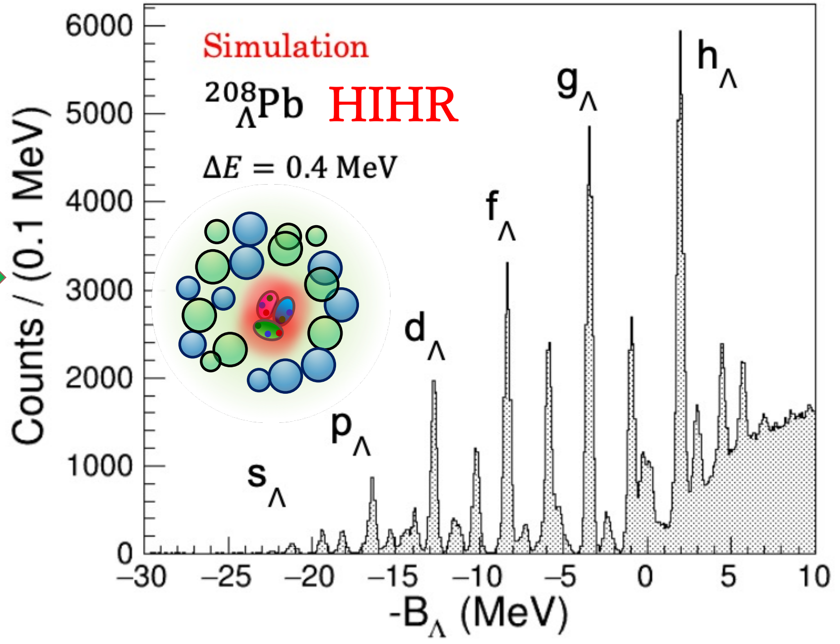

Precise Λ binding energies
for wide-mass range

Density dependence of ΛN interaction (ΛNN interaction)

Calculate U_Λ at high density region
Untangle hyperon puzzle in neutron star

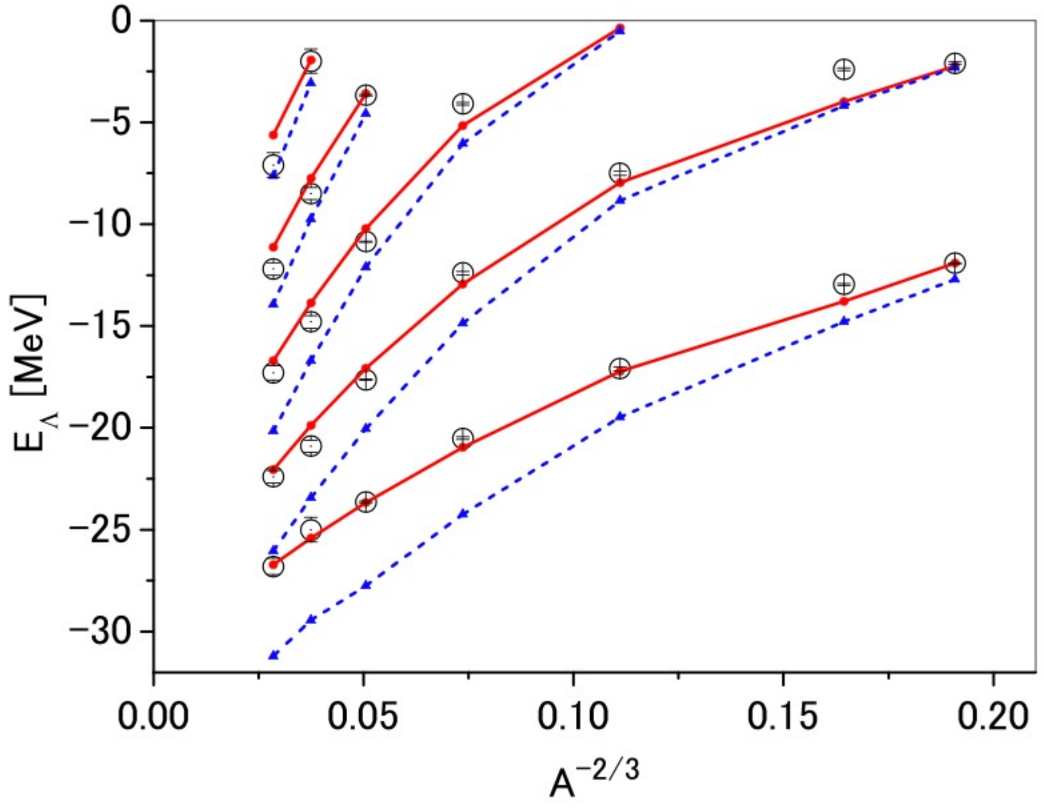

0
−5
−10
−15
−20
−25
−30
E_Λ [MeV]
0.00
0.05
0.10
0.15
0.20
A^−2/3

Chiral EFT

- Underlying chiral symmetry in QCD
- Power counting feature to improve calculation systematically by going to higher order
- Multi baryon force appear naturally and automatically in a consistent implementation of the framework

YN interaction at NLO

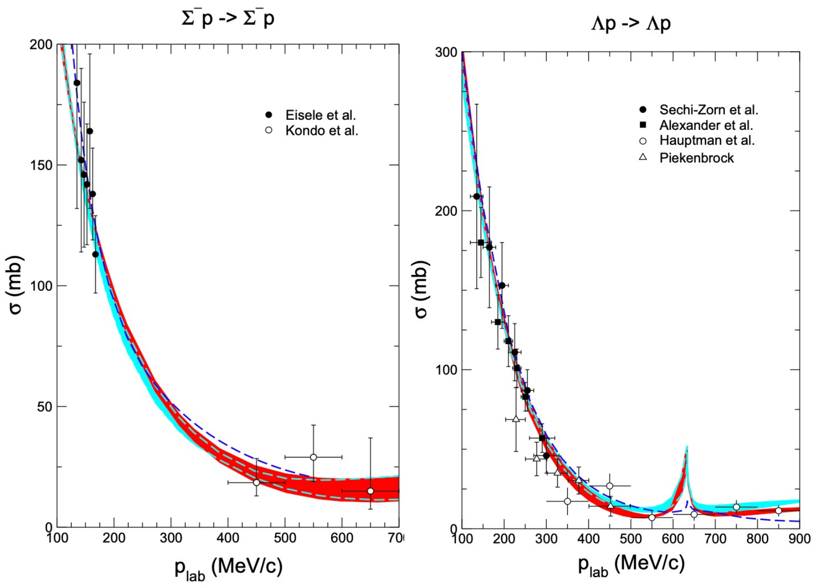

J. Haidenbauer et al., Eur. Phys. J. A (2020) 56:91

J. Haidenbauer et al., Nucl. Phys. A 915 (2013) 24

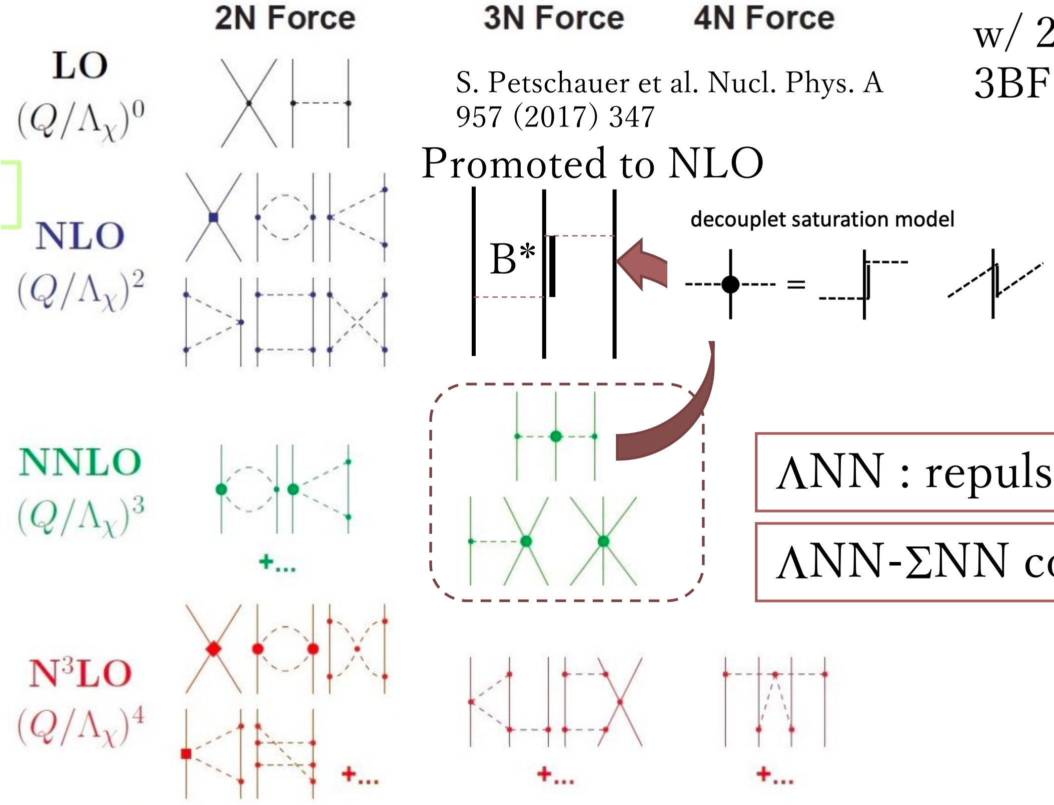

S. Petschauer et al. Nucl. Phys. A 957 (2017) 347

From slide by M. Kohno

Density-dependent effective potential w/ 2π-exchange ΛNN and ΛNN-ΣNN 3BF

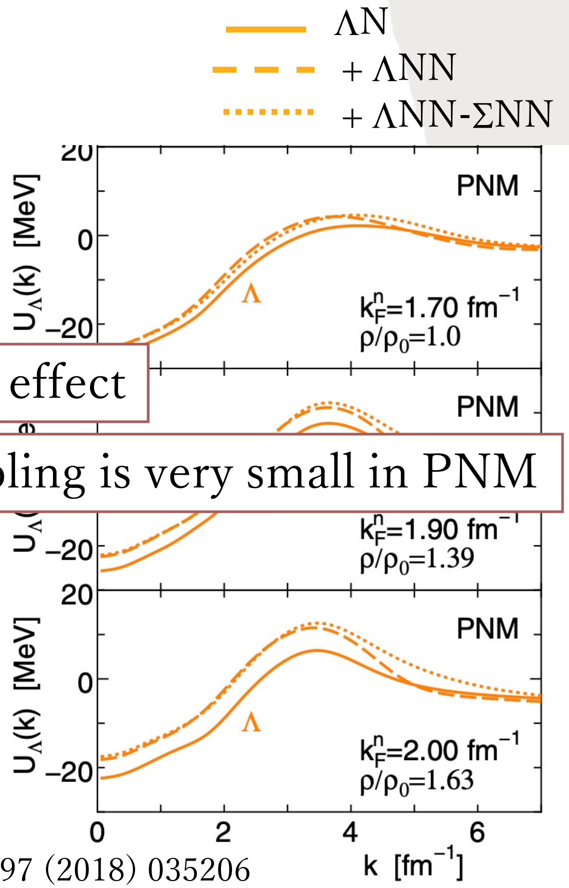

ΛNN : repulsive effect

ΛNN-ΣNN coupling is very small in PNM

M. Kohno, Phys. Rev. C 97 (2018) 035206

Λ binding energy and ΛNN interaction

Energy spectra of $^{13}_{\Lambda}$C, $^{16}_{\Lambda}$O, $^{28}_{\Lambda}$Si, $^{51}_{\Lambda}$V, $^{89}_{\Lambda}$Y, $^{139}_{\Lambda}$La, $^{208}_{\Lambda}$Pb with ESC16 model

M.M. Nagels et al. Phys. Rev. C99, 044003 (2019)

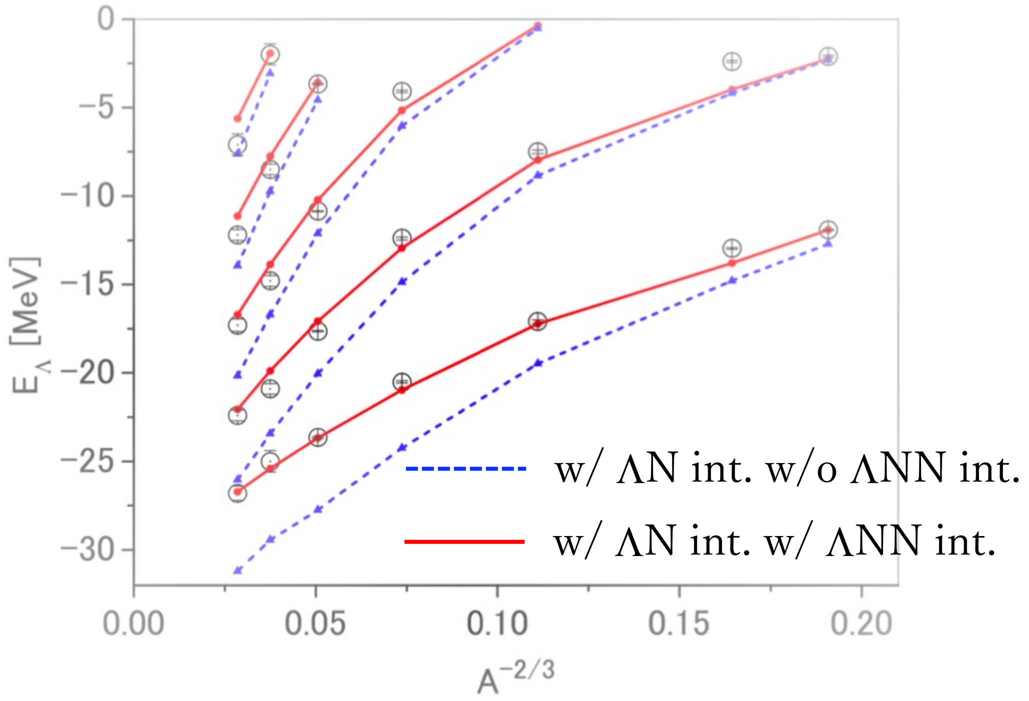

ESC16 need ΛNN repulsive interaction to explain Λ hypernuclear bounding energy

Λ hypernuclei with chiral YN potential

J. Haidenbauer, I. Vidana, Eur. Phys. J. A (2020) 56:55

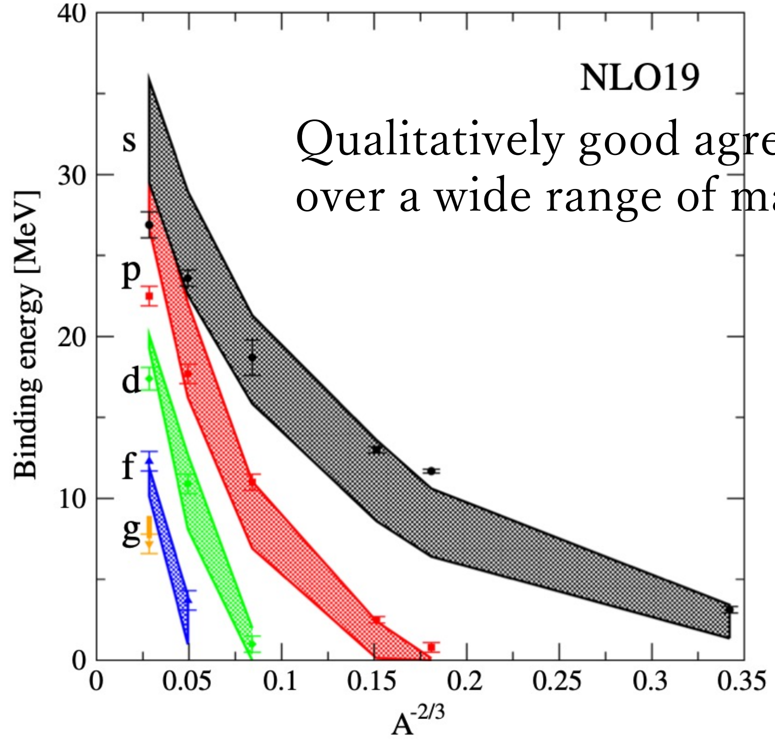

Qualitatively good agreement with data over a wide range of mass number

Sizable cutoff dependence

→ Would be reduced at higher order and after inclusion of 3BF

Toward construction of realistic YN interaction

Even for YN case

We need help of theorist and experience of NN experimentalist.
We are very happy if we make a such collaboration for the phase-shift analysis

Two-body scattering data → Phase-shift analysis

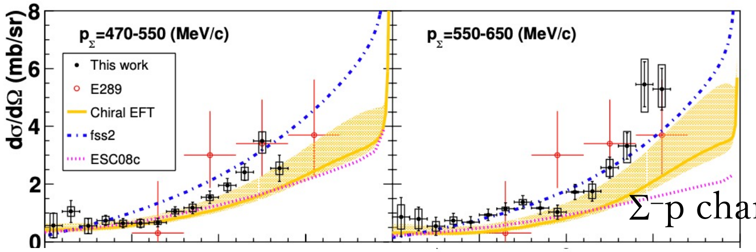

Σ^-p channel

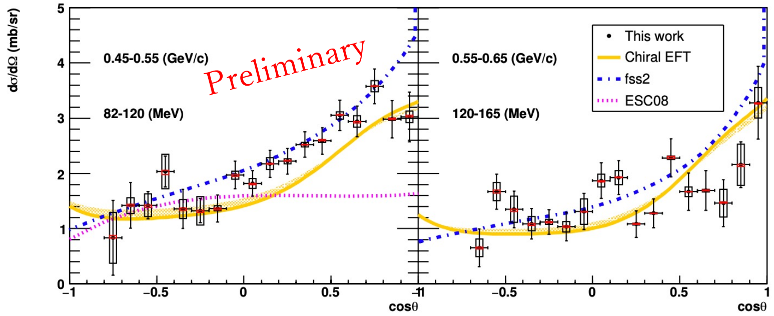

$\Sigma^-p \rightarrow \Lambda n$ channel

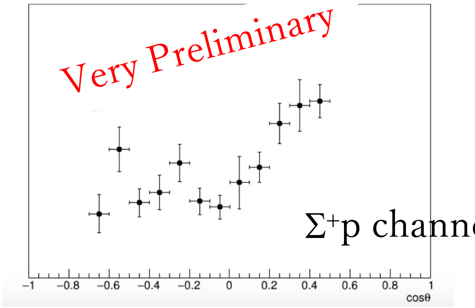

Σ^+p channel

ΣN channel would be available in very near future

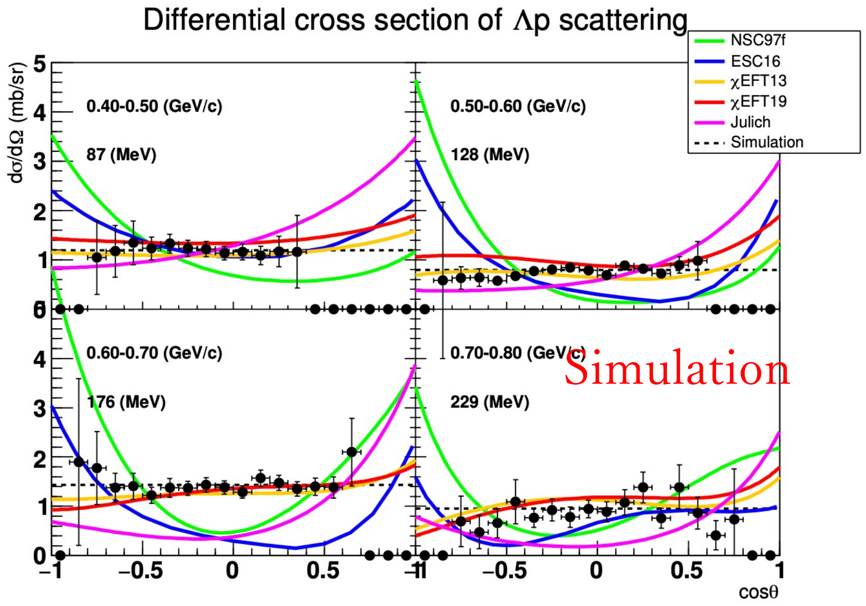

Simulation

ΛN channel will be measured after hall extension project

HIHR/K1.1 p

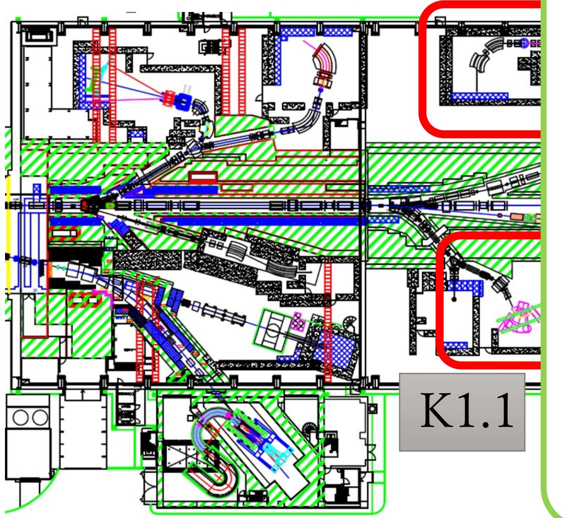

Femtoscopy at HIC

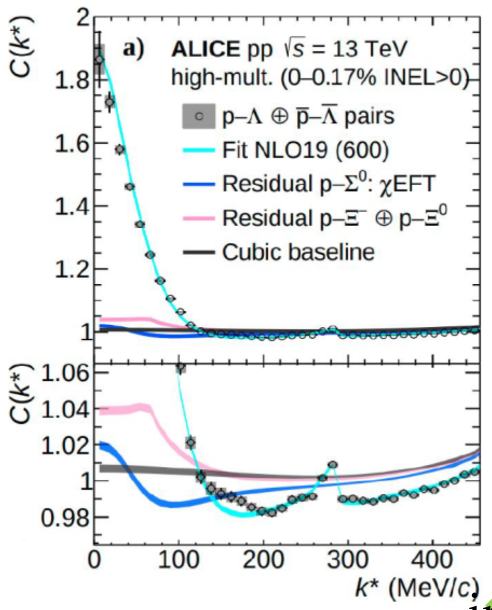

input

gh-Intensity and High-Resolution beam line

Dispersion-matching beam line → NO need to track beam particles

Potential high-intensity beam at J-PARC can be used

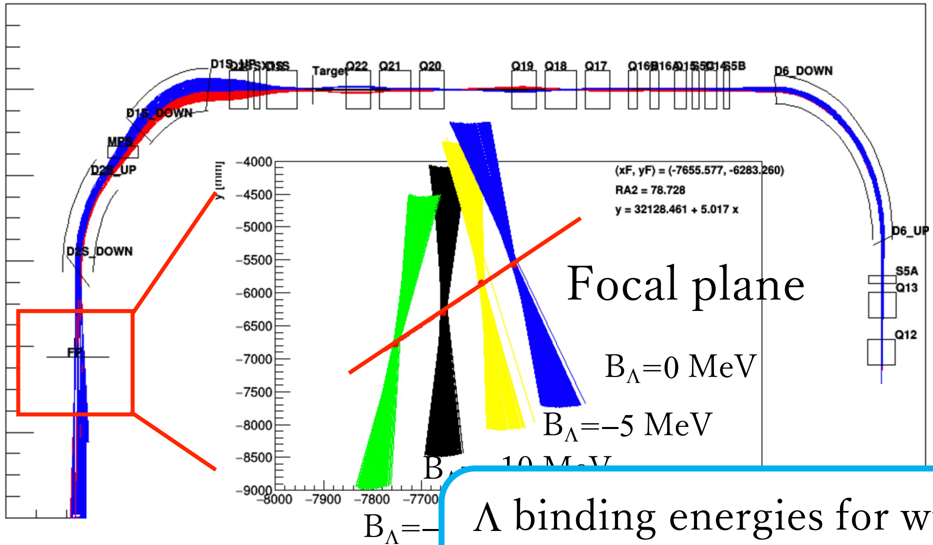

K1.1 beam line

Optimized for S=-1 physics

Suitable to produce → polarized Λ

Σp data at K1.8

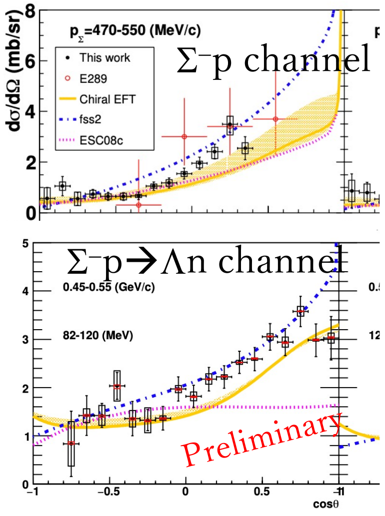

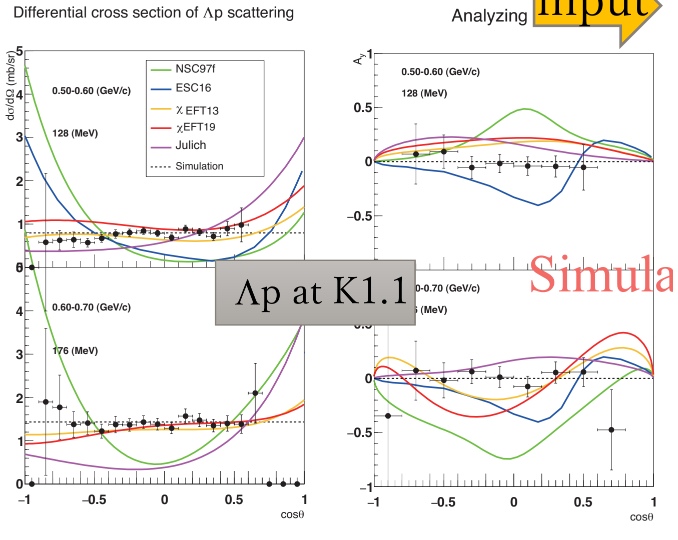

input

Realistic BB interaction model

SU(3) Chiral EFT

Nijmegen models

Potential from Lattice

Theoretical calculation of Λ single-particle energies

EOS, Neutron star matter

Λ binding energies for wide-mass numbe

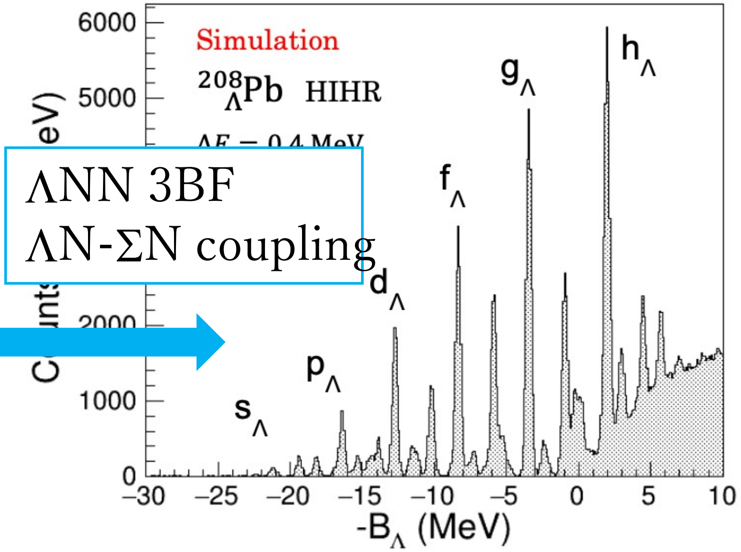

ΛNN 3BF

ΛN-ΣN coupling

Single particle potential at nuclear density

Accumulated hypernucler data

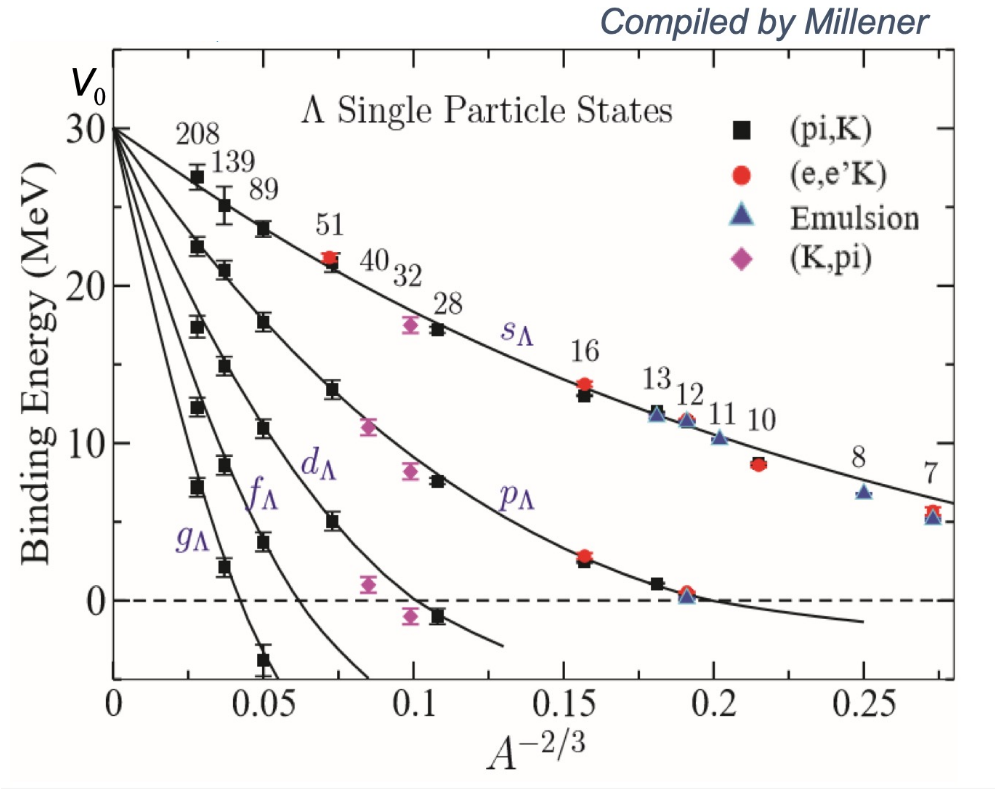

$U_\Lambda(\rho_0)$~-30 MeV

Attractive potential at normal nuclear density

J-PARC E07

M. Yoshimoto et al., arXiv:2103.08793

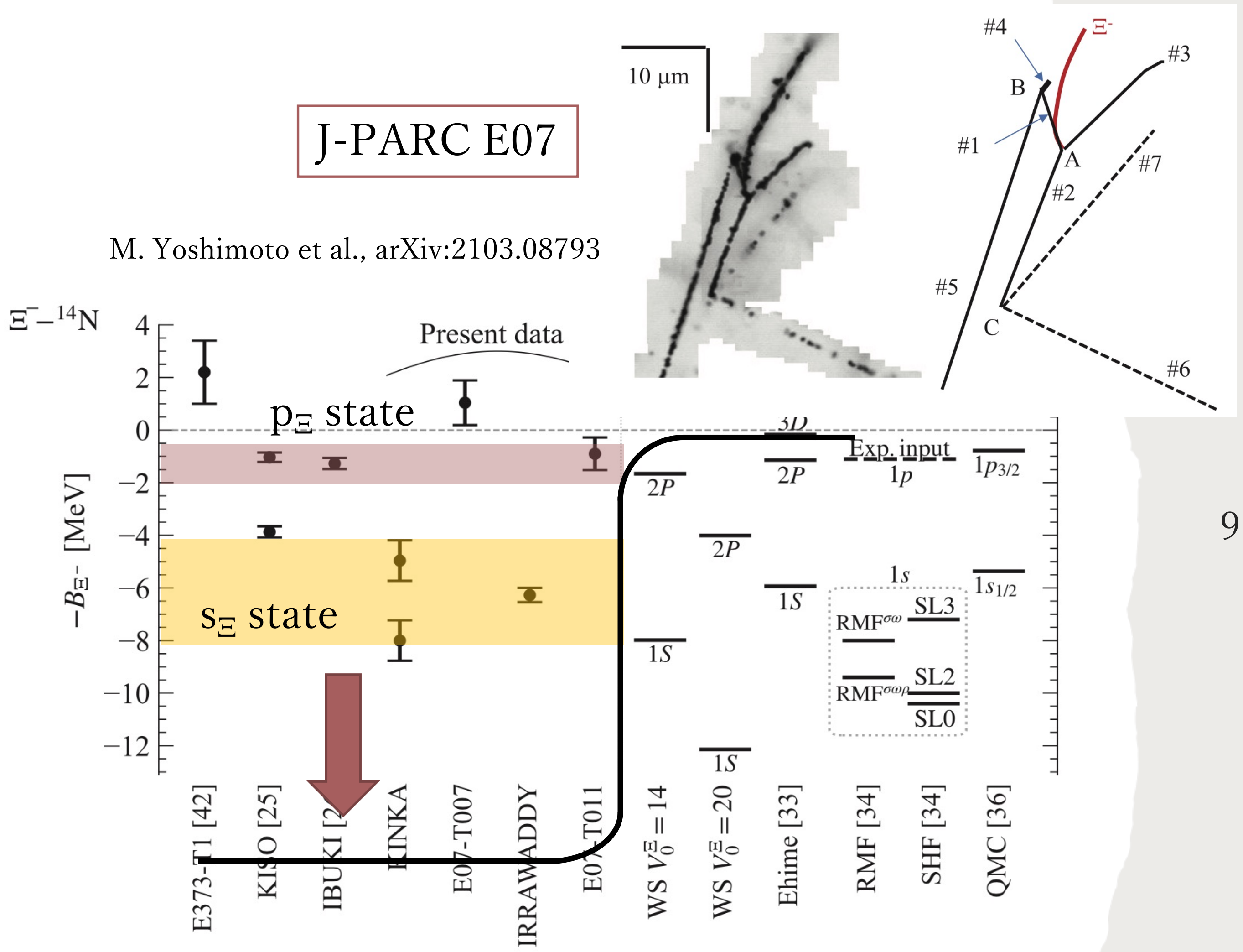

$U_\Xi(\rho_0)$ will be determined by J-PARC experiment

Emulsion (E07) + Ξ hypernuclear spectroscopy (E70)

Other experiment

LN interaction

LN interaction can be modified easily due to the LN-SN coupling

LN interaction in free space should be determined.